Exhibit EE

Exhibit D-7

Invalidity of U.S. Patent No. 6,922,632 ("'632 Patent") under Pre-AIA Section 102 or Section 103 in view of Welch et al., "SCAAT: Incremental Tracking with Incomplete Information," Univ. of N.C. at Chapel Hill, 1997 ("Welch 1997")[1]

Welch 1997 was published in 1997. Plaintiffs belatedly asserted a priority date of June 13, 2001 for the '632 Patent on December 22, 2021, 71 days after the Court's deadline. Defendants have reviewed Plaintiffs' alleged evidence of the purported June 13, 2001 priority date, and maintain that the '632 Patent is not entitled to this priority date. *See* Defendants' March 15, 2022 Supplemental Invalidity Contentions. Defendants reserve their objections to Plaintiffs' belated assertion of the new priority date and expressly reserve all rights to challenge this alleged new priority date. As such, Defendants assume for the sake of these invalidity contentions, that the priority date for the '632 Patent is August 9, 2002 based on the first filed Provisional Application from which the '632 Patent claims priority. (Defendants do not concede nor agree that Plaintiffs are even entitled to this date.) Assuming this priority date, Welch 1997 qualifies as prior art under at least pre-AIA Sections 102(a) and (b) to the '632 Patent.

As described herein, the asserted claims of the '632 Patent are invalid (a) under one or more sections of 35 U.S.C. § 102 as anticipated expressly or inherently by Welch 1997 (including the documents incorporated into Welch 1997 by reference), and (b) under 35 U.S.C. § 103 as obvious in view of Welch 1997 standing alone, and additionally, in combination with the knowledge of one of ordinary skill in the art, and/or other prior art, including but not limited to the prior art identified in Defendants' Invalidity Contentions and the prior art described in the claim charts attached in Exhibits D-1 – D-22. With respect to the proposed modifications to Welch 1997, as of the priority date of the '632 Patent, such modification would have been obvious to try, an obvious combination of prior art elements according to known methods to yield predictable results, a simple substitution of one known element for another to obtain predictable results, a use of known techniques to improve a similar device or method in the same way, an application of a known technique to a known device or method ready for improvement to yield predictable results, a variation of a known work in one field of endeavor for use in either the same field or a different one based on design incentives or other market forces with variations that are predictable to one of ordinary skill in the art, and/or obvious in view of teachings, suggestions, and motivations in the prior art that would have led one of ordinary skill to modify or combine the prior art references.

[1] Discovery in this case is ongoing and, accordingly, this invalidity chart is not to be considered final. Defendants have conducted the invalidity analysis herein without having fully undergone claim construction and a *Markman* hearing. By charting the prior art against the claim(s) herein, Defendants are not admitting nor agreeing to Plaintiffs' interpretation of the claims at issue in this case. Additionally, these charts provide representative examples of portions of the charted references that disclose the indicated limitations under Plaintiffs' application of the claims; additional portions of these references other than the representative examples provided herein may also disclose the indicated limitation(s) and Defendants contend that the asserted claim(s) are invalid in light of the charted reference(s) as a whole. Defendants reserve the right to rely on additional citations or sources of evidence that also may be applicable, or that may become applicable in light of claim construction, changes in Plaintiffs' infringement contentions, and/or information obtained during discovery as the case progresses. Further, by submitting these invalidity contentions, Defendants do not waive and hereby expressly reserve their right to raise other invalidity defenses, including but not limited to defenses under Sections 101 and 112. Defendants reserve the right to amend or supplement this claim chart at a later date, including after the Court's order construing disputed claim terms.

Exhibit D-7

All cross-references should be understood to include material that is cross-referenced within the cross-reference. Where a particular figure is cited, the citation should be understood to encompass the caption and description of the figure as well as any text relating to or describing the figure. Conversely, where particular text referring to a figure is cited, the citation should be understood to include the figure as well.

A. Independent Claim 1

Claim 1	Welch 1997
[1.pre] A method for tracking an object comprising:	At least under Plaintiffs' apparent infringement theory, Welch 1997 discloses, either expressly or inherently, a method for tracking an object. No party has yet asserted that the preamble is limiting, nor has the Court construed the preamble as limiting. However, to the extent that the preamble is limiting, it is disclosed by Welch 1997. In the alternative, this element would be obvious over Welch 1997 in light of the other references disclosed in Defendants' Invalidity Contentions and/or the knowledge of one of ordinary skill in the art. *See, e.g.*: We present a promising new **mathematical method for tracking a user's pose (position and orientation) for interactive computer graphics. The method,** which is applicable to a wide variety of both commercial and experimental systems, improves accuracy by properly assimilating sequential observations, filtering sensor measurements, and by concurrently autocalibrating source and sensor devices. It facilitates user motion prediction, multisensor data fusion, and higher report rates with lower latency than previous methods. Welch 1997 at Abstract. Our new approach **produces tracker reports as each new low-level sensor measurement is made** rather than waiting to form a complete collection of observations. Because single observations under-constrain the mathematical solution, we refer to our approach as single-constraint-at-a-time or SCAAT tracking. The key is that the single observations provide some information about the user's state, and thus can be used to incrementally improve a previous estimate. We recursively apply this principle, incorporating new sensor data as soon as it is measured. With this approach we are able to generate estimates more frequently, with less latency, and with

Exhibit D-7

CLAIM 1	Welch 1997
	improved accuracy. We present results from both an actual implementation, and from extensive simulations. Welch 1997 at Abstract. **The metho**d we present requires, we believe, a fundamental change in the way people think about estimating a set of unknowns in general, and tracking for virtual environments in particular. Most of us have the preconceived notion that to estimate a set of unknowns we need as many constraints as there are degrees of freedom at any particular instant in time. What we present instead is a method to constrain the unknowns over time, continually refining an estimate for the solution, a single constraint at a time. Welch 1997 at Section 1. **The SCAAT method employs a Kalman filter (KF)** in an unusual fashion. The Kalman filter is a mathematical procedure that provides an efficient computational (recursive) method for the least-squares estimation of a linear system. It does so in a predictor-corrector fashion, predicting short-term (since the last estimate) changes in the state using a dynamic model, and then correcting them with a measurement and a corresponding measurement model. The extended Kalman filter (EKF) is a variation of the Kalman filter that supports estimation of nonlinear systems, e.g. 3D position and orientation tracking systems. A basic introduction to the Kalman filter can be found in Chapter 1 of [31], while a more complete introductory discussion can be found in [40], which also contains some interesting historical narrative. More extensive references can be found in [7,18,24,28,31,46]. Welch 1997 at Section 3. The Kalman filter has been employed previously for virtual environment tracking estimation and prediction. For example see [2,5,12,14,42], and most recently [32]. In each of these cases however the filter was applied directly and only to the 6D pose estimates delivered by the off-the-shelf tracker. The SCAAT approach could be applied to either a hybrid system using off-the shelf and/or custom trackers, or it could be employed by tracker developers to improve the existing systems for the end-user graphics community. Welch 1997 at Section 3. In this section we describe **the method** in a manner that does not imply a specific tracking system. (In section 3.4 we present experimental results of a specific implementation, a SCAAT wide area optoelectronic tracking system.) In section 3.1 we describe **the method for tracking**, and in section 3.2 we describe **one possible method for concurrent autocalibration**. Welch 1997 at Section 3.

Exhibit D-7

CLAIM 1	Welch 1997
	3.1 Tracking **3.1.1 Main Tracker Filter** The use of a Kalman filter requires a mathematical (state-space) model for the dynamics of the process to be estimated, the target motion in this case. While several possible dynamic models and associated state configurations are possible, we have found a simple *position-velocity* model to suffice for the dynamics of our applications. In fact we use this same form of model, with different parameters, for all six of the position and orientation components $(x, y, z, \phi, \theta, \psi)$. Discussion of some other potential models and the associated trade-offs can be found in [7] pp. 415-420. Because our implementation is discrete with inter sample time δt we model the target's dynamic motion with the following linear difference equation: $\vec{x}(t+\delta t) = A(\delta t)\vec{x}(t) + \vec{w}(\delta t)$. (2) Welch 1997 at Section 3.1.

Exhibit D-7

CLAIM 1	Welch 1997
	In the standard model corresponding to equation (2), the n dimensional Kalman filter *state vector* $\vec{x}(t)$ would completely describe the target position and orientation at any time t. In practice we use a method similar to [2,6] and maintain the complete target orientation externally to the Kalman filter in order to avoid the nonlinearities associated with orientation computations. In the internal state vector $\vec{x}(t)$ we maintain the target position as the Cartesian coordinates (x, y, z), and the *incremental* orientation as small rotations (ϕ, θ, ψ) about the (x, y, z) axis. Externally we maintain the target orientation as the *external quaternion* $\vec{\alpha} = (\alpha_w, (\alpha_x, \alpha_y, \alpha_z))$. (See [9] for discussion of quaternions.) At each filter update step, the incremental orientations (ϕ, θ, ψ) are factored into the external quaternion $\vec{\alpha}$, and then zeroed as shown below. Thus the incremental orientations are linearized for the EKF, centered about zero. We maintain the derivatives of the target position and orientation internally, in the state vector $\vec{x}(t)$. We maintain the angular velocities internally because the angular velocities behave like orthogonal vectors and do not exhibit the nonlinearities of the angles themselves. The target state is then represented by the $n = 12$ element internal state vector $$\vec{x} = \left[x\ y\ z\ \dot{x}\ \dot{y}\ \dot{z}\ \phi\ \theta\ \psi\ \dot{\phi}\ \dot{\theta}\ \dot{\psi}\right]^T \quad (3)$$ and the four-element external orientation quaternion $$\vec{\alpha} = (\alpha_w, (\alpha_x, \alpha_y, \alpha_z)), \quad (4)$$ where the time designations have been omitted for clarity. Welch 1997 at Section 3.1.1.

Exhibit D-7

CLAIM 1	Welch 1997
	The $n \times n$ *state transition matrix* $A(\delta t)$ in (2) projects the state forward from time t to time $t + \delta t$. For our linear model, the matrix implements the relationships $$\begin{aligned} x(t+\delta t) &= x(t) + \dot{x}(t)\delta t \\ \dot{x}(t+\delta t) &= \dot{x}(t) \end{aligned} \quad (5)$$ and likewise for the remaining elements of (3). The $n \times 1$ *process noise vector* $\vec{w}(\delta t)$ in (2) is a normally-distributed zero-mean sequence that represents the uncertainty in the target state over any time interval δt. The corresponding $n \times n$ *process noise covariance matrix* is given by $$E\{\vec{w}(\delta t)\vec{w}^T(\delta t + \varepsilon)\} = \begin{cases} Q(\delta t), & \varepsilon = 0 \\ 0, & \varepsilon \neq 0 \end{cases}. \quad (6)$$ Because our implementation is discrete with inter sample time δt, we can use the transfer function method illustrated by [7] pp. 221-222 to compute a *sampled* process noise covariance matrix. (Because the associated random processes are presumed to be time stationary, we present the process noise covariance matrix as a function of the inter-sample duration δt only.) The non-zero elements of $Q(\delta t)$ are given by $$\begin{aligned} Q(\delta t)[i,i] &= \vec{\eta}[i]\frac{(\delta t)^3}{3} \\ Q(\delta t)[i,j] = Q(\delta t)[j,i] &= \vec{\eta}[i]\frac{(\delta t)^2}{2} \\ Q(\delta t)[j,j] &= \vec{\eta}[i](\delta t) \end{aligned} \quad (7)$$ for each pair $$(i,j) \in \{(x,\dot{x}), (y,\dot{y}), (z,\dot{z}), (\phi,\dot{\phi}), (\theta,\dot{\theta}), (\psi,\dot{\psi})\}.$$ Welch 1997 at Section 3.1.1.

Exhibit D-7

CLAIM 1	Welch 1997
	The $\vec{\eta}[i]$ in (7) are the *correlation kernels* of the (assumed constant) noise sources presumed to be driving the dynamic model. We determined a set of values using Powell's method, and then used these in both simulation and our real implementation. The values can be "tuned" for different dynamics, though we have found that the tracker works well over a broad range of values. The use of a Kalman filter requires not only a dynamic model as described above, but also a *measurement model* for each available type of measurement. The measurement model is used to predict the ideal noise-free response of each sensor and source pair, given the filter's current estimate of the target state as in equations (3) and (4). *It is the nature of the measurement models and indeed the actual sensor measurements that distinguishes a SCAAT Kalman filter from a well-constrained one.* For each sensor *type* σ we define the $m_\sigma \times 1$ *measurement vector* $\vec{z}_\sigma(t)$ and corresponding *measurement function* $\vec{h}_\sigma(\bullet)$ such that $$\vec{z}_{\sigma,t} = \vec{h}_\sigma(\vec{x}(t), \vec{b}_t, \vec{c}_t) + \vec{v}_\sigma(t) \,. \quad (8)$$ Note that in the "purest" SCAAT implementation $m_\sigma = 1$ and the measurements are incorporated as single scalar values. However if it is not possible or necessary to isolate the measurements, e.g. to perform autocalibration, then multi-dimensional measurements can be incorporated also. Guidelines presented in [47] lead to the following heuristic for choosing the SCAAT Kalman filter measurement elements (constraints): *During each SCAAT Kalman filter measurement update one should observe a single sensor and source pair only.* For example, to incorporate magnetic tracker data as an end-user, $m_\sigma = 7$ for the three position and four orientation (quaternion) Welch 1997 at Section 3.1.1.

Exhibit D-7

CLAIM 1	Welch 1997
	elements, while if the manufacturer were to use the SCAAT implementation, $m_\sigma = 3$ for each 3-axis electromagnetic response to a single excitation. For an image-based landmark tracker such as [41] the measurement function would, given estimates of the camera pose and a single landmark location, transform the landmark into camera space and then project it onto the camera image plane. In this case $m_\sigma = 2$ for the 2D image coordinates of the landmark. The $m_\sigma \times 1$ *measurement noise vector* $\vec{v}_\sigma(t)$ in (8) is a normally-distributed zero-mean sequence that represents any random error (e.g. electrical noise) in the measurement. This parameter can be determined from component design specifications, and (or) confirmed by off-line measurement. For our simulations we did both. The corresponding $m_\sigma \times m_\sigma$ *measurement noise covariance matrix* is given by $$E\{\vec{v}_\sigma(t)\vec{v}_\sigma^T(t+\varepsilon)\} = \begin{cases} R_\sigma(t), & \varepsilon = 0 \\ 0, & \varepsilon \neq 0 \end{cases}. \quad (9)$$ For each measurement function $\vec{h}_\sigma(\bullet)$ we determine the corresponding Jacobian function $$H_\sigma(\vec{x}(t), \vec{b}_t, \vec{c}_t)[i, j] \equiv \frac{\partial}{\partial \vec{x}[j]} \vec{h}_\sigma(\vec{x}(t), \vec{b}_t, \vec{c}_t)[i], \quad (10)$$ where $1 \leq i \leq m_\sigma$ and $1 \leq j \leq n$. Finally, we note the use of the standard (Kalman filter) $n \times n$ *error covariance matrix* $P(t)$ which maintains the covariance of the error in the estimated state. Welch 1997 at Section 3.1.1.

Exhibit D-7

CLAIM 1	Welch 1997
	3.1.2 Tracking Algorithm Given an initial state estimate $\hat{x}(0)$ and error covariance estimate $P(0)$, the SCAAT algorithm proceeds similarly to a conventional EKF, cycling through the following steps whenever a discrete measurement $\vec{z}_{\sigma,t}$ from some sensor (type σ) and source becomes available at time t: a. Compute the time δt since the previous estimate. b. Predict the state and error covariance. $\hat{x}^- = A(\delta t)\hat{x}(t-\delta t)$ $P^- = A(\delta t)P(t-\delta t)A^T(\delta t) + Q(\delta t)$ (11) c. Predict the measurement and compute the corresponding Jacobian. $\hat{z} = \vec{h}_\sigma(\hat{x}^-, \vec{b}_t, \vec{c}_t)$ $H = H_\sigma(\hat{x}^-, \vec{b}_t, \vec{c}_t)$ (12) d. Compute the *Kalman gain*. $K = P^-H^T(HP^-H^T + R_\sigma(t))^{-1}$ (13) e. Compute the *residual* between the actual sensor measurement $\vec{z}_{\sigma,t}$ and the predicted measurement from (12). $\overrightarrow{\Delta z} = \vec{z}_{\sigma,t} - \hat{z}$ (14) f. Correct the predicted tracker state estimate and error covariance from (11). $\hat{x}(t) = \hat{x}^- + K\overrightarrow{\Delta z}$ $P(t) = (I - KH)P^-$ (15) Welch 1997 at Section 3.1.2.

Exhibit D-7

CLAIM 1	Welch 1997
	g. Update the external orientation of equation (4) per the change indicated by the (ϕ, θ, ψ) elements of the state.* $$\begin{aligned}\Delta\hat{\alpha} &= \text{quaternion}(\hat{x}[\phi], \hat{x}[\theta], \hat{x}[\psi]) \\ \hat{\alpha} &= \hat{\alpha} \otimes \Delta\hat{\alpha}\end{aligned} \quad (16)$$ h. Zero the orientation elements of the state vector. $$\hat{x}[\phi] = \hat{x}[\theta] = \hat{x}[\psi] = 0 \quad (17)$$ The equations (11)-(17) may seem computationally complex, however they can be performed quite efficiently. The computations can be optimized to eliminate operations on matrix and vector elements that are known to be zero. For example, the elements of the Jacobian H in (12) that correspond to the velocities in the state $\hat{x}(t)$ will always be zero. In addition, the matrix inverted in the computation of K in (13) is of rank m_σ (2×2 for our example in section 3.4) which is smaller for a SCAAT filter than for a corresponding conventional EKF implementation. Finally, the increased data rate allows the use of the *small angle approximations* $\sin(\theta) = \theta$ and $\cos(\theta) = 1$ in $\vec{h}_\sigma(\bullet)$ and $H_\sigma(\bullet)$. The total *per estimate* computation time can therefore actually be less than that of a corresponding conventional implementation. (We are able to execute the SCAAT filter computations, with the autocalibration computations discussed in the next section, in approximately 100µs on a 200 MHz PC-compatible computer.) Welch 1997 at Section 3.1.2.

Exhibit D-7

<table>
<tr><th>CLAIM 1</th><th>Welch 1997</th></tr>
<tr><td></td><td>

3.1.3 Discussion

The key to the SCAAT method is the number of constraints provided by the measurement vector and measurement function in equation (8). For the 3D-tracking problem being solved, a unique solution requires $C = 6$ non-degenerate constraints to resolve six degrees of freedom. Because individual sensor measurements typically provide less than six constraints, conventional implementations usually construct a complete measurement vector

$$\vec{z}_t = \left[\vec{z}^T_{\sigma_1, t_1} \ \dots \ \vec{z}^T_{\sigma_N, t_N}\right]^T$$

from some group of $N \geq C$ individual sensor measurements over time $t_1 \dots t_N$, and *then* proceed to compute an estimate. Or a particular implementation may operate in a *moving-window* fashion, combining the most recent measurement with the $N-1$ previous measurements, possibly implementing a form of a finite-impulse-response filter. In any case, for such well-constrained systems complete observability is obtained at each step of the filter. Systems that collect measurements sequentially in this way inherently violate the simultaneity assumption, as well as increase the time δt between estimates.

Welch 1997 at Section 3.1.3.

</td></tr>
</table>

Exhibit D-7

CLAIM 1	Welch 1997
	In contrast, the SCAAT method blends individual measurements that each provide incomplete constraints into a complete state estimate. The EKF inherently provides the means for this blending, no matter how complete the information content of each individual measurement $\vec{z}_{\sigma,t}$. The EKF accomplishes this through the Kalman gain K which is computed in (13). The Kalman gain, which is used to adjust the state and the error covariance in (15), is optimal in the sense that it minimizes the error covariance if certain conditions are met. Note that the inversion in (13) forms a ratio that reflects the relative uncertainties of the state and the measurement. Note too that the ratio is affected by the use of the measurement function Jacobian H. Because the Jacobian reflects the rate of change of each measurement with respect to the current state, it indicates a direction in state space along which a measurement could *possibly* affect the state. Because the gain is recomputed at each step with the appropriate measurement function and associated Jacobian, it inherently reflects the amount and direction of information provided by the individual constraint. Welch 1997 at Section 3.1.3. **3.2 Autocalibration** The method we use for autocalibration involves *augmenting* the *main tracker filter* presented in section 3.1 to effectively implement a distinct *device filter*, a Kalman filter, for each source or sensor to be calibrated. (We use the word "device" here to include for example scene landmarks which can be thought of as passive sources, and cameras which are indeed sensors.) In general, any constant device-related parameters used by a measurement function $\vec{h}_\sigma(\bullet)$ from (8) are candidates for this autocalibration method. We assume that the parameters to be estimated are contained in the device parameter vectors $\vec{b}_t$ and $\vec{c}_t$, and we also present the case where both the source and sensor are to be calibrated since omission of one or the other is trivial. We note the following new convention. $\widehat{\alpha}$ = augmented matrix/vector (wide hat) Welch 1997 at Section 3.2

Exhibit D-7

CLAIM 1	Welch 1997
	3.2.1 Device Filters For each device (source, sensor, landmark, etc.) we create a distinct device filter as follows. Let $\vec{\pi}$ represent the corresponding device parameter vector and n_π = length($\vec{\pi}$). a. Allocate an $n_\pi \times 1$ state vector $\hat{x}_\pi$ for the device, initialize with the best *a priori* device parameter estimates, e.g. from design. b. Allocate an $n_\pi \times n_\pi$ noise covariance matrix $Q_\pi(\delta t)$, initialize with the expected parameter variances. c. Allocate an $n_\pi \times n_\pi$ error covariance matrix $P_\pi(t)$, initialize to indicate the level of confidence in the *a priori* device parameter estimates from (a) above. Welch 1997 at Section 3.2.1. **3.2.2 Revised Tracking Algorithm** The algorithm for tracking with concurrent autocalibration is the same as that presented in section 3.1, with the following exceptions. After step (a) in the original algorithm, we form augmented versions of the state vector $$\widehat{x}(t-\delta t) = \left[\hat{x}^T(t-\delta t)\ \ \hat{x}^T_{b,t}(t-\delta t)\ \ \hat{x}^T_{c,t}(t-\delta t)\right]^T, \quad (18)$$ the error covariance matrix $$\widehat{P}(t-\delta t) = \begin{bmatrix} P(t-\delta t) & 0 & 0 \\ 0 & P_{b,t}(t-\delta t) & 0 \\ 0 & 0 & P_{c,t}(t-\delta t) \end{bmatrix}, \quad (19)$$ the state transition matrix $$\widehat{A}(\delta t) = \begin{bmatrix} A(\delta t) & 0 & 0 \\ 0 & I & 0 \\ 0 & 0 & I \end{bmatrix}, \quad (20)$$ and the process noise matrix $$\widehat{Q}(\delta t) = \begin{bmatrix} Q(\delta t) & 0 & 0 \\ 0 & Q_{b,t}(\delta t) & 0 \\ 0 & 0 & Q_{c,t}(\delta t) \end{bmatrix}. \quad (21)$$ Welch 1997 at Section 3.2.2.

CLAIM 1	Welch 1997
	We then follow steps (b)-(h) from the original algorithm, making the appropriate substitutions of (18)-(21), and noting that the measurement and Jacobian functions used in step (c) have become $\vec{h}_{\sigma}(\overset{\frown}{x}(t))$ and $H_{\sigma}(\overset{\frown}{x}(t))$ because the estimates of parameters $\vec{b}_t$ and $\vec{c}_t$ ($\hat{x}_{b,t}$ and $\hat{x}_{c,t}$) are now contained in the augmented state vector $\overset{\frown}{x}$ per (18). After step (h) we finish by extracting and saving the device filter portions of the augmented state vector and error covariance matrix $\hat{x}_{b,t}(t) = \overset{\frown}{x}(t)[i \ldots j]$ $P_{b,t}(t) = \overset{\frown}{P}(t)[i \ldots j, i \ldots j]$ (22) $\hat{x}_{c,t}(t) = \overset{\frown}{x}(t)[k \ldots l]$ $P_{c,t}(t) = \overset{\frown}{P}(t)[k \ldots l, k \ldots l]$ where $i = n + 1$ $j = n + n_b$ $k = n + n_b + 1$ $l = n + n_b + n_c$ and n, n_b, and n_c are the dimensions of the state vectors for the main tracker filter, the source filter, and the sensor filter (respectively). We leave the main tracker filter state vector and error covariance matrix in their augmented counterparts, while we swap the device filter components in and out with each estimate. The result is that individual device filters are updated less frequently than the main tracker filter. The more a device is used, the more it is calibrated. If a device is never used, it is never calibrated. Welch 1997 at Section 3.2.2.

Exhibit D-7

CLAIM 1	Welch 1997
	With respect to added time complexity, the computations can again be optimized to eliminate operations on matrix and vector elements that are known to be zero: those places mentioned in section 3.1, and see (19)-(21). Also note that the size of and thus time for the matrix inversion in (13) has not changed. With respect to added space complexity, the autocalibration method requires storing a separate state vector and covariance matrix for each device—a fixed amount of (generally small) space per device. For example, consider autocalibrating the beacon (LED) positions for an optical tracking system with 3,000 beacons. For each beacon one would need 3 words for the beacon state (its 3D position), $3 \times 3 = 9$ words for the noise covariance matrix, and $3 \times 3 = 9$ words for the error covariance matrix. Assuming 8 bytes per word, this is only $3{,}000 \times 8 \times (3 + 9 + 9) = 504{,}000$ bytes. Welch 1997 at Section 3.2.2. **3.2.3 Discussion** The ability to simultaneously estimate two dependent sets of unknowns (the target and device states) is made possible by several factors. First, the dynamics of the two sets are very different as would be reflected in the process noise matrices. We assume the target is undergoing some random (constant) acceleration, reflected in the noise parameter η of $Q(\delta t)$ in (6). Conversely, we assume the device parameters are constant, and so the elements of $Q_{\pi}(\delta t)$ for a source or sensor simply reflect any allowed variances in the corresponding parameters: usually zero or extremely small. In addition, while the target is expected to be moving, the filter expects the motion between any two estimations to closely correspond to the velocity estimates in the state (3). If the tracker estimate rate is high enough, poorly estimated device parameters will result in what appears to be almost instantaneous target motion. The increased rate of the SCAAT method allows such motion to be recognized as unlikely, and attributed to poorly estimated device parameters. Welch 1997 at Section 3.2.3 *See also* Defendants' Invalidity Contentions for further discussion.

Exhibit D-7

CLAIM 1	Welch 1997
[1.a] coupling a sensor subsystem to an estimation subsystem, said sensor subsystem enabling measurement related to relative locations or orientations of sensing elements;	At least under Plaintiffs' apparent infringement theory, Welch 1997 discloses, either expressly or inherently, coupling a sensor subsystem to an estimation subsystem, said sensor subsystem enabling measurement related to relative locations or orientations of sensing elements. In the alternative, this element would be obvious over Welch 1997 in light of the other references disclosed in Defendants' Invalidity Contentions and/or the knowledge of one of ordinary skill in the art. *See, e.g.*: The Kalman filter [26] has been widely used for data fusion. For example in navigation systems [17,30], virtual environment tracking systems [5,12,14], and in 3D scene modeling [20,42]. However **the SCAAT method represents a new approach to Kalman filter based multi-sensor data fusion.** Because constraints are intentionally incorporated one at a time, one can pick and choose which ones to add, and when to add them. This means that information from different sensors or modalities can be woven together in a common, flexible, and expeditious fashion. Furthermore, one can use the approach to ensure that each estimate is computed from the most recently obtained constraint. Welch 1997 at Section 2.4. Consider for a moment the UNC hybrid landmark-magnetic presented at SIGGRAPH 96 [41]. This system uses an off-the-shelf **Ascension magnetic tracking system** along with a **vision-based landmark recognition system** to achieve superior **synthetic and real image registration** for augmented reality assisted medical procedures. The vision-based component attempts to identify and locate multiple known landmarks in a single image before applying a correction to the magnetic readings. A SCAAT implementation would instead identify and locate only one landmark per update, using a new image (frame) each time. Not only would this approach increase the frequency of landmark based correction (given the necessary image processing) but it would offer the added benefit that unlike the implementation presented in [41], no special processing would be needed for the cases where the number of visible landmarks falls below the number C necessary to determine a complete position and orientation solution. The SCAAT implementation would simply cycle through any available landmarks, one at a time. Even with only one visible landmark the method would continue to operate as usual, using the information provided by the landmark sighting to refine the estimate where possible, while increasing the uncertainty where not. Welch 1997 at Section 2.4. The SCAAT method employs a Kalman filter (KF) in an unusual fashion. The Kalman filter is a mathematical procedure that provides an efficient computational (recursive) method for the least-squares estimation of a linear

CLAIM 1	Welch 1997
	system. It does so in a predictor-corrector fashion, predicting short-term (since the last estimate) changes in the state using a dynamic model, and then correcting them with a measurement and a corresponding measurement model. The extended Kalman filter (EKF) is a variation of the Kalman filter that supports estimation of nonlinear systems, e.g. 3D position and orientation tracking systems. A basic introduction to the Kalman filter can be found in Chapter 1 of [31], while a more complete introductory discussion can be found in [40], which also contains some interesting historical narrative. More extensive references can be found in [7,18,24,28,31,46]. Welch 1997 at Section 3. The Kalman filter has been employed previously for virtual environment tracking estimation and prediction. For example see [2,5,12,14,42], and most recently [32]. In each of these cases however the filter was applied directly and only to the 6D pose estimates delivered by the off-the-shelf tracker. The SCAAT approach could be applied to either a hybrid system using off-the shelf and/or custom trackers, or it could be employed by tracker developers to improve the existing systems for the end-user graphics community. Welch 1997 at Section 3. In this section we describe the method in a manner that does not imply a specific tracking system. (In section 3.4 we present experimental results of a specific implementation, a SCAAT wide area optoelectronic tracking system.) In section 3.1 we describe the method for tracking, and in section 3.2 we describe one possible method for concurrent autocalibration. Welch 1997 at Section 3.

Exhibit D-7

CLAIM 1	Welch 1997
	Throughout we use the following conventions. x = scalar (lower case) $\vec{x}$ = general vector (lower case, arrow) indexed as $\vec{x}[r]$ $\hat{x}$ = filter estimate vector (lower case, hat) A = matrix (capital letters) indexed as $A[r, c]$ A^{-1} = matrix inverse I = the identity matrix β^- = matrix/vector *prediction* (super minus) β^T = matrix/vector transpose (super T) α_i = matrix/vector/scalar identifier (subscript) $E\{\bullet\}$ = mathematical expectation Welch 1997 at Section 3. **3.1 Tracking** **3.1.1 Main Tracker Filter** The use of a Kalman filter requires a mathematical (state-space) model for the dynamics of the process to be estimated, the target motion in this case. While several possible dynamic models and associated state configurations are possible, we have found a simple *position-velocity* model to suffice for the dynamics of our applications. In fact we use this same form of model, with different parameters, for all six of the position and orientation components $(x, y, z, \phi, \theta, \psi)$. Discussion of some other potential models and the associated trade-offs can be found in [7] pp. 415-420. Because our implementation is discrete with inter sample time δt we model the target's dynamic motion with the following linear difference equation: $\vec{x}(t+\delta t) = A(\delta t)\vec{x}(t) + \vec{w}(\delta t)$. (2) Welch 1997 at Section 3.1.

Exhibit D-7

CLAIM 1	Welch 1997
	In the standard model corresponding to equation (2), the n dimensional Kalman filter *state vector* $\vec{x}(t)$ would completely describe the target position and orientation at any time t. In practice we use a method similar to [2,6] and maintain the complete target orientation externally to the Kalman filter in order to avoid the nonlinearities associated with orientation computations. In the internal state vector $\vec{x}(t)$ we maintain the target position as the Cartesian coordinates (x, y, z), and the *incremental* orientation as small rotations (ϕ, θ, ψ) about the (x, y, z) axis. Externally we maintain the target orientation as the *external quaternion* $\vec{\alpha} = (\alpha_w, (\alpha_x, \alpha_y, \alpha_z))$. (See [9] for discussion of quaternions.) At each filter update step, the incremental orientations (ϕ, θ, ψ) are factored into the external quaternion $\vec{\alpha}$, and then zeroed as shown below. Thus the incremental orientations are linearized for the EKF, centered about zero. We maintain the derivatives of the target position and orientation internally, in the state vector $\vec{x}(t)$. We maintain the angular velocities internally because the angular velocities behave like orthogonal vectors and do not exhibit the nonlinearities of the angles themselves. The target state is then represented by the $n = 12$ element internal state vector $$\vec{x} = \left[x\ y\ z\ \dot{x}\ \dot{y}\ \dot{z}\ \phi\ \theta\ \psi\ \dot{\phi}\ \dot{\theta}\ \dot{\psi}\right]^T \qquad (3)$$ and the four-element external orientation quaternion $$\vec{\alpha} = (\alpha_w, (\alpha_x, \alpha_y, \alpha_z)), \qquad (4)$$ where the time designations have been omitted for clarity. Welch 1997 at Section 3.1.1.

Exhibit D-7

CLAIM 1	Welch 1997
	The $n \times n$ *state transition matrix* $A(\delta t)$ in (2) projects the state forward from time t to time $t + \delta t$. For our linear model, the matrix implements the relationships $$\begin{aligned} x(t+\delta t) &= x(t) + \dot{x}(t)\delta t \\ \dot{x}(t+\delta t) &= \dot{x}(t) \end{aligned} \qquad (5)$$ and likewise for the remaining elements of (3). The $n \times 1$ *process noise vector* $\vec{w}(\delta t)$ in (2) is a normally-distributed zero-mean sequence that represents the uncertainty in the target state over any time interval δt. The corresponding $n \times n$ *process noise covariance matrix* is given by $$E\{\vec{w}(\delta t)\vec{w}^T(\delta t + \varepsilon)\} = \begin{cases} Q(\delta t), & \varepsilon = 0 \\ 0, & \varepsilon \neq 0 \end{cases}. \qquad (6)$$ Because our implementation is discrete with inter sample time δt, we can use the transfer function method illustrated by [7] pp. 221-222 to compute a *sampled* process noise covariance matrix. (Because the associated random processes are presumed to be time stationary, we present the process noise covariance matrix as a function of the inter-sample duration δt only.) The non-zero elements of $Q(\delta t)$ are given by $$\begin{aligned} Q(\delta t)[i,i] &= \vec{\eta}[i]\frac{(\delta t)^3}{3} \\ Q(\delta t)[i,j] = Q(\delta t)[j,i] &= \vec{\eta}[i]\frac{(\delta t)^2}{2} \\ Q(\delta t)[j,j] &= \vec{\eta}[i](\delta t) \end{aligned} \qquad (7)$$ for each pair $$(i,j) \in \{(x,\dot{x}), (y,\dot{y}), (z,\dot{z}), (\phi,\dot{\phi}), (\theta,\dot{\theta}), (\psi,\dot{\psi})\}.$$ Welch 1997 at Section 3.1.1.

Exhibit D-7

CLAIM 1	Welch 1997
	The $\vec{\eta}[i]$ in (7) are the *correlation kernels* of the (assumed constant) noise sources presumed to be driving the dynamic model. We determined a set of values using Powell's method, and then used these in both simulation and our real implementation. The values can be "tuned" for different dynamics, though we have found that the tracker works well over a broad range of values. The use of a Kalman filter requires not only a dynamic model as described above, but also a *measurement model* for each available type of measurement. The measurement model is used to predict the ideal noise-free response of each sensor and source pair, given the filter's current estimate of the target state as in equations (3) and (4). *It is the nature of the measurement models and indeed the actual sensor measurements that distinguishes a SCAAT Kalman filter from a well-constrained one.* For each sensor *type* σ we define the $m_\sigma \times 1$ *measurement vector* $\vec{z}_\sigma(t)$ and corresponding *measurement function* $\vec{h}_\sigma(\bullet)$ such that $\vec{z}_{\sigma,t} = \vec{h}_\sigma(\vec{x}(t), \vec{b}_t, \vec{c}_t) + \vec{v}_\sigma(t)$. (8) Note that in the "purest" SCAAT implementation $m_\sigma = 1$ and the measurements are incorporated as single scalar values. However if it is not possible or necessary to isolate the measurements, e.g. to perform autocalibration, then multi-dimensional measurements can be incorporated also. Guidelines presented in [47] lead to the following heuristic for choosing the SCAAT Kalman filter measurement elements (constraints): *During each SCAAT Kalman filter measurement update one should observe a single sensor and source pair only.* For example, to incorporate magnetic tracker data as an end-user, $m_\sigma = 7$ for the three position and four orientation (quaternion) Welch 1997 at Section 3.1.1.

Exhibit D-7

CLAIM 1	Welch 1997
	elements, while if the manufacturer were to use the SCAAT implementation, $m_\sigma = 3$ for each 3-axis electromagnetic response to a single excitation. For an image-based landmark tracker such as [41] the measurement function would, given estimates of the camera pose and a single landmark location, transform the landmark into camera space and then project it onto the camera image plane. In this case $m_\sigma = 2$ for the 2D image coordinates of the landmark. The $m_\sigma \times 1$ *measurement noise vector* $\vec{v}_\sigma(t)$ in (8) is a normally-distributed zero-mean sequence that represents any random error (e.g. electrical noise) in the measurement. This parameter can be determined from component design specifications, and (or) confirmed by off-line measurement. For our simulations we did both. The corresponding $m_\sigma \times m_\sigma$ *measurement noise covariance matrix* is given by $$E\{\vec{v}_\sigma(t)\vec{v}_\sigma^T(t+\varepsilon)\} = \begin{cases} R_\sigma(t), & \varepsilon = 0 \\ 0, & \varepsilon \neq 0 \end{cases}. \quad (9)$$ For each measurement function $\vec{h}_\sigma(\bullet)$ we determine the corresponding Jacobian function $$H_\sigma(\hat{x}(t), \vec{b}_t, \vec{c}_t)[i, j] \equiv \frac{\partial}{\partial \hat{x}[j]} \vec{h}_\sigma(\hat{x}(t), \vec{b}_t, \vec{c}_t)[i], \quad (10)$$ where $1 \leq i \leq m_\sigma$ and $1 \leq j \leq n$. Finally, we note the use of the standard (Kalman filter) $n \times n$ *error covariance matrix* $P(t)$ which maintains the covariance of the error in the estimated state. Welch 1997 at Section 3.1.1.

CLAIM 1	Welch 1997
	3.1.2 Tracking Algorithm Given an initial state estimate $\hat{x}(0)$ and error covariance estimate $P(0)$, the SCAAT algorithm proceeds similarly to a conventional EKF, cycling through the following steps whenever a discrete measurement $\vec{z}_{\sigma,t}$ from some sensor (type σ) and source becomes available at time t: a. Compute the time δt since the previous estimate. b. Predict the state and error covariance. $\hat{x}^- = A(\delta t)\hat{x}(t-\delta t)$ $P^- = A(\delta t)P(t-\delta t)A^T(\delta t) + Q(\delta t)$ (11) c. Predict the measurement and compute the corresponding Jacobian. $\hat{z} = \vec{h}_\sigma(\hat{x}^-, \vec{b}_t, \vec{c}_t)$ $H = H_\sigma(\hat{x}^-, \vec{b}_t, \vec{c}_t)$ (12) d. Compute the *Kalman gain*. $K = P^- H^T (HP^- H^T + R_\sigma(t))^{-1}$ (13) e. Compute the *residual* between the actual sensor measurement $\vec{z}_{\sigma,t}$ and the predicted measurement from (12). $\overrightarrow{\Delta z} = \vec{z}_{\sigma,t} - \hat{z}$ (14) f. Correct the predicted tracker state estimate and error covariance from (11). $\hat{x}(t) = \hat{x}^- + K\overrightarrow{\Delta z}$ $P(t) = (I - KH)P^-$ (15) Welch 1997 at Section 3.1.2.

Exhibit D-7

CLAIM 1	Welch 1997
	g. Update the external orientation of equation (4) per the change indicated by the (ϕ, θ, ψ) elements of the state.* $$\begin{aligned} \Delta\hat{\alpha} &= \text{quaternion}(\hat{x}[\phi], \hat{x}[\theta], \hat{x}[\psi]) \\ \hat{\alpha} &= \hat{\alpha} \otimes \Delta\hat{\alpha} \end{aligned} \qquad (16)$$ h. Zero the orientation elements of the state vector. $$\hat{x}[\phi] = \hat{x}[\theta] = \hat{x}[\psi] = 0 \qquad (17)$$ The equations (11)-(17) may seem computationally complex, however they can be performed quite efficiently. The computations can be optimized to eliminate operations on matrix and vector elements that are known to be zero. For example, the elements of the Jacobian H in (12) that correspond to the velocities in the state $\hat{x}(t)$ will always be zero. In addition, the matrix inverted in the computation of K in (13) is of rank m_σ (2×2 for our example in section 3.4) which is smaller for a SCAAT filter than for a corresponding conventional EKF implementation. Finally, the increased data rate allows the use of the *small angle approximations* $\sin(\theta) = \theta$ and $\cos(\theta) = 1$ in $\vec{h}_\sigma(\bullet)$ and $H_\sigma(\bullet)$. The total *per estimate* computation time can therefore actually be less than that of a corresponding conventional implementation. (We are able to execute the SCAAT filter computations, with the autocalibration computations discussed in the next section, in approximately $100 \mu s$ on a 200 MHz PC-compatible computer.) Welch 1997 at Section 3.1.2.

Exhibit D-7

CLAIM 1	Welch 1997
	3.1.3 Discussion The key to the SCAAT method is the number of constraints provided by the measurement vector and measurement function in equation (8). For the 3D-tracking problem being solved, a unique solution requires $C = 6$ non-degenerate constraints to resolve six degrees of freedom. Because individual sensor measurements typically provide less than six constraints, conventional implementations usually construct a complete measurement vector $$\vec{z}_t = \left[\vec{z}^T_{\sigma_1, t_1} \ \cdots \ \vec{z}^T_{\sigma_N, t_N}\right]^T$$ from some group of $N \geq C$ individual sensor measurements over time $t_1 \ldots t_N$, and *then* proceed to compute an estimate. Or a particular implementation may operate in a *moving-window* fashion, combining the most recent measurement with the $N-1$ previous measurements, possibly implementing a form of a finite-impulse-response filter. In any case, for such well-constrained systems complete observability is obtained at each step of the filter. Systems that collect measurements sequentially in this way inherently violate the simultaneity assumption, as well as increase the time δt between estimates. Welch 1997 at Section 3.1.3. In contrast, the SCAAT method blends individual measurements that each provide incomplete constraints into a complete state estimate. The EKF inherently provides the means for this blending, no matter how complete the information content of each individual measurement $\vec{z}_{\sigma, t}$. The EKF accomplishes this through the Kalman gain K which is computed in (13). The Kalman gain, which is used to adjust the state and the error covariance in (15), is optimal in the sense that it minimizes the error covariance if certain conditions are met. Note that the inversion in (13) forms a ratio that reflects the relative uncertainties of the state and the measurement. Note too that the ratio is affected by the use of the measurement function Jacobian H. Because the Jacobian reflects the rate of change of each measurement with respect to the current state, it indicates a direction in state space along which a measurement could *possibly* affect the state. Because the gain is recomputed at each step with the appropriate measurement function and associated Jacobian, it inherently reflects the amount and direction of information provided by the individual constraint. Welch 1997 at Section 3.1.3.

CLAIM 1	Welch 1997
	3.3 Stability Because the SCAAT method uses individual measurements with insufficient information, one might be concerned about the potential for instability or divergence. A linear system is said to be stable if its response to any input tends to a finite steady value after the input is removed [24]. For the Kalman filter in general this is certainly not a new concern, and there are standard requirements and corresponding tests that ensure or detect stability (see [18], p. 132): a. The filter must be uniformly completely observable, b. the dynamic and measurement noise matrices in equations (6) and (9) must be bounded from above and below, and c. the dynamic behavior represented by in equation (2) must be bounded from above. As it turns out, these conditions and their standard tests are equally applicable to a SCAAT implementation. For the SCAAT method the conditions mean that the user dynamics between estimates must be bounded, the measurement noise must be bounded, one must incorporate a sufficient set of non-degenerate constraints over time. In particular, the constraints must be incorporated in less than 1/2 the time of the user motion time-constant in order to avoid tracking an alias of the true motion. In general these conditions are easily met for systems and circumstances that would otherwise be stable with a multiple-constraint implementation. A complete stability analysis is beyond the scope of this paper, and is presented in [47]. Welch 1997 at Section 3.3. [47] Greg Welch, 1996. “SCAAT: Incremental Tracking with Incomplete Information,” University of North Carolina at Chapel Hill, doctoral dissertation, TR 96-051. Welch 1997 at References. *See also* Defendants’ Invalidity Contentions for further discussion.
[1.b] accepting configuration data from the sensor subsystem;	At least under Plaintiffs’ apparent infringement theory, Welch 1997 discloses, either expressly or inherently, accepting configuration data from the sensor subsystem. In the alternative, this element would be obvious over Welch 1997 in light of the other references disclosed in Defendants’ Invalidity Contentions and/or the knowledge of one of ordinary skill in the art. *See, e.g.*:

Exhibit D-7

CLAIM 1	Welch 1997
	1.1 Incomplete Information The idea that one might build a tracking system that generates a new estimate with each individual sensor measurement or *observation* is a very interesting one. After all, individual observations usually provide only partial information about a user's complete state (pose), i.e. they are "incomplete" observations. For example, for a camera observing landmarks in a scene, only limited information is obtained from observations of any single landmark. In terms of control theory, a system designed to operate with only such incomplete measurements is characterized as *unobservable* because the user state cannot be observed (determined) from the measurements. The notion of observability can also be described in terms of constraints on the unknown parameters of the system being estimated, e.g. constraints on the unknown elements of the system state. Given a particular system, and the corresponding set of unknowns that are to be estimated, let C be defined as the minimal number of independent simultaneous constraints necessary to uniquely determine a solution, let N be the number actually used to generate a new estimate, and let N_{ind} be the number of *independent* constraints that can be formed from the N constraints. For any $N \geq N_{ind}$ constraints, if $N_{ind} = C$ the problem is *well constrained*, if $N_{ind} > C$ it is *over constrained*, and if $N_{ind} < C$ it is *under-constrained*. (See Figure 1.) Welch 1997 at Section 1.1.

Exhibit D-7

CLAIM 1	Welch 1997
	1.2 Landmark Tracking Consider for example a system in which a single camera is used to observe known scene points to determine the camera position and orientation. In this case, the constraints provided by the observations are multi-dimensional: 2D image coordinates of 3D scene points. Given the internal camera parameters, a set of four known coplanar scene points, and the corresponding image coordinates, the camera position and orientation can be uniquely determined in closed-form [16]. In other words if $N = C = 4$ constraints (2D image points) are used to estimate the camera position and orientation, the system is completely observable. On the other hand, if $N < C$ then there are multiple solutions. For example with only $N = 3$ non-collinear points, there are up to 4 solutions. Even worse, with $N = 2$ or $N = 1$ points, there are infinite combinations of position and orientation that could result in the same camera images. Welch 1997 at Section 1.2. In general, for closed-form tracking approaches, a well or over-constrained system with $N \geq C$ is observable, an under-constrained system with $N < C$ is not. Therefore, if the individual observations provide only partial information, i.e. the measurements provide insufficient constraints, then multiple devices or landmarks must be excited and (or) sensed prior to estimating a solution. Sometimes the necessary observations can be obtained simultaneously, and sometimes they can not. Magnetic trackers such as those made by Polhemus and Ascension perform three *sequential* source excitations, each in conjunction with a complete sensor unit observation. And while a camera can indeed observe multiple landmarks simultaneously in a single image, the image processing to identify and locate the individual landmarks must be done sequentially for a single CPU system. If the landmarks can move independently over time, for example if they are artificial marks placed on the skin of an ultrasound patient for the purpose of landmark-based tracking [41], batch processing of the landmarks can reduce the effectiveness of the system. A SCAAT implementation might grab an image, extract a *single* landmark, update the estimates of both the camera *and* landmark positions, and then throw-away the image. In this way estimates are generated faster and with the most recent landmark configurations. Welch 1997 at Section 1.2.

Exhibit D-7

CLAIM 1	Welch 1997
	1.3 Putting the Pieces Together Given a tracker that uses multiple constraints that are each individually incomplete, a *measurement model* for any one of incomplete constraints would be characterized as *locally unobservable*. Such a system must incorporate a sufficient set of these incomplete constraints so that the resulting overall system is observable. The corresponding aggregate measurement model can then be characterized as *globally observable*. Global observability can be obtained over *space* or over *time*. The SCAAT method adopts the latter scheme, even in some cases where the former is possible. Welch 1997 at Section 1.3. *See also* Defendants' Invalidity Contentions for further discussion.
[1.c] configuring the estimation system according to the accepted configuration data;	At least under Plaintiffs' apparent infringement theory, Welch 1997 discloses, either expressly or inherently, configuring the estimation system according to the accepted configuration data. In the alternative, this element would be obvious over Welch 1997 in light of the other references disclosed in Defendants' Invalidity Contentions and/or the knowledge of one of ordinary skill in the art. *See, e.g.*:

Exhibit D-7

CLAIM 1	Welch 1997
	1.1 Incomplete Information The idea that one might build a tracking system that generates a new estimate with each individual sensor measurement or *observation* is a very interesting one. After all, individual observations usually provide only partial information about a user's complete state (pose), i.e. they are "incomplete" observations. For example, for a camera observing landmarks in a scene, only limited information is obtained from observations of any single landmark. In terms of control theory, a system designed to operate with only such incomplete measurements is characterized as *unobservable* because the user state cannot be observed (determined) from the measurements. The notion of observability can also be described in terms of constraints on the unknown parameters of the system being estimated, e.g. constraints on the unknown elements of the system state. Given a particular system, and the corresponding set of unknowns that are to be estimated, let C be defined as the minimal number of independent simultaneous constraints necessary to uniquely determine a solution, let N be the number actually used to generate a new estimate, and let N_{ind} be the number of *independent* constraints that can be formed from the N constraints. For any $N \geq N_{ind}$ constraints, if $N_{ind} = C$ the problem is *well constrained*, if $N_{ind} > C$ it is *over constrained*, and if $N_{ind} < C$ it is *under-constrained*. (See Figure 1.) Welch 1997 at Section 1.1.

Exhibit D-7

CLAIM 1	Welch 1997
	1.2 Landmark Tracking Consider for example a system in which a single camera is used to observe known scene points to determine the camera position and orientation. In this case, the constraints provided by the observations are multi-dimensional: 2D image coordinates of 3D scene points. Given the internal camera parameters, a set of four known coplanar scene points, and the corresponding image coordinates, the camera position and orientation can be uniquely determined in closed-form [16]. In other words if $N = C = 4$ constraints (2D image points) are used to estimate the camera position and orientation, the system is completely observable. On the other hand, if $N < C$ then there are multiple solutions. For example with only $N = 3$ non-collinear points, there are up to 4 solutions. Even worse, with $N = 2$ or $N = 1$ points, there are infinite combinations of position and orientation that could result in the same camera images. Welch 1997 at Section 1.2. In general, for closed-form tracking approaches, a well or over-constrained system with $N \geq C$ is observable, an under-constrained system with $N < C$ is not. Therefore, if the individual observations provide only partial information, i.e. the measurements provide insufficient constraints, then multiple devices or landmarks must be excited and (or) sensed prior to estimating a solution. Sometimes the necessary observations can be obtained simultaneously, and sometimes they can not. Magnetic trackers such as those made by Polhemus and Ascension perform three *sequential* source excitations, each in conjunction with a complete sensor unit observation. And while a camera can indeed observe multiple landmarks simultaneously in a single image, the image processing to identify and locate the individual landmarks must be done sequentially for a single CPU system. If the landmarks can move independently over time, for example if they are artificial marks placed on the skin of an ultrasound patient for the purpose of landmark-based tracking [41], batch processing of the landmarks can reduce the effectiveness of the system. A SCAAT implementation might grab an image, extract a *single* landmark, update the estimates of both the camera *and* landmark positions, and then throw-away the image. In this way estimates are generated faster and with the most recent landmark configurations. Welch 1997 at Section 1.2.

Exhibit D-7

CLAIM 1	Welch 1997
	1.3 Putting the Pieces Together Given a tracker that uses multiple constraints that are each individually incomplete, a *measurement model* for any one of incomplete constraints would be characterized as *locally unobservable*. Such a system must incorporate a sufficient set of these incomplete constraints so that the resulting overall system is observable. The corresponding aggregate measurement model can then be characterized as *globally observable*. Global observability can be obtained over *space* or over *time*. The SCAAT method adopts the latter scheme, even in some cases where the former is possible. Welch 1997 at Section 1.3. *See also* Defendants' Invalidity Contentions for further discussion.
[1.d] repeatedly updating a state estimate, including accepting measurement information from the sensor subsystem, and updating the state estimate according to the accepted configuration data and the accepted measurement data.	At least under Plaintiffs' apparent infringement theory, Welch 1997 discloses, either expressly or inherently, repeatedly updating a state estimate, including accepting measurement information from the sensor subsystem, and updating the state estimate according to the accepted configuration data and the accepted measurement data. In the alternative, this element would be obvious over Welch 1997 in light of the other references disclosed in Defendants' Invalidity Contentions and/or the knowledge of one of ordinary skill in the art. *See, e.g.*: The SCAAT method employs a Kalman filter (KF) in an unusual fashion. The Kalman filter is a mathematical procedure that provides an efficient computational (recursive) method for the least-squares estimation of a linear system. **It does so in a predictor-corrector fashion, predicting short-term (since the last estimate) changes in the state using a dynamic model, and then correcting them with a measurement and a corresponding measurement model. The extended Kalman filter (EKF) is a variation of the Kalman filter that supports estimation of nonlinear systems, e.g. 3D position and orientation tracking systems.** A basic introduction to the Kalman filter can be found in Chapter 1 of [31], while a more complete introductory discussion can be found in [40], which also contains some interesting historical narrative. More extensive references can be found in [7,18,24,28,31,46]. Welch 1997 at Section 3. The Kalman filter has been employed previously for virtual environment tracking estimation and prediction. For example see [2,5,12,14,42], and most recently [32]. In each of these cases however the filter was applied directly

CLAIM 1	Welch 1997
	and only to the 6D pose estimates delivered by the off-the-shelf tracker. The SCAAT approach could be applied to either a hybrid system using off-the shelf and/or custom trackers, or it could be employed by tracker developers to improve the existing systems for the end-user graphics community. Welch 1997 at Section 3. In this section we describe the method in a manner that does not imply a specific tracking system. (In section 3.4 we present experimental results of a specific implementation, a SCAAT wide area optoelectronic tracking system.) In section 3.1 we describe the method for tracking, and in section 3.2 we describe one possible method for concurrent autocalibration. Welch 1997 at Section 3. Throughout we use the following conventions. x = scalar (lower case) $\vec{x}$ = general vector (lower case, arrow) indexed as $\vec{x}[r]$ $\hat{x}$ = filter estimate vector (lower case, hat) A = matrix (capital letters) indexed as $A[r, c]$ A^{-1} = matrix inverse I = the identity matrix β^{-} = matrix/vector *prediction* (super minus) β^{T} = matrix/vector transpose (super T) α_i = matrix/vector/scalar identifier (subscript) $E\{\bullet\}$ = mathematical expectation Welch 1997 at Section 3.

Exhibit D-7

CLAIM 1	Welch 1997
	3.1 Tracking **3.1.1 Main Tracker Filter** The use of a Kalman filter requires a mathematical (state-space) model for the dynamics of the process to be estimated, the target motion in this case. While several possible dynamic models and associated state configurations are possible, we have found a simple *position-velocity* model to suffice for the dynamics of our applications. In fact we use this same form of model, with different parameters, for all six of the position and orientation components $(x, y, z, \phi, \theta, \psi)$. Discussion of some other potential models and the associated trade-offs can be found in [7] pp. 415-420. Because our implementation is discrete with inter sample time δt we model the target's dynamic motion with the following linear difference equation: $\vec{x}(t + \delta t) = A(\delta t)\vec{x}(t) + \vec{w}(\delta t)$. (2) Welch 1997 at Section 3.1.

Exhibit D-7

CLAIM 1	Welch 1997
	In the standard model corresponding to equation (2), the n dimensional Kalman filter *state vector* $\hat{x}(t)$ would completely describe the target position and orientation at any time t. In practice we use a method similar to [2,6] and maintain the complete target orientation externally to the Kalman filter in order to avoid the nonlinearities associated with orientation computations. In the internal state vector $\hat{x}(t)$ we maintain the target position as the Cartesian coordinates (x, y, z), and the *incremental* orientation as small rotations (ϕ, θ, ψ) about the (x, y, z) axis. Externally we maintain the target orientation as the *external quaternion* $\vec{\alpha} = (\alpha_w, (\alpha_x, \alpha_y, \alpha_z))$. (See [9] for discussion of quaternions.) At each filter update step, the incremental orientations (ϕ, θ, ψ) are factored into the external quaternion $\vec{\alpha}$, and then zeroed as shown below. Thus the incremental orientations are linearized for the EKF, centered about zero. We maintain the derivatives of the target position and orientation internally, in the state vector $\hat{x}(t)$. We maintain the angular velocities internally because the angular velocities behave like orthogonal vectors and do not exhibit the nonlinearities of the angles themselves. The target state is then represented by the $n = 12$ element internal state vector $$\hat{x} = \left[x\ y\ z\ \dot{x}\ \dot{y}\ \dot{z}\ \phi\ \theta\ \psi\ \dot{\phi}\ \dot{\theta}\ \dot{\psi}\right]^T \quad (3)$$ and the four-element external orientation quaternion $$\vec{\alpha} = (\alpha_w, (\alpha_x, \alpha_y, \alpha_z)), \quad (4)$$ where the time designations have been omitted for clarity. Welch 1997 at Section 3.1.1.

Exhibit D-7

CLAIM 1	Welch 1997
	The $n \times n$ *state transition matrix* $A(\delta t)$ in (2) projects the state forward from time t to time $t + \delta t$. For our linear model, the matrix implements the relationships $$\begin{aligned} x(t+\delta t) &= x(t) + \dot{x}(t)\delta t \\ \dot{x}(t+\delta t) &= \dot{x}(t) \end{aligned} \quad (5)$$ and likewise for the remaining elements of (3). The $n \times 1$ *process noise vector* $\vec{w}(\delta t)$ in (2) is a normally-distributed zero-mean sequence that represents the uncertainty in the target state over any time interval δt. The corresponding $n \times n$ *process noise covariance matrix* is given by $$E\{\vec{w}(\delta t)\vec{w}^T(\delta t + \varepsilon)\} = \begin{cases} Q(\delta t), & \varepsilon = 0 \\ 0, & \varepsilon \neq 0 \end{cases}. \quad (6)$$ Because our implementation is discrete with inter sample time δt, we can use the transfer function method illustrated by [7] pp. 221-222 to compute a *sampled* process noise covariance matrix. (Because the associated random processes are presumed to be time stationary, we present the process noise covariance matrix as a function of the inter-sample duration δt only.) The non-zero elements of $Q(\delta t)$ are given by $$\begin{aligned} Q(\delta t)[i,i] &= \vec{\eta}[i]\frac{(\delta t)^3}{3} \\ Q(\delta t)[i,j] = Q(\delta t)[j,i] &= \vec{\eta}[i]\frac{(\delta t)^2}{2} \\ Q(\delta t)[j,j] &= \vec{\eta}[i](\delta t) \end{aligned} \quad (7)$$ for each pair $$(i,j) \in \{(x,\dot{x}), (y,\dot{y}), (z,\dot{z}), (\phi,\dot{\phi}), (\theta,\dot{\theta}), (\psi,\dot{\psi})\}.$$ Welch 1997 at Section 3.1.1.

Exhibit D-7

CLAIM 1	Welch 1997
	The $\vec{\eta}[i]$ in (7) are the *correlation kernels* of the (assumed constant) noise sources presumed to be driving the dynamic model. We determined a set of values using Powell's method, and then used these in both simulation and our real implementation. The values can be "tuned" for different dynamics, though we have found that the tracker works well over a broad range of values. The use of a Kalman filter requires not only a dynamic model as described above, but also a *measurement model* for each available type of measurement. The measurement model is used to predict the ideal noise-free response of each sensor and source pair, given the filter's current estimate of the target state as in equations (3) and (4). *It is the nature of the measurement models and indeed the actual sensor measurements that distinguishes a SCAAT Kalman filter from a well-constrained one.* For each sensor *type* σ we define the $m_\sigma \times 1$ *measurement vector* $\vec{z}_\sigma(t)$ and corresponding *measurement function* $\vec{h}_\sigma(\bullet)$ such that $$\vec{z}_{\sigma,t} = \vec{h}_\sigma(\vec{x}(t), \vec{b}_t, \vec{c}_t) + \vec{v}_\sigma(t) . \quad (8)$$ Note that in the "purest" SCAAT implementation $m_\sigma = 1$ and the measurements are incorporated as single scalar values. However if it is not possible or necessary to isolate the measurements, e.g. to perform autocalibration, then multi-dimensional measurements can be incorporated also. Guidelines presented in [47] lead to the following heuristic for choosing the SCAAT Kalman filter measurement elements (constraints): *During each SCAAT Kalman filter measurement update one should observe a single sensor and source pair only.* For example, to incorporate magnetic tracker data as an end-user, $m_\sigma = 7$ for the three position and four orientation (quaternion) Welch 1997 at Section 3.1.1.

Exhibit D-7

CLAIM 1	Welch 1997
	elements, while if the manufacturer were to use the SCAAT implementation, $m_\sigma = 3$ for each 3-axis electromagnetic response to a single excitation. For an image-based landmark tracker such as [41] the measurement function would, given estimates of the camera pose and a single landmark location, transform the landmark into camera space and then project it onto the camera image plane. In this case $m_\sigma = 2$ for the 2D image coordinates of the landmark. The $m_\sigma \times 1$ *measurement noise vector* $\vec{v}_\sigma(t)$ in (8) is a normally-distributed zero-mean sequence that represents any random error (e.g. electrical noise) in the measurement. This parameter can be determined from component design specifications, and (or) confirmed by off-line measurement. For our simulations we did both. The corresponding $m_\sigma \times m_\sigma$ *measurement noise covariance matrix* is given by $$E\{\vec{v}_\sigma(t)\vec{v}_\sigma^T(t+\varepsilon)\} = \begin{cases} R_\sigma(t), & \varepsilon = 0 \\ 0, & \varepsilon \neq 0 \end{cases}. \quad (9)$$ For each measurement function $\vec{h}_\sigma(\bullet)$ we determine the corresponding Jacobian function $$H_\sigma(\hat{x}(t), \vec{b}_t, \vec{c}_t)[i, j] \equiv \frac{\partial}{\partial \hat{x}[j]} \vec{h}_\sigma(\hat{x}(t), \vec{b}_t, \vec{c}_t)[i], \quad (10)$$ where $1 \leq i \leq m_\sigma$ and $1 \leq j \leq n$. Finally, we note the use of the standard (Kalman filter) $n \times n$ *error covariance matrix* $P(t)$ which maintains the covariance of the error in the estimated state. Welch 1997 at Section 3.1.1.

Exhibit D-7

CLAIM 1	Welch 1997
	3.1.2 Tracking Algorithm Given an initial state estimate $\hat{x}(0)$ and error covariance estimate $P(0)$, the SCAAT algorithm proceeds similarly to a conventional EKF, cycling through the following steps whenever a discrete measurement $\vec{z}_{\sigma,t}$ from some sensor (type σ) and source becomes available at time t: a. Compute the time δt since the previous estimate. b. Predict the state and error covariance. $$\begin{aligned} \hat{x}^- &= A(\delta t)\hat{x}(t-\delta t) \\ P^- &= A(\delta t)P(t-\delta t)A^T(\delta t)+Q(\delta t) \end{aligned} \quad (11)$$ c. Predict the measurement and compute the corresponding Jacobian. $$\begin{aligned} \hat{z} &= \vec{h}_\sigma(\hat{x}^-, \vec{b}_t, \vec{c}_t) \\ H &= H_\sigma(\hat{x}^-, \vec{b}_t, \vec{c}_t) \end{aligned} \quad (12)$$ d. Compute the *Kalman gain*. $$K = P^-H^T(HP^-H^T+R_\sigma(t))^{-1} \quad (13)$$ e. Compute the *residual* between the actual sensor measurement $\vec{z}_{\sigma,t}$ and the predicted measurement from (12). $$\overrightarrow{\Delta z} = \vec{z}_{\sigma,t} - \hat{z} \quad (14)$$ f. Correct the predicted tracker state estimate and error covariance from (11). $$\begin{aligned} \hat{x}(t) &= \hat{x}^- + K\overrightarrow{\Delta z} \\ P(t) &= (I-KH)P^- \end{aligned} \quad (15)$$ Welch 1997 at Section 3.1.2.

Exhibit D-7

CLAIM 1	Welch 1997
	g. Update the external orientation of equation (4) per the change indicated by the (ϕ, θ, ψ) elements of the state.* $$\begin{aligned} \Delta\hat{\alpha} &= \text{quaternion}(\hat{x}[\phi], \hat{x}[\theta], \hat{x}[\psi]) \\ \hat{\alpha} &= \hat{\alpha} \otimes \Delta\hat{\alpha} \end{aligned} \quad (16)$$ h. Zero the orientation elements of the state vector. $$\hat{x}[\phi] = \hat{x}[\theta] = \hat{x}[\psi] = 0 \quad (17)$$ The equations (11)-(17) may seem computationally complex, however they can be performed quite efficiently. The computations can be optimized to eliminate operations on matrix and vector elements that are known to be zero. For example, the elements of the Jacobian H in (12) that correspond to the velocities in the state $\hat{x}(t)$ will always be zero. In addition, the matrix inverted in the computation of K in (13) is of rank m_σ (2×2 for our example in section 3.4) which is smaller for a SCAAT filter than for a corresponding conventional EKF implementation. Finally, the increased data rate allows the use of the *small angle approximations* $\sin(\theta) = \theta$ and $\cos(\theta) = 1$ in $\vec{h}_\sigma(\bullet)$ and $H_\sigma(\bullet)$. The total *per estimate* computation time can therefore actually be less than that of a corresponding conventional implementation. (We are able to execute the SCAAT filter computations, with the autocalibration computations discussed in the next section, in approximately $100\mu s$ on a 200 MHz PC-compatible computer.) Welch 1997 at Section 3.1.2.

Exhibit D-7

CLAIM 1	Welch 1997
	3.1.3 Discussion The key to the SCAAT method is the number of constraints provided by the measurement vector and measurement function in equation (8). For the 3D-tracking problem being solved, a unique solution requires $C = 6$ non-degenerate constraints to resolve six degrees of freedom. Because individual sensor measurements typically provide less than six constraints, conventional implementations usually construct a complete measurement vector $$\vec{z}_t = \left[\vec{z}^T_{\sigma_1, t_1} \; \dots \; \vec{z}^T_{\sigma_N, t_N}\right]^T$$ from some group of $N \geq C$ individual sensor measurements over time $t_1 \dots t_N$, and *then* proceed to compute an estimate. Or a particular implementation may operate in a *moving-window* fashion, combining the most recent measurement with the $N - 1$ previous measurements, possibly implementing a form of a finite-impulse-response filter. In any case, for such well-constrained systems complete observability is obtained at each step of the filter. Systems that collect measurements sequentially in this way inherently violate the simultaneity assumption, as well as increase the time δt between estimates. Welch 1997 at Section 3.1.3. In contrast, the SCAAT method blends individual measurements that each provide incomplete constraints into a complete state estimate. The EKF inherently provides the means for this blending, no matter how complete the information content of each individual measurement $\vec{z}_{\sigma, t}$. The EKF accomplishes this through the Kalman gain K which is computed in (13). The Kalman gain, which is used to adjust the state and the error covariance in (15), is optimal in the sense that it minimizes the error covariance if certain conditions are met. Note that the inversion in (13) forms a ratio that reflects the relative uncertainties of the state and the measurement. Note too that the ratio is affected by the use of the measurement function Jacobian H. Because the Jacobian reflects the rate of change of each measurement with respect to the current state, it indicates a direction in state space along which a measurement could *possibly* affect the state. Because the gain is recomputed at each step with the appropriate measurement function and associated Jacobian, it inherently reflects the amount and direction of information provided by the individual constraint. Welch 1997 at Section 3.1.3.

Exhibit D-7

CLAIM 1	Welch 1997
	3.2 Autocalibration The method we use for autocalibration involves *augmenting* the *main tracker filter* presented in section 3.1 to effectively implement a distinct *device filter*, a Kalman filter, for each source or sensor to be calibrated. (We use the word "device" here to include for example scene landmarks which can be thought of as passive sources, and cameras which are indeed sensors.) In general, any constant device-related parameters used by a measurement function $\vec{h}_{\sigma}(\bullet)$ from (8) are candidates for this autocalibration method. We assume that the parameters to be estimated are contained in the device parameter vectors $\vec{b}_t$ and $\vec{c}_t$, and we also present the case where both the source and sensor are to be calibrated since omission of one or the other is trivial. We note the following new convention. $\widehat{\alpha}$ = augmented matrix/vector (wide hat) Welch 1997 at Section 3.2. **3.2.1 Device Filters** For each device (source, sensor, landmark, etc.) we create a distinct device filter as follows. Let $\vec{\pi}$ represent the corresponding device parameter vector and n_{π} = length($\vec{\pi}$). a. Allocate an $n_{\pi} \times 1$ state vector $\hat{x}_{\pi}$ for the device, initialize with the best *a priori* device parameter estimates, e.g. from design. b. Allocate an $n_{\pi} \times n_{\pi}$ noise covariance matrix $Q_{\pi}(\delta t)$, initialize with the expected parameter variances. c. Allocate an $n_{\pi} \times n_{\pi}$ error covariance matrix $P_{\pi}(t)$, initialize to indicate the level of confidence in the *a priori* device parameter estimates from (a) above. Welch 1997 at Section 3.2.1.

Exhibit D-7

CLAIM 1	Welch 1997
	3.2.2 Revised Tracking Algorithm The algorithm for tracking with concurrent autocalibration is the same as that presented in section 3.1, with the following exceptions. After step (a) in the original algorithm, we form augmented versions of the state vector $$\widehat{x}(t-\delta t) = \left[\hat{x}^T(t-\delta t)\ \hat{x}^T_{b,t}(t-\delta t)\ \hat{x}^T_{c,t}(t-\delta t)\right]^T, \quad (18)$$ the error covariance matrix $$\widehat{P}(t-\delta t) = \begin{bmatrix} P(t-\delta t) & 0 & 0 \\ 0 & P_{b,t}(t-\delta t) & 0 \\ 0 & 0 & P_{c,t}(t-\delta t) \end{bmatrix}, \quad (19)$$ the state transition matrix $$\widehat{A}(\delta t) = \begin{bmatrix} A(\delta t) & 0 & 0 \\ 0 & I & 0 \\ 0 & 0 & I \end{bmatrix}, \quad (20)$$ and the process noise matrix $$\widehat{Q}(\delta t) = \begin{bmatrix} Q(\delta t) & 0 & 0 \\ 0 & Q_{b,t}(\delta t) & 0 \\ 0 & 0 & Q_{c,t}(\delta t) \end{bmatrix}. \quad (21)$$ Welch 1997 at Section 3.2.2.

Exhibit D-7

CLAIM 1	Welch 1997
	We then follow steps (b)-(h) from the original algorithm, making the appropriate substitutions of (18)-(21), and noting that the measurement and Jacobian functions used in step (c) have become $\vec{h}_\sigma(\widehat{x}(t))$ and $H_\sigma(\widehat{x}(t))$ because the estimates of parameters $\vec{b}_t$ and $\vec{c}_t$ ($\hat{x}_{b,t}$ and $\hat{x}_{c,t}$) are now contained in the augmented state vector $\widehat{x}$ per (18). After step (h) we finish by extracting and saving the device filter portions of the augmented state vector and error covariance matrix $$\begin{aligned} \hat{x}_{b,t}(t) &= \widehat{x}(t)[i\ldots j] \\ P_{b,t}(t) &= \widehat{P}(t)[i\ldots j, i\ldots j] \\ \hat{x}_{c,t}(t) &= \widehat{x}(t)[k\ldots l] \\ P_{c,t}(t) &= \widehat{P}(t)[k\ldots l, k\ldots l] \end{aligned} \quad (22)$$ where $$\begin{aligned} i &= n+1 \\ j &= n+n_b \\ k &= n+n_b+1 \\ l &= n+n_b+n_c \end{aligned}$$ Welch 1997 at Section 3.2.2.

Exhibit D-7

CLAIM 1	Welch 1997
	and n, n_b, and n_c are the dimensions of the state vectors for the main tracker filter, the source filter, and the sensor filter (respectively). We leave the main tracker filter state vector and error covariance matrix in their augmented counterparts, while we swap the device filter components in and out with each estimate. The result is that individual device filters are updated less frequently than the main tracker filter. The more a device is used, the more it is calibrated. If a device is never used, it is never calibrated. With respect to added time complexity, the computations can again be optimized to eliminate operations on matrix and vector elements that are known to be zero: those places mentioned in section 3.1, and see (19)-(21). Also note that the size of and thus time for the matrix inversion in (13) has not changed. With respect to added space complexity, the autocalibration method requires storing a separate state vector and covariance matrix for each device—a fixed amount of (generally small) space per device. For example, consider autocalibrating the beacon (LED) positions for an optical tracking system with 3,000 beacons. For each beacon one would need 3 words for the beacon state (its 3D position), $3 \times 3 = 9$ words for the noise covariance matrix, and $3 \times 3 = 9$ words for the error covariance matrix. Assuming 8 bytes per word, this is only $3{,}000 \times 8 \times (3 + 9 + 9) = 504{,}000$ bytes. Welch 1997 at Section 3.2.2.

Exhibit D-7

CLAIM 1	Welch 1997
	 Figure 3: The HiBall is shown here with the internal circuitry exposed and the lenses removed. The sensors, which can be seen through the lens openings, are mounted on PC boards that fold-up into the HiBall upon assembly. The mechanical pencil at the bottom conveys an indication of the relative size of the unit. Welch 1997 at Figure 3.

Exhibit D-7

CLAIM 1	Welch 1997
	4.1 Tracker Filter The 12 element state vector $\hat{x}(t)$ for the main tracker filter contained the elements shown in (3). Each of the 3000 beacon filters was allocated a 3 element state vector $$\hat{x}_b = \left[x_b \; y_b \; z_b\right]^T$$ where (x_b, y_b, z_b) represents the beacon's estimated position in cartesian (world) coordinates. The 12×12 state transition matrix for the main tracker filter was formed as discussed section 3.1, and for each beacon filter it was the 3×3 identity matrix. The 12×12 process noise matrix for the main tracker was computed using (7), using elements of $\vec{\eta}$ that were determined off-line using Powell's method and a variety of real motion data. For each beacon filter we used an identical noise covariance matrix $$Q_b(\delta t)[i, j] = \begin{cases} \eta_b & \text{if } i = j \\ 0 & \text{otherwise} \end{cases}$$ for $1 \le i, j \le 3$, with beacon position variance η_b also determined off-line. (See [47] for the complete details.) At each estimate step, the *augmented* 15 element state vector, 15×15 process noise matrix, 15×15 state transition matrix, and 15×15 error covariance matrix all resembled (18)-(21) (without the camera parameter components). The measurement noise model was distance dependent (beacon light falls-off with distance) so $R_\sigma(t)$ from (9) was computed prior to step (d), by using a beacon distance estimate (obtained from the user and beacon positions in the predicted state $\hat{x}^-$) to project a distance-dependent electrical variance onto the camera. Welch 1997 at Section 4.1. *See also* Defendants' Invalidity Contentions for further discussion.

B. DEPENDENT CLAIM 2

CLAIM 2	Welch 1997
[2] The method of claim 1 wherein coupling the	At least under Plaintiffs' apparent infringement theory, Welch 1997 discloses, either expressly or inherently, the method of claim 1 wherein coupling the sensor subsystem to the estimation subsystem includes coupling software

Exhibit D-7

CLAIM 2	Welch 1997
sensor subsystem to the estimation subsystem includes coupling software modules each associated with one or more of the sensing elements.	modules each associated with one or more of the sensing elements. In the alternative, this element would be obvious over Welch 1997 in light of the other references disclosed in Defendants' Invalidity Contentions and/or the knowledge of one of ordinary skill in the art. *See, e.g.*: **1.2 Landmark Tracking** Consider for example a system in which a single camera is used to observe known scene points to determine the camera position and orientation. In this case, the constraints provided by the observations are multi-dimensional: 2D image coordinates of 3D scene points. Given the internal camera parameters, a set of four known coplanar scene points, and the corresponding image coordinates, the camera position and orientation can be uniquely determined in closed-form [16]. In other words if $N = C = 4$ constraints (2D image points) are used to estimate the camera position and orientation, the system is completely observable. On the other hand, if $N < C$ then there are multiple solutions. For example with only $N = 3$ non-collinear points, there are up to 4 solutions. Even worse, with $N = 2$ or $N = 1$ points, there are infinite combinations of position and orientation that could result in the same camera images. Welch 1997 at Section 1.2.

CLAIM 2	Welch 1997
	In general, for closed-form tracking approaches, a well or over-constrained system with $N \geq C$ is observable, an under-constrained system with $N < C$ is not. Therefore, if the individual observations provide only partial information, i.e. the measurements provide insufficient constraints, then multiple devices or landmarks must be excited and (or) sensed prior to estimating a solution. Sometimes the necessary observations can be obtained simultaneously, and sometimes they can not. Magnetic trackers such as those made by Polhemus and Ascension perform three *sequential* source excitations, each in conjunction with a complete sensor unit observation. And while a camera can indeed observe multiple landmarks simultaneously in a single image, the image processing to identify and locate the individual landmarks must be done sequentially for a single CPU system. If the landmarks can move independently over time, for example if they are artificial marks placed on the skin of an ultrasound patient for the purpose of landmark-based tracking [41], batch processing of the landmarks can reduce the effectiveness of the system. A SCAAT implementation might grab an image, extract a *single* landmark, update the estimates of both the camera *and* landmark positions, and then throw-away the image. In this way estimates are generated faster and with the most recent landmark configurations. Welch 1997 at Section 1.2.

Exhibit D-7

CLAIM 2	Welch 1997
	 Figure 3: The HiBall is shown here with the internal circuitry exposed and the lenses removed. The sensors, which can be seen through the lens openings, are mounted on PC boards that fold-up into the HiBall upon assembly. The mechanical pencil at the bottom conveys an indication of the relative size of the unit. Welch 1997 at Figure 3.

Exhibit D-7

CLAIM 2	Welch 1997
	3.2.1 Device Filters For each device (source, sensor, landmark, etc.) we create a distinct device filter as follows. Let $\vec{\pi}$ represent the corresponding device parameter vector and n_π = length($\vec{\pi}$). a. Allocate an $n_\pi \times 1$ state vector $\hat{x}_\pi$ for the device, initialize with the best *a priori* device parameter estimates, e.g. from design. b. Allocate an $n_\pi \times n_\pi$ noise covariance matrix $Q_\pi(\delta t)$, initialize with the expected parameter variances. c. Allocate an $n_\pi \times n_\pi$ error covariance matrix $P_\pi(t)$, initialize to indicate the level of confidence in the *a priori* device parameter estimates from (a) above. Welch 1997 at Section 3.2.1 *See* Disclosures with respect to Claim 1, *supra*; *see also* Defendants' Invalidity Contentions for further discussion.

C. DEPENDENT CLAIM 5

CLAIM 5	Welch 1997
[5] The method of claim 1 wherein the state estimate characterizes an estimate of a location of the object.	At least under Plaintiffs' apparent infringement theory, Welch 1997 discloses, either expressly or inherently, the method of claim 1 wherein the state estimate characterizes an estimate of a location of the object. In the alternative, this element would be obvious over Welch 1997 in light of the other references disclosed in Defendants' Invalidity Contentions and/or the knowledge of one of ordinary skill in the art. *See, e.g.*: We present a promising new mathematical method for tracking a user's **pose (position and orientation)** for interactive computer graphics. The method, which is applicable to a wide variety of both commercial and experimental systems, improves accuracy by properly assimilating sequential observations, filtering sensor

CLAIM 5	Welch 1997
	measurements, and by concurrently autocalibrating source and sensor devices. It facilitates user motion prediction, multisensor data fusion, and higher report rates with lower latency than previous methods. Tracking systems **determine the user's pose by measuring signals from low-level hardware sensors.** For reasons of physics and economics, most systems make multiple sequential measurements which are then combined to produce a single tracker report. For example, commercial magnetic trackers using the SPASYN (Space Synchro) system sequentially measure three magnetic vectors and then combine them mathematically to produce a report of the **sensor pose.** Our new approach produces tracker reports as each new low-level sensor measurement is made rather than waiting to form a complete collection of observations. Because single observations under-constrain the mathematical solution, we refer to our approach as single-constraint-at-a-time or SCAAT tracking. The key is that the single observations provide some information about the user's state, and thus can be used to incrementally improve a previous estimate. We recursively apply this principle, incorporating new sensor data as soon as it is measured. With this approach we are able to generate estimates more frequently, with less latency, and with improved accuracy. We present results from both an actual implementation, and from extensive simulations. Welch 1997 at Abstract. *See* Disclosures with respect to Claim 1, *supra*; *see also* Defendants' Invalidity Contentions for further discussion.

D. DEPENDENT CLAIM 6

CLAIM 6	Welch 1997
[6] The method of claim 1 wherein the state estimate characterizes configuration information for one or more sensing elements fixed to the object.	At least under Plaintiffs' apparent infringement theory, Welch 1997 discloses, either expressly or inherently, the method of claim 1 wherein the state estimate characterizes configuration information for one or more sensing elements fixed to the object. In the alternative, this element would be obvious over Welch 1997 in light of the other references disclosed in Defendants' Invalidity Contentions and/or the knowledge of one of ordinary skill in the art. *See, e.g.*:

Exhibit D-7

CLAIM 6	Welch 1997
	3.1 Tracking **3.1.1 Main Tracker Filter** The use of a Kalman filter requires a mathematical (state-space) model for the dynamics of the process to be estimated, the target motion in this case. While several possible dynamic models and associated state configurations are possible, we have found a simple *position-velocity* model to suffice for the dynamics of our applications. In fact we use this same form of model, with different parameters, for all six of the position and orientation components $(x, y, z, \phi, \theta, \psi)$. Discussion of some other potential models and the associated trade-offs can be found in [7] pp. 415-420. Because our implementation is discrete with inter sample time δt we model the target's dynamic motion with the following linear difference equation: $\vec{x}(t+\delta t) = A(\delta t)\vec{x}(t) + \vec{w}(\delta t)$. (2) Welch 1997 at Section 3.1.

Exhibit D-7

CLAIM 6	Welch 1997
	In the standard model corresponding to equation (2), the n dimensional Kalman filter *state vector* $\hat{x}(t)$ would completely describe the target position and orientation at any time t. In practice we use a method similar to [2,6] and maintain the complete target orientation externally to the Kalman filter in order to avoid the nonlinearities associated with orientation computations. In the internal state vector $\hat{x}(t)$ we maintain the target position as the Cartesian coordinates (x, y, z), and the *incremental* orientation as small rotations (ϕ, θ, ψ) about the (x, y, z) axis. Externally we maintain the target orientation as the *external quaternion* $\vec{\alpha} = (\alpha_w, (\alpha_x, \alpha_y, \alpha_z))$. (See [9] for discussion of quaternions.) At each filter update step, the incremental orientations (ϕ, θ, ψ) are factored into the external quaternion $\vec{\alpha}$, and then zeroed as shown below. Thus the incremental orientations are linearized for the EKF, centered about zero. We maintain the derivatives of the target position and orientation internally, in the state vector $\hat{x}(t)$. We maintain the angular velocities internally because the angular velocities behave like orthogonal vectors and do not exhibit the nonlinearities of the angles themselves. The target state is then represented by the $n = 12$ element internal state vector $$\hat{x} = \begin{bmatrix} x & y & z & \dot{x} & \dot{y} & \dot{z} & \phi & \theta & \psi & \dot{\phi} & \dot{\theta} & \dot{\psi} \end{bmatrix}^T \quad (3)$$ and the four-element external orientation quaternion $$\vec{\alpha} = (\alpha_w, (\alpha_x, \alpha_y, \alpha_z)), \quad (4)$$ where the time designations have been omitted for clarity. Welch 1997 at Section 3.1.1.

Exhibit D-7

CLAIM 6	Welch 1997
	The $n \times n$ *state transition matrix* $A(\delta t)$ in (2) projects the state forward from time t to time $t + \delta t$. For our linear model, the matrix implements the relationships $$\begin{aligned} x(t+\delta t) &= x(t) + \dot{x}(t)\delta t \\ \dot{x}(t+\delta t) &= \dot{x}(t) \end{aligned} \quad (5)$$ and likewise for the remaining elements of (3). The $n \times 1$ *process noise vector* $\vec{w}(\delta t)$ in (2) is a normally-distributed zero-mean sequence that represents the uncertainty in the target state over any time interval δt. The corresponding $n \times n$ *process noise covariance matrix* is given by $$E\{\vec{w}(\delta t)\vec{w}^T(\delta t + \varepsilon)\} = \begin{cases} Q(\delta t), & \varepsilon = 0 \\ 0, & \varepsilon \neq 0 \end{cases} . \quad (6)$$ Because our implementation is discrete with inter sample time δt, we can use the transfer function method illustrated by [7] pp. 221-222 to compute a *sampled* process noise covariance matrix. (Because the associated random processes are presumed to be time stationary, we present the process noise covariance matrix as a function of the inter-sample duration δt only.) The non-zero elements of $Q(\delta t)$ are given by $$\begin{aligned} Q(\delta t)[i,i] &= \vec{\eta}[i]\frac{(\delta t)^3}{3} \\ Q(\delta t)[i,j] = Q(\delta t)[j,i] &= \vec{\eta}[i]\frac{(\delta t)^2}{2} \\ Q(\delta t)[j,j] &= \vec{\eta}[i](\delta t) \end{aligned} \quad (7)$$ for each pair $$(i,j) \in \{(x,\dot{x}), (y,\dot{y}), (z,\dot{z}), (\phi,\dot{\phi}), (\theta,\dot{\theta}), (\psi,\dot{\psi})\} .$$ Welch 1997 at Section 3.1.1.

Exhibit D-7

CLAIM 6	Welch 1997
	The $\vec{\eta}[i]$ in (7) are the *correlation kernels* of the (assumed constant) noise sources presumed to be driving the dynamic model. We determined a set of values using Powell's method, and then used these in both simulation and our real implementation. The values can be "tuned" for different dynamics, though we have found that the tracker works well over a broad range of values. The use of a Kalman filter requires not only a dynamic model as described above, but also a *measurement model* for each available type of measurement. The measurement model is used to predict the ideal noise-free response of each sensor and source pair, given the filter's current estimate of the target state as in equations (3) and (4). *It is the nature of the measurement models and indeed the actual sensor measurements that distinguishes a SCAAT Kalman filter from a well-constrained one.* For each sensor *type* σ we define the $m_\sigma \times 1$ *measurement vector* $\vec{z}_\sigma(t)$ and corresponding *measurement function* $\vec{h}_\sigma(\bullet)$ such that $$\vec{z}_{\sigma,t} = \vec{h}_\sigma(\vec{x}(t), \vec{b}_t, \vec{c}_t) + \vec{v}_\sigma(t) . \qquad (8)$$ Note that in the "purest" SCAAT implementation $m_\sigma = 1$ and the measurements are incorporated as single scalar values. However if it is not possible or necessary to isolate the measurements, e.g. to perform autocalibration, then multi-dimensional measurements can be incorporated also. Guidelines presented in [47] lead to the following heuristic for choosing the SCAAT Kalman filter measurement elements (constraints): *During each SCAAT Kalman filter measurement update one should observe a single sensor and source pair only.* For example, to incorporate magnetic tracker data as an end-user, $m_\sigma = 7$ for the three position and four orientation (quaternion) Welch 1997 at Section 3.1.1.

Exhibit D-7

CLAIM 6	Welch 1997
	elements, while if the manufacturer were to use the SCAAT implementation, $m_\sigma = 3$ for each 3-axis electromagnetic response to a single excitation. For an image-based landmark tracker such as [41] the measurement function would, given estimates of the camera pose and a single landmark location, transform the landmark into camera space and then project it onto the camera image plane. In this case $m_\sigma = 2$ for the 2D image coordinates of the landmark. The $m_\sigma \times 1$ *measurement noise vector* $\vec{v}_\sigma(t)$ in (8) is a normally-distributed zero-mean sequence that represents any random error (e.g. electrical noise) in the measurement. This parameter can be determined from component design specifications, and (or) confirmed by off-line measurement. For our simulations we did both. The corresponding $m_\sigma \times m_\sigma$ *measurement noise covariance matrix* is given by $$E\{\vec{v}_\sigma(t)\vec{v}_\sigma^T(t+\varepsilon)\} = \begin{cases} R_\sigma(t), & \varepsilon = 0 \\ 0, & \varepsilon \neq 0 \end{cases}. \quad (9)$$ For each measurement function $\vec{h}_\sigma(\bullet)$ we determine the corresponding Jacobian function $$H_\sigma(\hat{x}(t), \vec{b}_t, \vec{c}_t)[i, j] \equiv \frac{\partial}{\partial \hat{x}[j]} \vec{h}_\sigma(\hat{x}(t), \vec{b}_t, \vec{c}_t)[i], \quad (10)$$ where $1 \leq i \leq m_\sigma$ and $1 \leq j \leq n$. Finally, we note the use of the standard (Kalman filter) $n \times n$ *error covariance matrix* $P(t)$ which maintains the covariance of the error in the estimated state. Welch 1997 at Section 3.1.1.

Exhibit D-7

CLAIM 6	Welch 1997
	3.2 Autocalibration The method we use for autocalibration involves *augmenting* the *main tracker filter* presented in section 3.1 to effectively implement a distinct *device filter*, a Kalman filter, for each source or sensor to be calibrated. (We use the word "device" here to include for example scene landmarks which can be thought of as passive sources, and cameras which are indeed sensors.) In general, any constant device-related parameters used by a measurement function $\vec{h}_\sigma(\bullet)$ from (8) are candidates for this autocalibration method. We assume that the parameters to be estimated are contained in the device parameter vectors $\vec{b}_t$ and $\vec{c}_t$, and we also present the case where both the source and sensor are to be calibrated since omission of one or the other is trivial. We note the following new convention. $\widehat{\alpha}$ = augmented matrix/vector (wide hat) Welch 1997 at Section 3.2 **3.2.1 Device Filters** For each device (source, sensor, landmark, etc.) we create a distinct device filter as follows. Let $\vec{\pi}$ represent the corresponding device parameter vector and n_π = length($\vec{\pi}$). a. Allocate an $n_\pi \times 1$ state vector $\hat{x}_\pi$ for the device, initialize with the best *a priori* device parameter estimates, e.g. from design. b. Allocate an $n_\pi \times n_\pi$ noise covariance matrix $Q_\pi(\delta t)$, initialize with the expected parameter variances. c. Allocate an $n_\pi \times n_\pi$ error covariance matrix $P_\pi(t)$, initialize to indicate the level of confidence in the *a priori* device parameter estimates from (a) above. Welch 1997 at Section 3.2.1.

CLAIM 6	Welch 1997
	3.2.2 Revised Tracking Algorithm The algorithm for tracking with concurrent autocalibration is the same as that presented in section 3.1, with the following exceptions. After step (a) in the original algorithm, we form augmented versions of the state vector $$\widehat{x}(t-\delta t) = \left[\hat{x}^T(t-\delta t)\ \ \hat{x}^T_{b,t}(t-\delta t)\ \ \hat{x}^T_{c,t}(t-\delta t)\right]^T, \quad (18)$$ the error covariance matrix $$\widehat{P}(t-\delta t) = \begin{bmatrix} P(t-\delta t) & 0 & 0 \\ 0 & P_{b,t}(t-\delta t) & 0 \\ 0 & 0 & P_{c,t}(t-\delta t) \end{bmatrix}, \quad (19)$$ the state transition matrix $$\widehat{A}(\delta t) = \begin{bmatrix} A(\delta t) & 0 & 0 \\ 0 & I & 0 \\ 0 & 0 & I \end{bmatrix}, \quad (20)$$ and the process noise matrix $$\widehat{Q}(\delta t) = \begin{bmatrix} Q(\delta t) & 0 & 0 \\ 0 & Q_{b,t}(\delta t) & 0 \\ 0 & 0 & Q_{c,t}(\delta t) \end{bmatrix}. \quad (21)$$ Welch 1997 at Section 3.2.2.

Exhibit D-7

CLAIM 6	Welch 1997
	We then follow steps (b)-(h) from the original algorithm, making the appropriate substitutions of (18)-(21), and noting that the measurement and Jacobian functions used in step (c) have become $\vec{h}_\sigma(\overline{x}(t))$ and $H_\sigma(\overline{x}(t))$ because the estimates of parameters $\vec{b}_t$ and $\vec{c}_t$ ($\hat{x}_{b,t}$ and $\hat{x}_{c,t}$) are now contained in the augmented state vector $\overline{x}$ per (18). After step (h) we finish by extracting and saving the device filter portions of the augmented state vector and error covariance matrix $$\begin{aligned} \hat{x}_{b,t}(t) &= \widehat{x}(t)[i \dots j] \\ P_{b,t}(t) &= \widehat{P}(t)[i \dots j, i \dots j] \\ \hat{x}_{c,t}(t) &= \widehat{x}(t)[k \dots l] \\ P_{c,t}(t) &= \widehat{P}(t)[k \dots l, k \dots l] \end{aligned} \qquad (22)$$ where $$\begin{aligned} i &= n+1 \\ j &= n+n_b \\ k &= n+n_b+1 \\ l &= n+n_b+n_c \end{aligned}$$ and n, n_b, and n_c are the dimensions of the state vectors for the main tracker filter, the source filter, and the sensor filter (respectively). We leave the main tracker filter state vector and error covariance matrix in their augmented counterparts, while we swap the device filter components in and out with each estimate. The result is that individual device filters are updated less frequently than the main tracker filter. The more a device is used, the more it is calibrated. If a device is never used, it is never calibrated. Welch 1997 at Section 3.2.2.

Exhibit D-7

CLAIM 6	Welch 1997
	With respect to added time complexity, the computations can again be optimized to eliminate operations on matrix and vector elements that are known to be zero: those places mentioned in section 3.1, and see (19)-(21). Also note that the size of and thus time for the matrix inversion in (13) has not changed. With respect to added space complexity, the autocalibration method requires storing a separate state vector and covariance matrix for each device—a fixed amount of (generally small) space per device. For example, consider autocalibrating the beacon (LED) positions for an optical tracking system with 3,000 beacons. For each beacon one would need 3 words for the beacon state (its 3D position), $3 \times 3 = 9$ words for the noise covariance matrix, and $3 \times 3 = 9$ words for the error covariance matrix. Assuming 8 bytes per word, this is only $3{,}000 \times 8 \times (3 + 9 + 9) = 504{,}000$ bytes. Welch 1997 at Section 3.2.2. **3.2.3 Discussion** The ability to simultaneously estimate two dependent sets of unknowns (the target and device states) is made possible by several factors. First, the dynamics of the two sets are very different as would be reflected in the process noise matrices. We assume the target is undergoing some random (constant) acceleration, reflected in the noise parameter η of $Q(\delta t)$ in (6). Conversely, we assume the device parameters are constant, and so the elements of $Q_{\pi}(\delta t)$ for a source or sensor simply reflect any allowed variances in the corresponding parameters: usually zero or extremely small. In addition, while the target is expected to be moving, the filter expects the motion between any two estimations to closely correspond to the velocity estimates in the state (3). If the tracker estimate rate is high enough, poorly estimated device parameters will result in what appears to be almost instantaneous target motion. The increased rate of the SCAAT method allows such motion to be recognized as unlikely, and attributed to poorly estimated device parameters. Welch 1997 at Section 3.2.3 3.3 Stability Because the SCAAT method uses individual measurements with insufficient information, one might be concerned about the potential for instability or divergence. A linear system is said to be stable if its response to any input

CLAIM 6	Welch 1997
	tends to a finite steady value after the input is removed [24]. For the Kalman filter in general this is certainly not a new concern, and there are standard requirements and corresponding tests that ensure or detect stability (see [18], p. 132): a. The filter must be uniformly completely observable, b. the dynamic and measurement noise matrices in equations (6) and (9) must be bounded from above and below, and c. the dynamic behavior represented by in equation (2) must be bounded from above. As it turns out, these conditions and their standard tests are equally applicable to a SCAAT implementation. For the SCAAT method the conditions mean that the user dynamics between estimates must be bounded, the measurement noise must be bounded, one must incorporate a sufficient set of non-degenerate constraints over time. In particular, the constraints must be incorporated in less than 1/2 the time of the user motion time-constant in order to avoid tracking an alias of the true motion. In general these conditions are easily met for systems and circumstances that would otherwise be stable with a multiple-constraint implementation. A complete stability analysis is beyond the scope of this paper, and is presented in [47]. Welch 1997 at Section 3.3. [47] Greg Welch, 1996. "SCAAT: Incremental Tracking with Incomplete Information," University of North Carolina at Chapel Hill, doctoral dissertation, TR 96-051. Welch 1997 at References. *See* Disclosures with respect to Claim 1, *supra*; *see also* Defendants' Invalidity Contentions for further discussion.

E. DEPENDENT CLAIM 7

CLAIM 7	Welch 1997
[7] The method of claim 6 wherein the configuration information for the one	At least under Plaintiffs' apparent infringement theory, Welch 1997 discloses, either expressly or inherently, the method of claim 6 wherein the configuration information for the one or more sensing elements fixed to the object includes information related to position or orientation of said sensing elements relative to the object. In the

Exhibit D-7

CLAIM 7	Welch 1997
or more sensing elements fixed to the object includes information related to position or orientation of said sensing elements relative to the object.	alternative, this element would be obvious over Welch 1997 in light of the other references disclosed in Defendants' Invalidity Contentions and/or the knowledge of one of ordinary skill in the art. *See, e.g.*: **Knowledge about source and sensor imperfections can be used to improve the accuracy of tracking systems.** While intrinsic sensor parameters can often be determined off-line, e.g. by the manufacturer, this is generally not the case for extrinsic parameters. **For example it can be difficult to determine the exact geometric relationship between the various sensors** of a hybrid system. **Consider that the coordinate system of a magnetic sensor is located at some unknown location inside the sensor unit. Similarly the precise geometric relationship between visible landmarks used in a vision-based system is often difficult to determine.** Even worse, landmark positions can change over time as, for example, a patient's skin deforms with pressure from an ultrasound probe. In general, goals such as flexibility, ease of use, and lower cost, make the notion of self-calibration or autocalibration attractive. The general idea for autocalibration is not new. See for example [19,45]. However, because the SCAAT method isolates the measurements provided by each sensor or modality, the method provides a new and elegant means to autocalibrate concurrently while tracking. Because the SCAAT method isolates the individual measurements, or measurement dimensions, individual source and sensor imperfections are more easily identified and dealt with. Furthermore, because the simultaneity assumption is avoided, the motion restrictions discussed in section 2.1 would be removed, and autocalibration could be performed while concurrently tracking a target. The isolation enforced by the SCAAT approach can improve results even if the constraints are obtained simultaneously through multidimensional measurements. An intuitive explanation is that if the elements (dimensions) are corrupted by independent noise, then incorporating the elements independently can offer improved filtering over a batch or ensemble estimation scheme. Welch 1997 at Sec. 2.2

CLAIM 7	Welch 1997
	2.3 Temporal Improvements Per Shannon's sampling theorem [24] the measurement or *sampling* frequency should be at least twice the true target motion bandwidth, or an estimator may track an alias of the true motion. Given that common arm and head motion bandwidth specifications range from 2 to 20 Hz [13,14,36], the *sampling* rate should ideally be greater than 40 Hz. Furthermore, the *estimate* rate should be as high as possible so that normally-distributed white estimate error can be discriminated from any non-white error that might be observed during times of significant target dynamics, and so estimates will always reflect the most recent user motion. In addition to increasing the estimate rate, we want to reduce the latency associated with generating an improved estimate, thus reducing the overall latency between target motion and visual feedback in virtual environment systems [34]. If too high, such latency can impair adaptation and the illusion of presence [22], and can cause motion discomfort or sickness. Increased latency also contributes to problems with head-mounted display registration [23] and with motion prediction [4,15,29]. Finally, post-rendering Welch 1997 at Section 2.3.

Exhibit D-7

CLAIM 7	Welch 1997
	image deflection techniques are sometimes employed in an attempt to address latency variability in the rendering pipeline [32,39]. Such methods are most effective when they have access to (or generate) accurate motion predictions and low-latency tracker updates. With accurate prediction the best possible position and orientation information can be used to render a preliminary image. With fast tracker updates there is higher probability that when the preliminary image is ready for final deflection, recent user motion has been detected and incorporated into the deflection. With these requirements in mind, let us examine the effect of the measurements on the estimate latency and rate. Let t_m be the time needed to determine one constraint, e.g. to measure a sensor or extract a scene landmark, let N be the number of (sequential) constraints used to compute a complete estimate, and let t_c be the time needed to actually compute that estimate. Then the estimate latency t_e and rate r_e are $t_e = Nt_m + t_c$, $r_e = \frac{1}{t_e} = \frac{1}{Nt_m + t_c}$. (1) Welch 1997 at Section 2.3.

Exhibit D-7

CLAIM 7	Welch 1997
	As the number of constraints N increases, equation (1) shows how the estimate latency and rate increase and decrease respectively. For example the Polhemus Fastrak, which uses the SPASYN (*Space Synchro*) method for determining relative position and orientation, employs $N = 3$ sequential electromagnetic excitations and measurements per estimate [25,27,37], the original University of North Carolina (UNC) optoelectronic tracking system sequentially observed $10 \leq N \leq 20$ beacons per estimate [3,44], and the current UNC hybrid landmark-magnetic tracking system extracts (from a camera image) and then incorporates $N = 4$ landmarks per update. The SCAAT method seeks to improve the latencies and data rates of such systems by updating the current estimate with each new (individual) constraint, i.e. by fixing N at 1. In other words, it increases the estimate rate to approximately the rate that individual constraints can be obtained and likewise decreases the estimate latency to approximately the time required to obtain a single constraint, e.g. to perform a single measurement of a single sensor, or to extract a single landmark. Figure 2 illustrates the increased data rate with a timing diagram that compares the SPASYN (Polhemus Navigation Systems) magnetic position and orientation tracking system with a hypothetical SCAAT implementation. In contrast to the SPASYN system, a SCAAT implementation would generate a new estimate after sensing each *individual* excitation vector rather than waiting for a complete pattern. Welch 1997 at Section 2.3.

Exhibit D-7

CLAIM 7	Welch 1997
	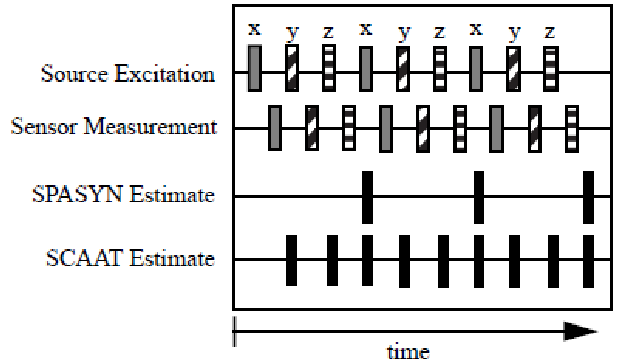 Figure 2: A timing diagram comparing the SPASYN (Polhemus Navigation Systems) magnetic position and orientation tracking system with a hypothetical SCAAT implementation. Welch 1997 at Figure 2. **3.1 Tracking** **3.1.1 Main Tracker Filter** The use of a Kalman filter requires a mathematical (state-space) model for the dynamics of the process to be estimated, the target motion in this case. While several possible dynamic models and associated state configurations are possible, we have found a simple *position-velocity* model to suffice for the dynamics of our applications. In fact we use this same form of model, with different parameters, for all six of the position and orientation components $(x, y, z, \phi, \theta, \psi)$. Discussion of some other potential models and the associated trade-offs can be found in [7] pp. 415-420. Because our implementation is discrete with inter sample time δt we model the target's dynamic motion with the following linear difference equation: $\vec{x}(t+\delta t) = A(\delta t)\vec{x}(t) + \vec{w}(\delta t)$. (2)

CLAIM 7	Welch 1997
	Welch 1997 at Section 3.1. In the standard model corresponding to equation (2), the n dimensional Kalman filter *state vector* $\vec{x}(t)$ would completely describe the target position and orientation at any time t. In practice we use a method similar to [2,6] and maintain the complete target orientation externally to the Kalman filter in order to avoid the nonlinearities associated with orientation computations. In the internal state vector $\vec{x}(t)$ we maintain the target position as the Cartesian coordinates (x, y, z), and the *incremental* orientation as small rotations (ϕ, θ, ψ) about the (x, y, z) axis. Externally we maintain the target orientation as the *external quaternion* $\vec{\alpha} = (\alpha_w, (\alpha_x, \alpha_y, \alpha_z))$. (See [9] for discussion of quaternions.) At each filter update step, the incremental orientations (ϕ, θ, ψ) are factored into the external quaternion $\vec{\alpha}$, and then zeroed as shown below. Thus the incremental orientations are linearized for the EKF, centered about zero. We maintain the derivatives of the target position and orientation internally, in the state vector $\vec{x}(t)$. We maintain the angular velocities internally because the angular velocities behave like orthogonal vectors and do not exhibit the nonlinearities of the angles themselves. The target state is then represented by the $n = 12$ element internal state vector $$\vec{x} = \begin{bmatrix} x & y & z & \dot{x} & \dot{y} & \dot{z} & \phi & \theta & \psi & \dot{\phi} & \dot{\theta} & \dot{\psi} \end{bmatrix}^T \quad (3)$$ and the four-element external orientation quaternion $$\vec{\alpha} = (\alpha_w, (\alpha_x, \alpha_y, \alpha_z)), \quad (4)$$ where the time designations have been omitted for clarity. Welch 1997 at Section 3.1.1.

Exhibit D-7

CLAIM 7	Welch 1997
	The $n \times n$ *state transition matrix* $A(\delta t)$ in (2) projects the state forward from time t to time $t + \delta t$. For our linear model, the matrix implements the relationships $$\begin{aligned} x(t+\delta t) &= x(t) + \dot{x}(t)\delta t \\ \dot{x}(t+\delta t) &= \dot{x}(t) \end{aligned} \quad (5)$$ and likewise for the remaining elements of (3). The $n \times 1$ *process noise vector* $\vec{w}(\delta t)$ in (2) is a normally-distributed zero-mean sequence that represents the uncertainty in the target state over any time interval δt. The corresponding $n \times n$ *process noise covariance matrix* is given by $$E\{\vec{w}(\delta t)\vec{w}^T(\delta t + \varepsilon)\} = \begin{cases} Q(\delta t), & \varepsilon = 0 \\ 0, & \varepsilon \neq 0 \end{cases} . \quad (6)$$ Because our implementation is discrete with inter sample time δt, we can use the transfer function method illustrated by [7] pp. 221-222 to compute a *sampled* process noise covariance matrix. (Because the associated random processes are presumed to be time stationary, we present the process noise covariance matrix as a function of the inter-sample duration δt only.) The non-zero elements of $Q(\delta t)$ are given by $$\begin{aligned} Q(\delta t)[i,i] &= \vec{\eta}[i]\frac{(\delta t)^3}{3} \\ Q(\delta t)[i,j] = Q(\delta t)[j,i] &= \vec{\eta}[i]\frac{(\delta t)^2}{2} \\ Q(\delta t)[j,j] &= \vec{\eta}[i](\delta t) \end{aligned} \quad (7)$$ for each pair $$(i,j) \in \{(x,\dot{x}), (y,\dot{y}), (z,\dot{z}), (\phi,\dot{\phi}), (\theta,\dot{\theta}), (\psi,\dot{\psi})\}.$$ Welch 1997 at Section 3.1.1.

Exhibit D-7

CLAIM 7	Welch 1997
	The $\vec{\eta}[i]$ in (7) are the *correlation kernels* of the (assumed constant) noise sources presumed to be driving the dynamic model. We determined a set of values using Powell's method, and then used these in both simulation and our real implementation. The values can be "tuned" for different dynamics, though we have found that the tracker works well over a broad range of values. The use of a Kalman filter requires not only a dynamic model as described above, but also a *measurement model* for each available type of measurement. The measurement model is used to predict the ideal noise-free response of each sensor and source pair, given the filter's current estimate of the target state as in equations (3) and (4). *It is the nature of the measurement models and indeed the actual sensor measurements that distinguishes a SCAAT Kalman filter from a well-constrained one.* For each sensor *type* σ we define the $m_\sigma \times 1$ *measurement vector* $\vec{z}_\sigma(t)$ and corresponding *measurement function* $\vec{h}_\sigma(\bullet)$ such that $$\vec{z}_{\sigma,t} = \vec{h}_\sigma(\vec{x}(t), \vec{b}_t, \vec{c}_t) + \vec{v}_\sigma(t)\ . \quad (8)$$ Note that in the "purest" SCAAT implementation $m_\sigma = 1$ and the measurements are incorporated as single scalar values. However if it is not possible or necessary to isolate the measurements, e.g. to perform autocalibration, then multi-dimensional measurements can be incorporated also. Guidelines presented in [47] lead to the following heuristic for choosing the SCAAT Kalman filter measurement elements (constraints): *During each SCAAT Kalman filter measurement update one should observe a single sensor and source pair only.* For example, to incorporate magnetic tracker data as an end-user, $m_\sigma = 7$ for the three position and four orientation (quaternion) Welch 1997 at Section 3.1.1.

Exhibit D-7

CLAIM 7	Welch 1997
	elements, while if the manufacturer were to use the SCAAT implementation, $m_\sigma = 3$ for each 3-axis electromagnetic response to a single excitation. For an image-based landmark tracker such as [41] the measurement function would, given estimates of the camera pose and a single landmark location, transform the landmark into camera space and then project it onto the camera image plane. In this case $m_\sigma = 2$ for the 2D image coordinates of the landmark. The $m_\sigma \times 1$ *measurement noise vector* $\vec{v}_\sigma(t)$ in (8) is a normally-distributed zero-mean sequence that represents any random error (e.g. electrical noise) in the measurement. This parameter can be determined from component design specifications, and (or) confirmed by off-line measurement. For our simulations we did both. The corresponding $m_\sigma \times m_\sigma$ *measurement noise covariance matrix* is given by $$E\{\vec{v}_\sigma(t)\vec{v}_\sigma^T(t+\varepsilon)\} = \begin{cases} R_\sigma(t), & \varepsilon = 0 \\ 0, & \varepsilon \neq 0 \end{cases}. \quad (9)$$ For each measurement function $\vec{h}_\sigma(\bullet)$ we determine the corresponding Jacobian function $$H_\sigma(\hat{x}(t), \vec{b}_t, \vec{c}_t)[i, j] \equiv \frac{\partial}{\partial \hat{x}[j]} \vec{h}_\sigma(\hat{x}(t), \vec{b}_t, \vec{c}_t)[i], \quad (10)$$ where $1 \leq i \leq m_\sigma$ and $1 \leq j \leq n$. Finally, we note the use of the standard (Kalman filter) $n \times n$ *error covariance matrix* $P(t)$ which maintains the covariance of the error in the estimated state. Welch 1997 at Section 3.1.1.

Exhibit D-7

CLAIM 7	Welch 1997
	3.2 Autocalibration The method we use for autocalibration involves *augmenting* the *main tracker filter* presented in section 3.1 to effectively implement a distinct *device filter*, a Kalman filter, for each source or sensor to be calibrated. (We use the word "device" here to include for example scene landmarks which can be thought of as passive sources, and cameras which are indeed sensors.) In general, any constant device-related parameters used by a measurement function $\vec{h}_\sigma(\bullet)$ from (8) are candidates for this autocalibration method. We assume that the parameters to be estimated are contained in the device parameter vectors $\vec{b}_t$ and $\vec{c}_t$, and we also present the case where both the source and sensor are to be calibrated since omission of one or the other is trivial. We note the following new convention. $\widehat{\alpha}$ = augmented matrix/vector (wide hat) Welch 1997 at Section 3.2 **3.2.3 Discussion** The ability to simultaneously estimate two dependent sets of unknowns (the target and device states) is made possible by several factors. First, the dynamics of the two sets are very different as would be reflected in the process noise matrices. We assume the target is undergoing some random (constant) acceleration, reflected in the noise parameter η of $Q(\delta t)$ in (6). Conversely, we assume the device parameters are constant, and so the elements of $Q_\pi(\delta t)$ for a source or sensor simply reflect any allowed variances in the corresponding parameters: usually zero or extremely small. In addition, while the target is expected to be moving, the filter expects the motion between any two estimations to closely correspond to the velocity estimates in the state (3). If the tracker estimate rate is high enough, poorly estimated device parameters will result in what appears to be almost instantaneous target motion. The increased rate of the SCAAT method allows such motion to be recognized as unlikely, and attributed to poorly estimated device parameters. Welch 1997 at Section 3.2.3

Exhibit D-7

CLAIM 7	Welch 1997
	3.3 Stability Because the SCAAT method uses individual measurements with insufficient information, one might be concerned about the potential for instability or divergence. A linear system is said to be stable if its response to any input tends to a finite steady value after the input is removed [24]. For the Kalman filter in general this is certainly not a new concern, and there are standard requirements and corresponding tests that ensure or detect stability (see [18], p. 132): a. The filter must be uniformly completely observable, b. the dynamic and measurement noise matrices in equations (6) and (9) must be bounded from above and below, and c. the dynamic behavior represented by in equation (2) must be bounded from above. As it turns out, these conditions and their standard tests are equally applicable to a SCAAT implementation. For the SCAAT method the conditions mean that the user dynamics between estimates must be bounded, the measurement noise must be bounded, one must incorporate a sufficient set of non-degenerate constraints over time. In particular, the constraints must be incorporated in less than 1/2 the time of the user motion time-constant in order to avoid tracking an alias of the true motion. In general these conditions are easily met for systems and circumstances that would otherwise be stable with a multiple-constraint implementation. A complete stability analysis is beyond the scope of this paper, and is presented in [47]. Welch 1997 at Section 3.3. [47] Greg Welch, 1996. "SCAAT: Incremental Tracking with Incomplete Information," University of North Carolina at Chapel Hill, doctoral dissertation, TR 96-051. Welch 1997 at References. *See* Disclosures with respect to Claim 6, *supra*; *see also* Defendants' Invalidity Contentions for further discussion.

Exhibit D-7

F. DEPENDENT CLAIM 8

CLAIM 8	Welch 1997
[8] The method of claim 6 wherein the configuration information for the one or more sensing elements fixed to the object includes operational parameters for the one or more sensing elements.	At least under Plaintiffs' apparent infringement theory, Welch 1997 discloses, either expressly or inherently, the method of claim 6 wherein the configuration information for the one or more sensing elements fixed to the object includes operational parameters for the one or more sensing elements. In the alternative, this element would be obvious over Welch 1997 in light of the other references disclosed in Defendants' Invalidity Contentions and/or the knowledge of one of ordinary skill in the art. *See, e.g.*: **3.1 Tracking** **3.1.1 Main Tracker Filter** The use of a Kalman filter requires a mathematical (state-space) model for the dynamics of the process to be estimated, the target motion in this case. While several possible dynamic models and associated state configurations are possible, we have found a simple *position-velocity* model to suffice for the dynamics of our applications. In fact we use this same form of model, with different parameters, for all six of the position and orientation components $(x, y, z, \phi, \theta, \psi)$. Discussion of some other potential models and the associated trade-offs can be found in [7] pp. 415-420. Because our implementation is discrete with inter sample time δt we model the target's dynamic motion with the following linear difference equation: $\vec{x}(t+\delta t) = A(\delta t)\vec{x}(t) + \vec{w}(\delta t)$. (2) Welch 1997 at Section 3.1.

Exhibit D-7

CLAIM 8	Welch 1997
	In the standard model corresponding to equation (2), the n dimensional Kalman filter *state vector* $\vec{x}(t)$ would completely describe the target position and orientation at any time t. In practice we use a method similar to [2,6] and maintain the complete target orientation externally to the Kalman filter in order to avoid the nonlinearities associated with orientation computations. In the internal state vector $\vec{x}(t)$ we maintain the target position as the Cartesian coordinates (x, y, z), and the *incremental* orientation as small rotations (ϕ, θ, ψ) about the (x, y, z) axis. Externally we maintain the target orientation as the *external quaternion* $\vec{\alpha} = (\alpha_w, (\alpha_x, \alpha_y, \alpha_z))$. (See [9] for discussion of quaternions.) At each filter update step, the incremental orientations (ϕ, θ, ψ) are factored into the external quaternion $\vec{\alpha}$, and then zeroed as shown below. Thus the incremental orientations are linearized for the EKF, centered about zero. We maintain the derivatives of the target position and orientation internally, in the state vector $\vec{x}(t)$. We maintain the angular velocities internally because the angular velocities behave like orthogonal vectors and do not exhibit the nonlinearities of the angles themselves. The target state is then represented by the $n = 12$ element internal state vector $$\vec{x} = \begin{bmatrix} x & y & z & \dot{x} & \dot{y} & \dot{z} & \phi & \theta & \psi & \dot{\phi} & \dot{\theta} & \dot{\psi} \end{bmatrix}^T \quad (3)$$ and the four-element external orientation quaternion $$\vec{\alpha} = (\alpha_w, (\alpha_x, \alpha_y, \alpha_z)), \quad (4)$$ where the time designations have been omitted for clarity. Welch 1997 at Section 3.1.1.

Exhibit D-7

CLAIM 8	Welch 1997
	The $n \times n$ *state transition matrix* $A(\delta t)$ in (2) projects the state forward from time t to time $t + \delta t$. For our linear model, the matrix implements the relationships $$\begin{aligned} x(t+\delta t) &= x(t) + \dot{x}(t)\delta t \\ \dot{x}(t+\delta t) &= \dot{x}(t) \end{aligned} \quad (5)$$ and likewise for the remaining elements of (3). The $n \times 1$ *process noise vector* $\vec{w}(\delta t)$ in (2) is a normally-distributed zero-mean sequence that represents the uncertainty in the target state over any time interval δt. The corresponding $n \times n$ *process noise covariance matrix* is given by $$E\{\vec{w}(\delta t)\vec{w}^T(\delta t + \varepsilon)\} = \begin{cases} Q(\delta t), & \varepsilon = 0 \\ 0, & \varepsilon \neq 0 \end{cases}. \quad (6)$$ Because our implementation is discrete with inter sample time δt, we can use the transfer function method illustrated by [7] pp. 221-222 to compute a *sampled* process noise covariance matrix. (Because the associated random processes are presumed to be time stationary, we present the process noise covariance matrix as a function of the inter-sample duration δt only.) The non-zero elements of $Q(\delta t)$ are given by $$\begin{aligned} Q(\delta t)[i,i] &= \vec{\eta}[i]\frac{(\delta t)^3}{3} \\ Q(\delta t)[i,j] = Q(\delta t)[j,i] &= \vec{\eta}[i]\frac{(\delta t)^2}{2} \\ Q(\delta t)[j,j] &= \vec{\eta}[i](\delta t) \end{aligned} \quad (7)$$ for each pair $$(i,j) \in \{(x,\dot{x}), (y,\dot{y}), (z,\dot{z}), (\phi,\dot{\phi}), (\theta,\dot{\theta}), (\psi,\dot{\psi})\}.$$ Welch 1997 at Section 3.1.1.

Exhibit D-7

CLAIM 8	Welch 1997
	The $\vec{\eta}[i]$ in (7) are the *correlation kernels* of the (assumed constant) noise sources presumed to be driving the dynamic model. We determined a set of values using Powell's method, and then used these in both simulation and our real implementation. The values can be "tuned" for different dynamics, though we have found that the tracker works well over a broad range of values. The use of a Kalman filter requires not only a dynamic model as described above, but also a *measurement model* for each available type of measurement. The measurement model is used to predict the ideal noise-free response of each sensor and source pair, given the filter's current estimate of the target state as in equations (3) and (4). *It is the nature of the measurement models and indeed the actual sensor measurements that distinguishes a SCAAT Kalman filter from a well-constrained one.* For each sensor *type* σ we define the $m_\sigma \times 1$ *measurement vector* $\vec{z}_\sigma(t)$ and corresponding *measurement function* $\vec{h}_\sigma(\bullet)$ such that $$\vec{z}_{\sigma,t} = \vec{h}_\sigma(\vec{x}(t), \vec{b}_t, \vec{c}_t) + \vec{v}_\sigma(t) . \qquad (8)$$ Note that in the "purest" SCAAT implementation $m_\sigma = 1$ and the measurements are incorporated as single scalar values. However if it is not possible or necessary to isolate the measurements, e.g. to perform autocalibration, then multi-dimensional measurements can be incorporated also. Guidelines presented in [47] lead to the following heuristic for choosing the SCAAT Kalman filter measurement elements (constraints): *During each SCAAT Kalman filter measurement update one should observe a single sensor and source pair only.* For example, to incorporate magnetic tracker data as an end-user, $m_\sigma = 7$ for the three position and four orientation (quaternion) Welch 1997 at Section 3.1.1.

Exhibit D-7

CLAIM 8	Welch 1997
	elements, while if the manufacturer were to use the SCAAT implementation, $m_\sigma = 3$ for each 3-axis electromagnetic response to a single excitation. For an image-based landmark tracker such as [41] the measurement function would, given estimates of the camera pose and a single landmark location, transform the landmark into camera space and then project it onto the camera image plane. In this case $m_\sigma = 2$ for the 2D image coordinates of the landmark. The $m_\sigma \times 1$ *measurement noise vector* $\vec{v}_\sigma(t)$ in (8) is a normally-distributed zero-mean sequence that represents any random error (e.g. electrical noise) in the measurement. This parameter can be determined from component design specifications, and (or) confirmed by off-line measurement. For our simulations we did both. The corresponding $m_\sigma \times m_\sigma$ *measurement noise covariance matrix* is given by $$E\{\vec{v}_\sigma(t)\vec{v}_\sigma^T(t+\varepsilon)\} = \begin{cases} R_\sigma(t), & \varepsilon = 0 \\ 0, & \varepsilon \neq 0 \end{cases}. \quad (9)$$ For each measurement function $\vec{h}_\sigma(\bullet)$ we determine the corresponding Jacobian function $$H_\sigma(\hat{x}(t), \vec{b}_t, \vec{c}_t)[i, j] \equiv \frac{\partial}{\partial \hat{x}[j]} \vec{h}_\sigma(\hat{x}(t), \vec{b}_t, \vec{c}_t)[i], \quad (10)$$ where $1 \leq i \leq m_\sigma$ and $1 \leq j \leq n$. Finally, we note the use of the standard (Kalman filter) $n \times n$ *error covariance matrix* $P(t)$ which maintains the covariance of the error in the estimated state. Welch 1997 at Section 3.1.1.

Exhibit D-7

CLAIM 8	Welch 1997
	3.1.2 Tracking Algorithm Given an initial state estimate $\hat{x}(0)$ and error covariance estimate $P(0)$, the SCAAT algorithm proceeds similarly to a conventional EKF, cycling through the following steps whenever a discrete measurement $\vec{z}_{\sigma,t}$ from some sensor (type σ) and source becomes available at time t: a. Compute the time δt since the previous estimate. b. Predict the state and error covariance. $\hat{x}^- = A(\delta t)\hat{x}(t-\delta t)$ $P^- = A(\delta t)P(t-\delta t)A^T(\delta t) + Q(\delta t)$ (11) c. Predict the measurement and compute the corresponding Jacobian. $\hat{z} = \vec{h}_\sigma(\hat{x}^-, \vec{b}_t, \vec{c}_t)$ $H = H_\sigma(\hat{x}^-, \vec{b}_t, \vec{c}_t)$ (12) d. Compute the *Kalman gain*. $K = P^- H^T (HP^- H^T + R_\sigma(t))^{-1}$ (13) e. Compute the *residual* between the actual sensor measurement $\vec{z}_{\sigma,t}$ and the predicted measurement from (12). $\overrightarrow{\Delta z} = \vec{z}_{\sigma,t} - \hat{z}$ (14) f. Correct the predicted tracker state estimate and error covariance from (11). $\hat{x}(t) = \hat{x}^- + K\overrightarrow{\Delta z}$ $P(t) = (I - KH)P^-$ (15) Welch 1997 at Section 3.1.2.

Exhibit D-7

CLAIM 8	Welch 1997
	g. Update the external orientation of equation (4) per the change indicated by the (ϕ, θ, ψ) elements of the state. $$\begin{aligned} \Delta\hat{\alpha} &= \text{quaternion}(\hat{x}[\phi], \hat{x}[\theta], \hat{x}[\psi]) \\ \hat{\alpha} &= \hat{\alpha} \otimes \Delta\hat{\alpha} \end{aligned} \quad (16)$$ h. Zero the orientation elements of the state vector. $$\hat{x}[\phi] = \hat{x}[\theta] = \hat{x}[\psi] = 0 \quad (17)$$ The equations (11)-(17) may seem computationally complex, however they can be performed quite efficiently. The computations can be optimized to eliminate operations on matrix and vector elements that are known to be zero. For example, the elements of the Jacobian H in (12) that correspond to the velocities in the state $\hat{x}(t)$ will always be zero. In addition, the matrix inverted in the computation of K in (13) is of rank m_σ (2×2 for our example in section 3.4) which is smaller for a SCAAT filter than for a corresponding conventional EKF implementation. Finally, the increased data rate allows the use of the *small angle approximations* $\sin(\theta) = \theta$ and $\cos(\theta) = 1$ in $\vec{h}_\sigma(\bullet)$ and $H_\sigma(\bullet)$. The total *per estimate* computation time can therefore actually be less than that of a corresponding conventional implementation. (We are able to execute the SCAAT filter computations, with the autocalibration computations discussed in the next section, in approximately 100µs on a 200 MHz PC-compatible computer.) Welch 1997 at Section 3.1.2.

Exhibit D-7

CLAIM 8	Welch 1997
	3.2 Autocalibration The method we use for autocalibration involves *augmenting* the *main tracker filter* presented in section 3.1 to effectively implement a distinct *device filter*, a Kalman filter, for each source or sensor to be calibrated. (We use the word "device" here to include for example scene landmarks which can be thought of as passive sources, and cameras which are indeed sensors.) In general, any constant device-related parameters used by a measurement function $\vec{h}_\sigma(\cdot)$ from (8) are candidates for this autocalibration method. We assume that the parameters to be estimated are contained in the device parameter vectors $\vec{b}_t$ and $\vec{c}_t$, and we also present the case where both the source and sensor are to be calibrated since omission of one or the other is trivial. We note the following new convention. $\widehat{\alpha}$ = augmented matrix/vector (wide hat) Welch 1997 at Section 3.2. **3.2.1 Device Filters** For each device (source, sensor, landmark, etc.) we create a distinct device filter as follows. Let $\vec{\pi}$ represent the corresponding device parameter vector and n_π = length($\vec{\pi}$). a. Allocate an $n_\pi \times 1$ state vector $\hat{x}_\pi$ for the device, initialize with the best *a priori* device parameter estimates, e.g. from design. b. Allocate an $n_\pi \times n_\pi$ noise covariance matrix $Q_\pi(\delta t)$, initialize with the expected parameter variances. c. Allocate an $n_\pi \times n_\pi$ error covariance matrix $P_\pi(t)$, initialize to indicate the level of confidence in the *a priori* device parameter estimates from (a) above. Welch 1997 at Section 3.2.1.

Exhibit D-7

CLAIM 8	Welch 1997
	3.2.2 Revised Tracking Algorithm The algorithm for tracking with concurrent autocalibration is the same as that presented in section 3.1, with the following exceptions. After step (a) in the original algorithm, we form augmented versions of the state vector $\widehat{x}(t-\delta t) = \left[\hat{x}^T(t-\delta t)\ \ \hat{x}^T_{b,t}(t-\delta t)\ \ \hat{x}^T_{c,t}(t-\delta t)\right]^T, \quad (18)$ the error covariance matrix $\widehat{P}(t-\delta t) = \begin{bmatrix} P(t-\delta t) & 0 & 0 \\ 0 & P_{b,t}(t-\delta t) & 0 \\ 0 & 0 & P_{c,t}(t-\delta t) \end{bmatrix}, \quad (19)$ the state transition matrix $\widehat{A}(\delta t) = \begin{bmatrix} A(\delta t) & 0 & 0 \\ 0 & I & 0 \\ 0 & 0 & I \end{bmatrix}, \quad (20)$ and the process noise matrix $\widehat{Q}(\delta t) = \begin{bmatrix} Q(\delta t) & 0 & 0 \\ 0 & Q_{b,t}(\delta t) & 0 \\ 0 & 0 & Q_{c,t}(\delta t) \end{bmatrix}. \quad (21)$ Welch 1997 at Section 3.2.2.

Exhibit D-7

CLAIM 8	Welch 1997
	We then follow steps (b)-(h) from the original algorithm, making the appropriate substitutions of (18)-(21), and noting that the measurement and Jacobian functions used in step (c) have become $\vec{h}_{\sigma}(\widehat{x}(t))$ and $H_{\sigma}(\widehat{x}(t))$ because the estimates of parameters $\vec{b}_t$ and $\vec{c}_t$ ($\hat{x}_{b,t}$ and $\hat{x}_{c,t}$) are now contained in the augmented state vector $\widehat{x}$ per (18). After step (h) we finish by extracting and saving the device filter portions of the augmented state vector and error covariance matrix $$\begin{aligned} \hat{x}_{b,t}(t) &= \widehat{x}(t)[i \ldots j] \\ P_{b,t}(t) &= \widehat{P}(t)[i \ldots j, i \ldots j] \\ \hat{x}_{c,t}(t) &= \widehat{x}(t)[k \ldots l] \\ P_{c,t}(t) &= \widehat{P}(t)[k \ldots l, k \ldots l] \end{aligned} \quad (22)$$ where $$\begin{aligned} i &= n+1 \\ j &= n+n_b \\ k &= n+n_b+1 \\ l &= n+n_b+n_c \end{aligned}$$ and n, n_b, and n_c are the dimensions of the state vectors for the main tracker filter, the source filter, and the sensor filter (respectively). We leave the main tracker filter state vector and error covariance matrix in their augmented counterparts, while we swap the device filter components in and out with each estimate. The result is that individual device filters are updated less frequently than the main tracker filter. The more a device is used, the more it is calibrated. If a device is never used, it is never calibrated. Welch 1997 at Section 3.2.2.

CLAIM 8	Welch 1997
	With respect to added time complexity, the computations can again be optimized to eliminate operations on matrix and vector elements that are known to be zero: those places mentioned in section 3.1, and see (19)-(21). Also note that the size of and thus time for the matrix inversion in (13) has not changed. With respect to added space complexity, the autocalibration method requires storing a separate state vector and covariance matrix for each device—a fixed amount of (generally small) space per device. For example, consider autocalibrating the beacon (LED) positions for an optical tracking system with 3,000 beacons. For each beacon one would need 3 words for the beacon state (its 3D position), $3 \times 3 = 9$ words for the noise covariance matrix, and $3 \times 3 = 9$ words for the error covariance matrix. Assuming 8 bytes per word, this is only $3{,}000 \times 8 \times (3 + 9 + 9) = 504{,}000$ bytes. Welch 1997 at Section 3.2.2. **3.2.3 Discussion** The ability to simultaneously estimate two dependent sets of unknowns (the target and device states) is made possible by several factors. First, the dynamics of the two sets are very different as would be reflected in the process noise matrices. We assume the target is undergoing some random (constant) acceleration, reflected in the noise parameter η of $Q(\delta t)$ in (6). Conversely, we assume the device parameters are constant, and so the elements of $Q_{\pi}(\delta t)$ for a source or sensor simply reflect any allowed variances in the corresponding parameters: usually zero or extremely small. In addition, while the target is expected to be moving, the filter expects the motion between any two estimations to closely correspond to the velocity estimates in the state (3). If the tracker estimate rate is high enough, poorly estimated device parameters will result in what appears to be almost instantaneous target motion. The increased rate of the SCAAT method allows such motion to be recognized as unlikely, and attributed to poorly estimated device parameters. Welch 1997 at Section 3.2.3 *See* Disclosures with respect to Claim 6, *supra*; *see also* Defendants' Invalidity Contentions for further discussion.

Exhibit D-7

G. Dependent Claim 24

Claim 24	Welch 1997
[24] The method of claim 1 wherein updating the state estimate includes applying a Kalman Filter approach.	At least under Plaintiffs' apparent infringement theory, Welch 1997 discloses, either expressly or inherently, the method of claim 1 wherein updating the state estimate includes applying a Kalman Filter approach. In the alternative, this element would be obvious over Welch 1997 in light of the other references disclosed in Defendants' Invalidity Contentions and/or the knowledge of one of ordinary skill in the art. *See, e.g.*:

CLAIM 24	Welch 1997
	2.4 Data Fusion & Hybrid Systems The Kalman filter [26] has been widely used for data fusion. For example in navigation systems [17,30], virtual environment tracking systems [5,12,14], and in 3D scene modeling [20,42]. However the SCAAT method represents a new approach to Kalman filter based *multi-sensor data fusion*. Because constraints are intentionally incorporated one at a time, one can pick and choose which ones to add, and when to add them. This means that information from different sensors or modalities can be woven together in a common, flexible, and expeditious fashion. Furthermore, one can use the approach to ensure that each estimate is computed from the most recently obtained constraint. Consider for a moment the UNC hybrid landmark-magnetic presented at SIGGRAPH 96 [41]. This system uses an off-the-shelf Ascension magnetic tracking system along with a vision-based landmark recognition system to achieve superior synthetic and real image registration for augmented reality assisted medical procedures. The vision-based component attempts to identify and locate multiple known landmarks in a single image before applying a correction to the magnetic readings. A SCAAT implementation would instead identify and locate only one landmark per update, using a new image (frame) each time. Not only would this approach increase the frequency of landmark-based correction (given the necessary image processing) but it would offer the added benefit that unlike the implementation presented in [41], no special processing would be needed for the cases where the number of visible landmarks falls below the number C necessary to determine a complete position and orientation solution. The SCAAT implementation would simply cycle through any available landmarks, one at a time. Even with only one visible landmark the method would continue to operate as usual, using the information provided by the landmark sighting to refine the estimate where possible, while increasing the uncertainty where not. Welch 1997 at Section 2.4.

Exhibit D-7

CLAIM 24	**Welch 1997**
	3 METHOD The SCAAT method employs a *Kalman filter* (KF) in an unusual fashion. The Kalman filter is a mathematical procedure that provides an efficient computational (recursive) method for the least-squares estimation of a linear system. It does so in a *predictor-corrector* fashion, predicting short-term (since the last estimate) changes in the state using a *dynamic model*, and then correcting them with a measurement and a corresponding *measurement model*. The *extended* Kalman filter (EKF) is a variation of the Kalman filter that supports estimation of *nonlinear* systems, e.g. 3D position and orientation tracking systems. A basic introduction to the Kalman filter can be found in Chapter 1 of [31], while a more complete introductory discussion can be found in [40], which also contains some interesting historical narrative. More extensive references can be found in [7,18,24,28,31,46]. The Kalman filter has been employed previously for virtual environment tracking estimation and prediction. For example see [2,5,12,14,42], and most recently [32]. In each of these cases however the filter was applied directly and only to the 6D pose estimates delivered by the off-the-shelf tracker. The SCAAT approach could be applied to either a hybrid system using off-the-shelf and/or custom trackers, or it could be employed by tracker developers to improve the existing systems for the end-user graphics community. Welch 1997 at Section 3. *See* Disclosures with respect to Claim 1, *supra*; *see also* Defendants' Invalidity Contentions for further discussion.

H. DEPENDENT CLAIM 25

CLAIM 25	**Welch 1997**
[25] The method of claim 1 wherein each of	At least under Plaintiffs' apparent infringement theory, Welch 1997 discloses, either expressly or inherently, the method of claim 1 wherein each of said sensing elements comprises at least one of a sensor and a target. In the

Exhibit D-7

CLAIM 25	Welch 1997
said sensing elements comprises at least one of a sensor and a target.	alternative, this element would be obvious over Welch 1997 in light of the other references disclosed in Defendants' Invalidity Contentions and/or the knowledge of one of ordinary skill in the art. *See, e.g.*: **1.2 Landmark Tracking** Consider for example a system in which a single camera is used to observe known scene points to determine the camera position and orientation. In this case, the constraints provided by the observations are multi-dimensional: 2D image coordinates of 3D scene points. Given the internal camera parameters, a set of four known coplanar scene points, and the corresponding image coordinates, the camera position and orientation can be uniquely determined in closed-form [16]. In other words if $N = C = 4$ constraints (2D image points) are used to estimate the camera position and orientation, the system is completely observable. On the other hand, if $N < C$ then there are multiple solutions. For example with only $N = 3$ non-collinear points, there are up to 4 solutions. Even worse, with $N = 2$ or $N = 1$ points, there are infinite combinations of position and orientation that could result in the same camera images. Welch 1997 at Section 1.2.

Exhibit D-7

CLAIM 25	Welch 1997
	In general, for closed-form tracking approaches, a well or over-constrained system with $N \geq C$ is observable, an under-constrained system with $N < C$ is not. Therefore, if the individual observations provide only partial information, i.e. the measurements provide insufficient constraints, then multiple devices or landmarks must be excited and (or) sensed prior to estimating a solution. Sometimes the necessary observations can be obtained simultaneously, and sometimes they can not. Magnetic trackers such as those made by Polhemus and Ascension perform three *sequential* source excitations, each in conjunction with a complete sensor unit observation. And while a camera can indeed observe multiple landmarks simultaneously in a single image, the image processing to identify and locate the individual landmarks must be done sequentially for a single CPU system. If the landmarks can move independently over time, for example if they are artificial marks placed on the skin of an ultrasound patient for the purpose of landmark-based tracking [41], batch processing of the landmarks can reduce the effectiveness of the system. A SCAAT implementation might grab an image, extract a *single* landmark, update the estimates of both the camera *and* landmark positions, and then throw-away the image. In this way estimates are generated faster and with the most recent landmark configurations. Welch 1997 at Section 1.2.

Exhibit D-7

CLAIM 25	Welch 1997
	 Figure 3: The HiBall is shown here with the internal circuitry exposed and the lenses removed. The sensors, which can be seen through the lens openings, are mounted on PC boards that fold-up into the HiBall upon assembly. The mechanical pencil at the bottom conveys an indication of the relative size of the unit. Welch 1997 at Figure 3. We are using the SCAAT approach in the current version of the UNC wide-area optoelectronic tracking system known as the HiBall tracker. T**he HiBall, shown below in Figure 3, incorporates six optical sensors and six lenses with infrared filters into one golf ball sized sensing unit that can be worn on a user's head or hand.** The principal mechanical component of the HiBall, the senor housing unit, was fabricated by researchers at the University of Utah using their modeling environment. Because the HiBall sensors and lenses share a common transparent space in the center of the housing, a single sensor can actually sense light through more than one lens. By making use of all of these views we end up with effectively 26 "cameras". **These cameras are then used to observe ceiling-mounted light-emitting diodes (LEDs) to track the position and orientation of the HiBall.** This inside-looking-out approach was first used with

Exhibit D-7

CLAIM 25	Welch 1997
	the previous UNC optoelectronic tracking system [44] which spanned most of the user's head and weighed approximately ten pounds, not including a backpack containing some electronics. In contrast, the HiBall sensing unit is the size of a golf ball and weighs only five ounces, including the electronics. The combination of reduced weight, smaller packaging, and the new SCAAT algorithm results in a very ergonomic, fast, and accurate system. In this section we present results from both simulations performed during the design and development of the HiBall, and preliminary results from the actual implementation. The simulations are useful because we have control over the "truth" and can perform controlled experiments. The results from the actual implementation serve to demonstrate actual operation and to provide some support for our accuracy and stability claims. Welch 1997 at Sec. 4 With respect to the SCAAT implementation, the tracker *sensors* are the HiBall cameras and the tracker *sources* are the ceiling-mounted 2D array of approximately 3000 electronic beacons (LEDs). The cameras provide a single 2D measurement vector, i.e. a 2D constraint, which is the (u, v) image coordinates of the beacon as seen by the camera. So for this example, $m_\sigma = 2$ and $\hat{z}_\sigma = [u, v]^T$. The measurement function $\hat{h}_\sigma(\bullet)$ transforms the beacon into camera coordinates and then projects it onto the camera's image plane in order to predict the camera response. Welch 1997 at Sec. 4 *See* Disclosures with respect to Claim 1, *supra*; *see also* Defendants' Invalidity Contentions for further discussion.

I. DEPENDENT CLAIM 28

CLAIM 28	Welch 1997
[28] The method of claim 1 wherein the object is selected from a group consisting of a	At least under Plaintiffs' apparent infringement theory, Welch 1997 discloses, either expressly or inherently, the method of claim 1 wherein the object is selected from a group consisting of a vehicle, a robot, a person, a part of a person, a flying object, a floating object, an underwater moving object, an animal, a camera, a sensing apparatus, a helmet, a tool, a piece of sports equipment, a shoe, a boot, an article of clothing, a personal protective equipment,

CLAIM 28	Welch 1997
vehicle, a robot, a person, a part of a person, a flying object, a floating object, an underwater moving object, an animal, a camera, a sensing apparatus, a helmet, a tool, a piece of sports equipment, a shoe, a boot, an article of clothing, a personal protective equipment, a rigid object having a dimension between 1 nanometer to 109 meters.	a rigid object having a dimension between 1 nanometer to 109 meters. In the alternative, this element would be obvious over Welch 1997 in light of the other references disclosed in Defendants' Invalidity Contentions and/or the knowledge of one of ordinary skill in the art. *See* Disclosures with respect to Claim 1, *supra*; *see also* Defendants' Invalidity Contentions for further discussion.

J. DEPENDENT CLAIM 29

CLAIM 29	Welch 1997
[29] The method of claim 1 wherein the state estimate comprises information related to a position or an orientation of the object relative to a reference coordinate frame.	At least under Plaintiffs' apparent infringement theory, Welch 1997 discloses, either expressly or inherently, the method of claim 1 wherein the state estimate comprises information related to a position or an orientation of the object relative to a reference coordinate frame. In the alternative, this element would be obvious over Welch 1997 in light of the other references disclosed in Defendants' Invalidity Contentions and/or the knowledge of one of ordinary skill in the art. *See, e.g.*: At least under Plaintiffs' apparent infringement theory, Welch 1997 discloses, either expressly or inherently, the method of claim 1 wherein the state estimate characterizes configuration information for one or more sensing elements fixed to the object. In the alternative, this element would be obvious over Welch 1997 in light of the

Exhibit D-7

CLAIM 29	Welch 1997
	other references disclosed in Defendants' Invalidity Contentions and/or the knowledge of one of ordinary skill in the art. *See, e.g.*: **3.1 Tracking** **3.1.1 Main Tracker Filter** The use of a Kalman filter requires a mathematical (state-space) model for the dynamics of the process to be estimated, the target motion in this case. While several possible dynamic models and associated state configurations are possible, we have found a simple *position-velocity* model to suffice for the dynamics of our applications. In fact we use this same form of model, with different parameters, for all six of the position and orientation components $(x, y, z, \phi, \theta, \psi)$. Discussion of some other potential models and the associated trade-offs can be found in [7] pp. 415-420. Because our implementation is discrete with inter sample time δt we model the target's dynamic motion with the following linear difference equation: $\vec{x}(t+\delta t) = A(\delta t)\vec{x}(t) + \vec{w}(\delta t)$. (2) Welch 1997 at Section 3.1.

Exhibit D-7

CLAIM 29	Welch 1997
	In the standard model corresponding to equation (2), the n dimensional Kalman filter *state vector* $\vec{x}(t)$ would completely describe the target position and orientation at any time t. In practice we use a method similar to [2,6] and maintain the complete target orientation externally to the Kalman filter in order to avoid the nonlinearities associated with orientation computations. In the internal state vector $\vec{x}(t)$ we maintain the target position as the Cartesian coordinates (x, y, z), and the *incremental* orientation as small rotations (ϕ, θ, ψ) about the (x, y, z) axis. Externally we maintain the target orientation as the *external quaternion* $\vec{\alpha} = (\alpha_w, (\alpha_x, \alpha_y, \alpha_z))$. (See [9] for discussion of quaternions.) At each filter update step, the incremental orientations (ϕ, θ, ψ) are factored into the external quaternion $\vec{\alpha}$, and then zeroed as shown below. Thus the incremental orientations are linearized for the EKF, centered about zero. We maintain the derivatives of the target position and orientation internally, in the state vector $\vec{x}(t)$. We maintain the angular velocities internally because the angular velocities behave like orthogonal vectors and do not exhibit the nonlinearities of the angles themselves. The target state is then represented by the $n = 12$ element internal state vector $$\vec{x} = \left[x\ y\ z\ \dot{x}\ \dot{y}\ \dot{z}\ \phi\ \theta\ \psi\ \dot{\phi}\ \dot{\theta}\ \dot{\psi}\right]^T \quad (3)$$ and the four-element external orientation quaternion $$\vec{\alpha} = (\alpha_w, (\alpha_x, \alpha_y, \alpha_z)), \quad (4)$$ where the time designations have been omitted for clarity. Welch 1997 at Section 3.1.1.

Exhibit D-7

CLAIM 29	Welch 1997
	The $n \times n$ *state transition matrix* $A(\delta t)$ in (2) projects the state forward from time t to time $t + \delta t$. For our linear model, the matrix implements the relationships $$\begin{aligned} x(t+\delta t) &= x(t) + \dot{x}(t)\delta t \\ \dot{x}(t+\delta t) &= \dot{x}(t) \end{aligned} \quad (5)$$ and likewise for the remaining elements of (3). The $n \times 1$ *process noise vector* $\vec{w}(\delta t)$ in (2) is a normally-distributed zero-mean sequence that represents the uncertainty in the target state over any time interval δt. The corresponding $n \times n$ *process noise covariance matrix* is given by $$E\{\vec{w}(\delta t)\vec{w}^T(\delta t + \varepsilon)\} = \begin{cases} Q(\delta t), & \varepsilon = 0 \\ 0, & \varepsilon \neq 0 \end{cases}. \quad (6)$$ Because our implementation is discrete with inter sample time δt, we can use the transfer function method illustrated by [7] pp. 221-222 to compute a *sampled* process noise covariance matrix. (Because the associated random processes are presumed to be time stationary, we present the process noise covariance matrix as a function of the inter-sample duration δt only.) The non-zero elements of $Q(\delta t)$ are given by $$\begin{aligned} Q(\delta t)[i,i] &= \vec{\eta}[i]\frac{(\delta t)^3}{3} \\ Q(\delta t)[i,j] = Q(\delta t)[j,i] &= \vec{\eta}[i]\frac{(\delta t)^2}{2} \\ Q(\delta t)[j,j] &= \vec{\eta}[i](\delta t) \end{aligned} \quad (7)$$ for each pair $$(i,j) \in \{(x,\dot{x}), (y,\dot{y}), (z,\dot{z}), (\phi,\dot{\phi}), (\theta,\dot{\theta}), (\psi,\dot{\psi})\}.$$ Welch 1997 at Section 3.1.1.

Exhibit D-7

CLAIM 29	Welch 1997
	The $\vec{\eta}[i]$ in (7) are the *correlation kernels* of the (assumed constant) noise sources presumed to be driving the dynamic model. We determined a set of values using Powell's method, and then used these in both simulation and our real implementation. The values can be "tuned" for different dynamics, though we have found that the tracker works well over a broad range of values. The use of a Kalman filter requires not only a dynamic model as described above, but also a ***measurement model*** for each available type of measurement. The measurement model is used to predict the ideal noise-free response of each sensor and source pair, given the filter's current estimate of the target state as in equations (3) and (4). *It is the nature of the measurement models and indeed the actual sensor measurements that distinguishes a SCAAT Kalman filter from a well-constrained one.* For each sensor *type* σ we define the $m_\sigma \times 1$ *measurement vector* $\vec{z}_\sigma(t)$ and corresponding *measurement function* $\vec{h}_\sigma(\bullet)$ such that $$\vec{z}_{\sigma,t} = \vec{h}_\sigma(\vec{x}(t), \vec{b}_t, \vec{c}_t) + \vec{v}_\sigma(t). \quad (8)$$ Note that in the "purest" SCAAT implementation $m_\sigma = 1$ and the measurements are incorporated as single scalar values. However if it is not possible or necessary to isolate the measurements, e.g. to perform autocalibration, then multi-dimensional measurements can be incorporated also. Guidelines presented in [47] lead to the following heuristic for choosing the SCAAT Kalman filter measurement elements (constraints): *During each SCAAT Kalman filter measurement update one should observe a single sensor and source pair only.* For example, to incorporate magnetic tracker data as an end-user, $m_\sigma = 7$ for the three position and four orientation (quaternion) Welch 1997 at Section 3.1.1.

CLAIM 29	Welch 1997
	elements, while if the manufacturer were to use the SCAAT implementation, $m_\sigma = 3$ for each 3-axis electromagnetic response to a single excitation. For an image-based landmark tracker such as [41] the measurement function would, given estimates of the camera pose and a single landmark location, transform the landmark into camera space and then project it onto the camera image plane. In this case $m_\sigma = 2$ for the 2D image coordinates of the landmark. The $m_\sigma \times 1$ *measurement noise vector* $\vec{v}_\sigma(t)$ in (8) is a normally-distributed zero-mean sequence that represents any random error (e.g. electrical noise) in the measurement. This parameter can be determined from component design specifications, and (or) confirmed by off-line measurement. For our simulations we did both. The corresponding $m_\sigma \times m_\sigma$ *measurement noise covariance matrix* is given by $$E\{\vec{v}_\sigma(t)\vec{v}_\sigma^T(t+\varepsilon)\} = \begin{cases} R_\sigma(t), & \varepsilon = 0 \\ 0, & \varepsilon \neq 0 \end{cases}. \quad (9)$$ For each measurement function $\vec{h}_\sigma(\bullet)$ we determine the corresponding Jacobian function $$H_\sigma(\hat{x}(t), \vec{b}_t, \vec{c}_t)[i, j] \equiv \frac{\partial}{\partial \hat{x}[j]} \vec{h}_\sigma(\hat{x}(t), \vec{b}_t, \vec{c}_t)[i], \quad (10)$$ where $1 \leq i \leq m_\sigma$ and $1 \leq j \leq n$. Finally, we note the use of the standard (Kalman filter) $n \times n$ *error covariance matrix* $P(t)$ which maintains the covariance of the error in the estimated state. Welch 1997 at Section 3.1.1. *See* Disclosures with respect to Claim 1, *supra*; *see also* Defendants' Invalidity Contentions for further discussion.

K. INDEPENDENT CLAIM 47

CLAIM 47	Welch 1997
[47] A method of using multiple sensors in a	At least under Plaintiffs' apparent infringement theory, Welch 1997 discloses, either expressly or inherently, a method of using multiple sensors in a tracking system comprising: providing an estimation module; coupling one

Exhibit D-7

CLAIM 47	Welch 1997
tracking system comprising: providing an estimation module; coupling one or more sensor modules to the estimation module, each associated with a different set of one or more sensors; configuring the tracking system, including providing configuration information from each of the sensor modules to the estimation module regarding the characteristics of the sensors associated with the sensor module, and configuring the estimation module using the provided configuration information; maintaining estimates of tracking parameters in	or more sensor modules to the estimation module, each associated with a different set of one or more sensors; configuring the tracking system, including providing configuration information from each of the sensor modules to the estimation module regarding the characteristics of the sensors associated with the sensor module, and configuring the estimation module using the provided configuration information; maintaining estimates of tracking parameters in the estimation module, including repeatedly passing data based on the estimates of the tracking parameters from the estimation module to one or more of the sensor modules, receiving from said one or more sensor modules at the estimation module data based on measurements obtained from the associated sensors, and the data passed to the sensor modules, and combining the data received from said one or more sensor modules and the estimates of the tracking parameters in the estimation module to update the tracking parameters.. In the alternative, this element would be obvious over Welch 1997 in light of the other references disclosed in Defendants' Invalidity Contentions and/or the knowledge of one of ordinary skill in the art. *See, e.g.*: **Tracking systems determine the user's pose by measuring signals from low-level hardware sensors.** For reasons of physics and economics, most systems make multiple sequential measurements which are then combined to produce a single tracker report. For example, commercial magnetic trackers using the SPASYN (Space Synchro) system sequentially measure three magnetic vectors and then combine them mathematically to produce a report of the sensor pose. **Our new approach produces tracker reports as each new low-level sensor measurement is made rather than waiting to form a complete collection of observations.** Because single observations under-constrain the mathematical solution, we refer to our approach as single-constraint-at-a-time or SCAAT tracking. **The key is that the single observations provide some information about the user's state, and thus can be used to incrementally improve a previous estimate. We recursively apply this principle, incorporating new sensor data as soon as it is measured**. With this approach we are able to generate estimates more frequently, with less latency, and with improved accuracy. We present results from both an actual implementation, and from extensive simulations. Welch 1997 at Abstract. **The Kalman filter [26] has been widely used for data fusion.** For example in navigation systems [17,30], virtual environment tracking systems [5,12,14], and in 3D scene modeling [20,42]. However the SCAAT method represents a new approach to Kalman filter based multi-sensor data fusion. **Because constraints are intentionally incorporated one at a time, one can pick and choose which ones to add, and when to add**

Exhibit D-7

CLAIM 47	Welch 1997
the estimation module, including repeatedly passing data based on the estimates of the tracking parameters from the estimation module to one or more of the sensor modules, receiving from said one or more sensor modules at the estimation module data based on measurements obtained from the associated sensors, and the data passed to the sensor modules, and combining the data received from said one or more sensor modules and the estimates of the tracking parameters in the estimation module to update the tracking parameters.	**them. This means that information from different sensors or modalities can be woven together in a common, flexible, and expeditious fashion.** Furthermore, one can use the approach to ensure that each estimate is computed from the most recently obtained constraint. Welch 1997 at Section 2.4. Consider for a moment the UNC hybrid landmark-magnetic presented at SIGGRAPH 96 [41]. **This system uses an off-the-shelf Ascension magnetic tracking system along with a vision-based landmark recognition system to achieve superior synthetic and real image registration for augmented reality assisted medical procedures. The vision-based component attempts to identify and locate multiple known landmarks in a single image before applying a correction to the magnetic readings.** A SCAAT implementation would instead identify and locate only one landmark per update, using a new image (frame) each time. Not only would this approach increase the frequency of landmark based correction (given the necessary image processing) but it would offer the added benefit that unlike the implementation presented in [41], no special processing would be needed for the cases where the number of visible landmarks falls below the number *C* necessary to determine a complete position and orientation solution. The SCAAT implementation would simply cycle through any available landmarks, one at a time. Even with only one visible landmark the method would continue to operate as usual, using the information provided by the landmark sighting to refine the estimate where possible, while increasing the uncertainty where not. Welch 1997 at Section 2.4. **The SCAAT method employs a Kalman filter (KF) in an unusual fashion. The Kalman filter is a mathematical procedure that provides an efficient computational (recursive) method for the least-squares estimation of a linear system.** It does so in a predictor-corrector fashion, predicting short-term (since the last estimate) changes in the state using a dynamic model, and then correcting them with a measurement and a corresponding measurement model. The extended Kalman filter (EKF) is a variation of the Kalman filter that supports estimation of nonlinear systems, e.g. 3D position and orientation tracking systems. A basic introduction to the Kalman filter can be found in Chapter 1 of [31], while a more complete introductory discussion can be found in [40], which also contains some interesting historical narrative. More extensive references can be found in [7,18,24,28,31,46]. Welch 1997 at Section 3. **The Kalman filter has been employed previously for virtual environment tracking estimation and prediction.** For example see [2,5,12,14,42], and most recently [32]. In each of these cases however the filter was applied directly and only to the 6D pose estimates delivered by the off-the-shelf tracker. The SCAAT approach

Exhibit D-7

CLAIM 47	Welch 1997
	could be applied to either a hybrid system using off-the shelf and/or custom trackers, or it could be employed by tracker developers to improve the existing systems for the end-user graphics community. Welch 1997 at Section 3. In this section **we describe the method in a manner that does not imply a specific tracking system.** (In section 3.4 we present experimental results of a specific implementation, a SCAAT wide area optoelectronic tracking system.) In section 3.1 we describe the method for tracking, and in section 3.2 we describe one possible method for concurrent autocalibration. Welch 1997 at Section 3. Throughout we use the following conventions. x = scalar (lower case) $\vec{x}$ = general vector (lower case, arrow) indexed as $\vec{x}[r]$ $\hat{x}$ = filter estimate vector (lower case, hat) A = matrix (capital letters) indexed as $A[r, c]$ A^{-1} = matrix inverse I = the identity matrix β^- = matrix/vector *prediction* (super minus) β^T = matrix/vector transpose (super T) α_i = matrix/vector/scalar identifier (subscript) $E\{\bullet\}$ = mathematical expectation Welch 1997 at Section 3.

Exhibit D-7

CLAIM 47	Welch 1997
	3.1 Tracking **3.1.1 Main Tracker Filter** The use of a Kalman filter requires a mathematical (state-space) model for the dynamics of the process to be estimated, the target motion in this case. While several possible dynamic models and associated state configurations are possible, we have found a simple *position-velocity* model to suffice for the dynamics of our applications. In fact we use this same form of model, with different parameters, for all six of the position and orientation components $(x, y, z, \phi, \theta, \psi)$. Discussion of some other potential models and the associated trade-offs can be found in [7] pp. 415-420. Because our implementation is discrete with inter sample time δt we model the target's dynamic motion with the following linear difference equation: $\vec{x}(t+\delta t) = A(\delta t)\vec{x}(t) + \vec{w}(\delta t)$. (2) Welch 1997 at Section 3.1.

Exhibit D-7

CLAIM 47	Welch 1997
	In the standard model corresponding to equation (2), the n dimensional Kalman filter *state vector* $\hat{x}(t)$ would completely describe the target position and orientation at any time t. In practice we use a method similar to [2,6] and maintain the complete target orientation externally to the Kalman filter in order to avoid the nonlinearities associated with orientation computations. In the internal state vector $\hat{x}(t)$ we maintain the target position as the Cartesian coordinates (x, y, z), and the *incremental* orientation as small rotations (ϕ, θ, ψ) about the (x, y, z) axis. Externally we maintain the target orientation as the *external quaternion* $\vec{\alpha} = (\alpha_w, (\alpha_x, \alpha_y, \alpha_z))$. (See [9] for discussion of quaternions.) At each filter update step, the incremental orientations (ϕ, θ, ψ) are factored into the external quaternion $\vec{\alpha}$, and then zeroed as shown below. Thus the incremental orientations are linearized for the EKF, centered about zero. We maintain the derivatives of the target position and orientation internally, in the state vector $\hat{x}(t)$. We maintain the angular velocities internally because the angular velocities behave like orthogonal vectors and do not exhibit the nonlinearities of the angles themselves. The target state is then represented by the $n = 12$ element internal state vector $$\vec{x} = \left[x\ y\ z\ \dot{x}\ \dot{y}\ \dot{z}\ \phi\ \theta\ \psi\ \dot{\phi}\ \dot{\theta}\ \dot{\psi}\right]^T \quad (3)$$ and the four-element external orientation quaternion $$\vec{\alpha} = (\alpha_w, (\alpha_x, \alpha_y, \alpha_z)), \quad (4)$$ where the time designations have been omitted for clarity. Welch 1997 at Section 3.1.1.

Exhibit D-7

CLAIM 47	Welch 1997
	The $n \times n$ *state transition matrix* $A(\delta t)$ in (2) projects the state forward from time t to time $t + \delta t$. For our linear model, the matrix implements the relationships $$\begin{aligned} x(t+\delta t) &= x(t) + \dot{x}(t)\delta t \\ \dot{x}(t+\delta t) &= \dot{x}(t) \end{aligned} \qquad (5)$$ and likewise for the remaining elements of (3). The $n \times 1$ *process noise vector* $\vec{w}(\delta t)$ in (2) is a normally-distributed zero-mean sequence that represents the uncertainty in the target state over any time interval δt. The corresponding $n \times n$ *process noise covariance matrix* is given by $$E\{\vec{w}(\delta t)\vec{w}^T(\delta t + \varepsilon)\} = \begin{cases} Q(\delta t), & \varepsilon = 0 \\ 0, & \varepsilon \neq 0 \end{cases}. \qquad (6)$$ Because our implementation is discrete with inter sample time δt, we can use the transfer function method illustrated by [7] pp. 221-222 to compute a *sampled* process noise covariance matrix. (Because the associated random processes are presumed to be time stationary, we present the process noise covariance matrix as a function of the inter-sample duration δt only.) The non-zero elements of $Q(\delta t)$ are given by $$\begin{aligned} Q(\delta t)[i,i] &= \vec{\eta}[i]\frac{(\delta t)^3}{3} \\ Q(\delta t)[i,j] = Q(\delta t)[j,i] &= \vec{\eta}[i]\frac{(\delta t)^2}{2} \\ Q(\delta t)[j,j] &= \vec{\eta}[i](\delta t) \end{aligned} \qquad (7)$$ for each pair $$(i,j) \in \{(x,\dot{x}), (y,\dot{y}), (z,\dot{z}), (\phi,\dot{\phi}), (\theta,\dot{\theta}), (\psi,\dot{\psi})\}.$$ Welch 1997 at Section 3.1.1.

Exhibit D-7

CLAIM 47	Welch 1997
	The $\vec{\eta}[i]$ in (7) are the *correlation kernels* of the (assumed constant) noise sources presumed to be driving the dynamic model. We determined a set of values using Powell's method, and then used these in both simulation and our real implementation. The values can be "tuned" for different dynamics, though we have found that the tracker works well over a broad range of values. The use of a Kalman filter requires not only a dynamic model as described above, but also a *measurement model* for each available type of measurement. The measurement model is used to predict the ideal noise-free response of each sensor and source pair, given the filter's current estimate of the target state as in equations (3) and (4). *It is the nature of the measurement models and indeed the actual sensor measurements that distinguishes a SCAAT Kalman filter from a well-constrained one.* For each sensor *type* σ we define the $m_\sigma \times 1$ *measurement vector* $\vec{z}_\sigma(t)$ and corresponding *measurement function* $\vec{h}_\sigma(\bullet)$ such that $$\vec{z}_{\sigma,t} = \vec{h}_\sigma(\vec{x}(t), \vec{b}_t, \vec{c}_t) + \vec{v}_\sigma(t) . \quad (8)$$ Note that in the "purest" SCAAT implementation $m_\sigma = 1$ and the measurements are incorporated as single scalar values. However if it is not possible or necessary to isolate the measurements, e.g. to perform autocalibration, then multi-dimensional measurements can be incorporated also. Guidelines presented in [47] lead to the following heuristic for choosing the SCAAT Kalman filter measurement elements (constraints): *During each SCAAT Kalman filter measurement update one should observe a single sensor and source pair only.* For example, to incorporate magnetic tracker data as an end-user, $m_\sigma = 7$ for the three position and four orientation (quaternion) Welch 1997 at Section 3.1.1.

Exhibit D-7

CLAIM 47	Welch 1997
	elements, while if the manufacturer were to use the SCAAT implementation, $m_\sigma = 3$ for each 3-axis electromagnetic response to a single excitation. For an image-based landmark tracker such as [41] the measurement function would, given estimates of the camera pose and a single landmark location, transform the landmark into camera space and then project it onto the camera image plane. In this case $m_\sigma = 2$ for the 2D image coordinates of the landmark. The $m_\sigma \times 1$ *measurement noise vector* $\vec{v}_\sigma(t)$ in (8) is a normally-distributed zero-mean sequence that represents any random error (e.g. electrical noise) in the measurement. This parameter can be determined from component design specifications, and (or) confirmed by off-line measurement. For our simulations we did both. The corresponding $m_\sigma \times m_\sigma$ *measurement noise covariance matrix* is given by $$E\{\vec{v}_\sigma(t)\vec{v}_\sigma^T(t+\varepsilon)\} = \begin{cases} R_\sigma(t), & \varepsilon = 0 \\ 0, & \varepsilon \neq 0 \end{cases}. \quad (9)$$ For each measurement function $\vec{h}_\sigma(\bullet)$ we determine the corresponding Jacobian function $$H_\sigma(\vec{x}(t), \vec{b}_t, \vec{c}_t)[i, j] \equiv \frac{\partial}{\partial \vec{x}[j]} \vec{h}_\sigma(\vec{x}(t), \vec{b}_t, \vec{c}_t)[i], \quad (10)$$ where $1 \leq i \leq m_\sigma$ and $1 \leq j \leq n$. Finally, we note the use of the standard (Kalman filter) $n \times n$ *error covariance matrix* $P(t)$ which maintains the covariance of the error in the estimated state. Welch 1997 at Section 3.1.1.

Exhibit D-7

<table>
<tr><th>CLAIM 47</th><th>Welch 1997</th></tr>
<tr><td></td><td>

3.1.2 Tracking Algorithm

Given an initial state estimate $\hat{x}(0)$ and error covariance estimate $P(0)$, the SCAAT algorithm proceeds similarly to a conventional EKF, cycling through the following steps whenever a discrete measurement $\vec{z}_{\sigma,t}$ from some sensor (type σ) and source becomes available at time t:

a. Compute the time δt since the previous estimate.

b. Predict the state and error covariance.

$$\begin{aligned} \hat{x}^- &= A(\delta t)\hat{x}(t-\delta t) \\ P^- &= A(\delta t)P(t-\delta t)A^T(\delta t) + Q(\delta t) \end{aligned} \quad (11)$$

c. Predict the measurement and compute the corresponding Jacobian.

$$\begin{aligned} \hat{z} &= \vec{h}_\sigma(\hat{x}^-, \vec{b}_t, \vec{c}_t) \\ H &= H_\sigma(\hat{x}^-, \vec{b}_t, \vec{c}_t) \end{aligned} \quad (12)$$

d. Compute the *Kalman gain*.

$$K = P^- H^T (HP^- H^T + R_\sigma(t))^{-1} \quad (13)$$

e. Compute the *residual* between the actual sensor measurement $\vec{z}_{\sigma,t}$ and the predicted measurement from (12).

$$\overrightarrow{\Delta z} = \vec{z}_{\sigma,t} - \hat{z} \quad (14)$$

f. Correct the predicted tracker state estimate and error covariance from (11).

$$\begin{aligned} \hat{x}(t) &= \hat{x}^- + K\overrightarrow{\Delta z} \\ P(t) &= (I - KH)P^- \end{aligned} \quad (15)$$

Welch 1997 at Section 3.1.2.
</td></tr>
</table>

Exhibit D-7

CLAIM 47	Welch 1997
	g. Update the external orientation of equation (4) per the change indicated by the (ϕ, θ, ψ) elements of the state.* $$\begin{aligned} \Delta\hat{\alpha} &= \text{quaternion}(\hat{x}[\phi], \hat{x}[\theta], \hat{x}[\psi]) \\ \hat{\alpha} &= \hat{\alpha} \otimes \Delta\hat{\alpha} \end{aligned} \quad (16)$$ h. Zero the orientation elements of the state vector. $$\hat{x}[\phi] = \hat{x}[\theta] = \hat{x}[\psi] = 0 \quad (17)$$ The equations (11)-(17) may seem computationally complex, however they can be performed quite efficiently. The computations can be optimized to eliminate operations on matrix and vector elements that are known to be zero. For example, the elements of the Jacobian H in (12) that correspond to the velocities in the state $\hat{x}(t)$ will always be zero. In addition, the matrix inverted in the computation of K in (13) is of rank m_σ (2×2 for our example in section 3.4) which is smaller for a SCAAT filter than for a corresponding conventional EKF implementation. Finally, the increased data rate allows the use of the *small angle approximations* $\sin(\theta) = \theta$ and $\cos(\theta) = 1$ in $\vec{h}_\sigma(\bullet)$ and $H_\sigma(\bullet)$. The total *per estimate* computation time can therefore actually be less than that of a corresponding conventional implementation. (We are able to execute the SCAAT filter computations, with the autocalibration computations discussed in the next section, in approximately 100μs on a 200 MHz PC-compatible computer.) Welch 1997 at Section 3.1.2.

Exhibit D-7

CLAIM 47	Welch 1997
	3.1.3 Discussion The key to the SCAAT method is the number of constraints provided by the measurement vector and measurement function in equation (8). For the 3D-tracking problem being solved, a unique solution requires $C = 6$ non-degenerate constraints to resolve six degrees of freedom. Because individual sensor measurements typically provide less than six constraints, conventional implementations usually construct a complete measurement vector $$\hat{z}_t = \left[\hat{z}^T_{\sigma_1, t_1} \; \dots \; \hat{z}^T_{\sigma_N, t_N}\right]^T$$ from some group of $N \geq C$ individual sensor measurements over time $t_1 \dots t_N$, and *then* proceed to compute an estimate. Or a particular implementation may operate in a *moving-window* fashion, combining the most recent measurement with the $N-1$ previous measurements, possibly implementing a form of a finite-impulse-response filter. In any case, for such well-constrained systems complete observability is obtained at each step of the filter. Systems that collect measurements sequentially in this way inherently violate the simultaneity assumption, as well as increase the time δt between estimates. Welch 1997 at Section 3.1.3. In contrast, the SCAAT method blends individual measurements that each provide incomplete constraints into a complete state estimate. The EKF inherently provides the means for this blending, no matter how complete the information content of each individual measurement $\hat{z}_{\sigma, t}$. The EKF accomplishes this through the Kalman gain K which is computed in (13). The Kalman gain, which is used to adjust the state and the error covariance in (15), is optimal in the sense that it minimizes the error covariance if certain conditions are met. Note that the inversion in (13) forms a ratio that reflects the relative uncertainties of the state and the measurement. Note too that the ratio is affected by the use of the measurement function Jacobian H. Because the Jacobian reflects the rate of change of each measurement with respect to the current state, it indicates a direction in state space along which a measurement could *possibly* affect the state. Because the gain is recomputed at each step with the appropriate measurement function and associated Jacobian, it inherently reflects the amount and direction of information provided by the individual constraint. Welch 1997 at Section 3.1.3.

CLAIM 47	Welch 1997
	3.2 Autocalibration The method we use for autocalibration involves *augmenting* the *main tracker filter* presented in section 3.1 to effectively implement a distinct *device filter*, a Kalman filter, for each source or sensor to be calibrated. (We use the word "device" here to include for example scene landmarks which can be thought of as passive sources, and cameras which are indeed sensors.) In general, any constant device-related parameters used by a measurement function $\vec{h}_\sigma(\bullet)$ from (8) are candidates for this autocalibration method. We assume that the parameters to be estimated are contained in the device parameter vectors $\vec{b}_t$ and $\vec{c}_t$, and we also present the case where both the source and sensor are to be calibrated since omission of one or the other is trivial. We note the following new convention. $\widehat{\alpha}$ = augmented matrix/vector (wide hat) Welch 1997 at Section 3.2. **3.2.1 Device Filters** For each device (source, sensor, landmark, etc.) we create a distinct device filter as follows. Let $\vec{\pi}$ represent the corresponding device parameter vector and $n_\pi = \text{length}(\vec{\pi})$. a. Allocate an $n_\pi \times 1$ state vector $\hat{x}_\pi$ for the device, initialize with the best *a priori* device parameter estimates, e.g. from design. b. Allocate an $n_\pi \times n_\pi$ noise covariance matrix $Q_\pi(\delta t)$, initialize with the expected parameter variances. c. Allocate an $n_\pi \times n_\pi$ error covariance matrix $P_\pi(t)$, initialize to indicate the level of confidence in the *a priori* device parameter estimates from (a) above. Welch 1997 at Section 3.2.1.

Exhibit D-7

CLAIM 47	Welch 1997
	3.2.2 Revised Tracking Algorithm The algorithm for tracking with concurrent autocalibration is the same as that presented in section 3.1, with the following exceptions. After step (a) in the original algorithm, we form augmented versions of the state vector $$\widehat{x}(t-\delta t) = \left[\hat{x}^T(t-\delta t)\ \ \hat{x}_{b,t}^T(t-\delta t)\ \ \hat{x}_{c,t}^T(t-\delta t)\right]^T, \quad (18)$$ the error covariance matrix $$\widehat{P}(t-\delta t) = \begin{bmatrix} P(t-\delta t) & 0 & 0 \\ 0 & P_{b,t}(t-\delta t) & 0 \\ 0 & 0 & P_{c,t}(t-\delta t) \end{bmatrix}, \quad (19)$$ the state transition matrix $$\widehat{A}(\delta t) = \begin{bmatrix} A(\delta t) & 0 & 0 \\ 0 & I & 0 \\ 0 & 0 & I \end{bmatrix}, \quad (20)$$ and the process noise matrix $$\widehat{Q}(\delta t) = \begin{bmatrix} Q(\delta t) & 0 & 0 \\ 0 & Q_{b,t}(\delta t) & 0 \\ 0 & 0 & Q_{c,t}(\delta t) \end{bmatrix}. \quad (21)$$ Welch 1997 at Section 3.2.2.

CLAIM 47	Welch 1997
	We then follow steps (b)-(h) from the original algorithm, making the appropriate substitutions of (18)-(21), and noting that the measurement and Jacobian functions used in step (c) have become $\vec{h}_\sigma(\widehat{x}(t))$ and $H_\sigma(\widehat{x}(t))$ because the estimates of parameters $\vec{b}_t$ and $\vec{c}_t$ ($\hat{x}_{b,t}$ and $\hat{x}_{c,t}$) are now contained in the augmented state vector $\widehat{x}$ per (18). After step (h) we finish by extracting and saving the device filter portions of the augmented state vector and error covariance matrix $$\begin{aligned} \hat{x}_{b,t}(t) &= \widehat{x}(t)[i \ldots j] \\ P_{b,t}(t) &= \widehat{P}(t)[i \ldots j, i \ldots j] \\ \hat{x}_{c,t}(t) &= \widehat{x}(t)[k \ldots l] \\ P_{c,t}(t) &= \widehat{P}(t)[k \ldots l, k \ldots l] \end{aligned} \quad (22)$$ where $$\begin{aligned} i &= n+1 \\ j &= n+n_b \\ k &= n+n_b+1 \\ l &= n+n_b+n_c \end{aligned}$$ Welch 1997 at Section 3.2.2.

Exhibit D-7

CLAIM 47	Welch 1997
	and n, n_b, and n_c are the dimensions of the state vectors for the main tracker filter, the source filter, and the sensor filter (respectively). We leave the main tracker filter state vector and error covariance matrix in their augmented counterparts, while we swap the device filter components in and out with each estimate. The result is that individual device filters are updated less frequently than the main tracker filter. The more a device is used, the more it is calibrated. If a device is never used, it is never calibrated. With respect to added time complexity, the computations can again be optimized to eliminate operations on matrix and vector elements that are known to be zero: those places mentioned in section 3.1, and see (19)-(21). Also note that the size of and thus time for the matrix inversion in (13) has not changed. With respect to added space complexity, the autocalibration method requires storing a separate state vector and covariance matrix for each device—a fixed amount of (generally small) space per device. For example, consider autocalibrating the beacon (LED) positions for an optical tracking system with 3,000 beacons. For each beacon one would need 3 words for the beacon state (its 3D position), $3 \times 3 = 9$ words for the noise covariance matrix, and $3 \times 3 = 9$ words for the error covariance matrix. Assuming 8 bytes per word, this is only $3{,}000 \times 8 \times (3 + 9 + 9) = 504{,}000$ bytes. Welch 1997 at Section 3.2.2. 3.3 Stability Because the SCAAT method uses individual measurements with insufficient information, one might be concerned about the potential for instability or divergence. A linear system is said to be stable if its response to any input tends to a finite steady value after the input is removed [24]. For the Kalman filter in general this is certainly not a new concern, and there are standard requirements and corresponding tests that ensure or detect stability (see [18], p. 132): a. The filter must be uniformly completely observable, b. the dynamic and measurement noise matrices in equations (6) and (9) must be bounded from above and below, and c. the dynamic behavior represented by in equation (2) must be bounded from above. As it turns out, these conditions and their standard tests are equally applicable to a SCAAT implementation. For the SCAAT method the conditions mean that the user dynamics between estimates must be bounded, the

Exhibit D-7

CLAIM 47	Welch 1997
	measurement noise must be bounded, one must incorporate a sufficient set of non-degenerate constraints over time. In particular, the constraints must be incorporated in less than 1/2 the time of the user motion time-constant in order to avoid tracking an alias of the true motion. In general these conditions are easily met for systems and circumstances that would otherwise be stable with a multiple-constraint implementation. A complete stability analysis is beyond the scope of this paper, and is presented in [47]. Welch 1997 at Section 3.3. [47] Greg Welch, 1996. "SCAAT: Incremental Tracking with Incomplete Information," University of North Carolina at Chapel Hill, doctoral dissertation, TR 96-051. Welch 1997 at References.  Figure 3: The HiBall is shown here with the internal circuitry exposed and the lenses removed. The sensors, which can be seen through the lens openings, are mounted on PC boards that fold-up into the HiBall upon assembly. The mechanical pencil at the bottom conveys an indication of the relative size of the unit. Welch 1997 at Figure 3.

CLAIM 47	Welch 1997
	4.1 Tracker Filter The 12 element state vector $\hat{x}(t)$ for the main tracker filter contained the elements shown in (3). Each of the 3000 beacon filters was allocated a 3 element state vector $$\hat{x}_b = \left[x_b\ y_b\ z_b\right]^T$$ where (x_b, y_b, z_b) represents the beacon's estimated position in cartesian (world) coordinates. The 12×12 state transition matrix for the main tracker filter was formed as discussed section 3.1, and for each beacon filter it was the 3×3 identity matrix. The 12×12 process noise matrix for the main tracker was computed using (7), using elements of $\vec{\eta}$ that were determined off-line using Powell's method and a variety of real motion data. For each beacon filter we used an identical noise covariance matrix $$Q_b(\delta t)[i, j] = \begin{cases} \eta_b & \text{if } i = j \\ 0 & \text{otherwise} \end{cases}$$ for $1 \le i, j \le 3$, with beacon position variance η_b also determined off-line. (See [47] for the complete details.) At each estimate step, the *augmented* 15 element state vector, 15×15 process noise matrix, 15×15 state transition matrix, and 15×15 error covariance matrix all resembled (18)-(21) (without the camera parameter components). The measurement noise model was distance dependent (beacon light falls-off with distance) so $R_\sigma(t)$ from (9) was computed prior to step (d), by using a beacon distance estimate (obtained from the user and beacon positions in the predicted state $\widehat{x}^-$) to project a distance-dependent electrical variance onto the camera. Welch 1997 at Section 4.1. *See also* Defendants' Invalidity Contentions for further discussion.

L. DEPENDENT CLAIM 50

CLAIM 50	Welch 1997
[50] The method of claim 47 wherein	At least under Plaintiffs' apparent infringement theory, Welch 1997 discloses, either expressly or inherently, the method of claim 47 wherein providing the estimation module includes providing a module that is configurable to

Exhibit D-7

CLAIM 50	Welch 1997
providing the estimation module includes providing a module that is configurable to use different sets of sensor modules coupled to it.	use different sets of sensor modules coupled to it. In the alternative, this element would be obvious over Welch 1997 in light of the other references disclosed in Defendants' Invalidity Contentions and/or the knowledge of one of ordinary skill in the art. *See, e.g.*: Tracking systems determine the user's pose by measuring signals from low-level hardware sensors. For reasons of physics and economics, most systems make multiple sequential measurements which are then combined to produce a single tracker report. For example, commercial magnetic trackers using the SPASYN (Space Synchro) system sequentially measure three magnetic vectors and then combine them mathematically to produce a report of the sensor pose. Our new approach produces tracker reports as each new low-level sensor measurement is made rather than waiting to form a complete collection of observations. Because single observations under-constrain the mathematical solution, we refer to our approach as single-constraint-at-a-time or SCAAT tracking. **The key is that the single observations provide some information about the user's state, and thus can be used to incrementally improve a previous estimate. We recursively apply this principle, incorporating new sensor data as soon as it is measured. With this approach we are able to generate estimates more frequently, with less latency, and with improved accuracy. We present results from both an actual implementation, and from extensive simulations.** Welch 1997 at Abstract. **The Kalman filter has been employed previously for virtual environment tracking estimation and prediction.** For example see [2,5,12,14,42], and most recently [32]. In each of these cases however the filter was applied directly and only to the 6D pose estimates delivered by the off-the-shelf tracker. The SCAAT approach could be applied to either a hybrid system using off-the shelf and/or custom trackers, or it could be employed by tracker developers to improve the existing systems for the end-user graphics community. Welch 1997 at Section 3. In this section **we describe the method in a manner that does not imply a specific tracking system.** (In section 3.4 we present experimental results of a specific implementation, a SCAAT wide area optoelectronic tracking system.) In section 3.1 we describe the method for tracking, and in section 3.2 we describe one possible

CLAIM 50	Welch 1997
	method for concurrent autocalibration. Welch 1997 at Section 3. *See* Disclosures with respect to Claim 47, *supra*; *see also* Defendants' Invalidity Contentions for further discussion.

M. DEPENDENT CLAIM 51

CLAIM 51	Welch 1997
[51] The method of claim 47 wherein maintaining estimates of the tracking parameters in the estimation module includes using a stochastic model in the estimation module.	At least under Plaintiffs' apparent infringement theory, Welch 1997 discloses, either expressly or inherently, the method of claim 47 wherein maintaining estimates of the tracking parameters in the estimation module includes using a stochastic model in the estimation module. In the alternative, this element would be obvious over Welch 1997 in light of the other references disclosed in Defendants' Invalidity Contentions and/or the knowledge of one of ordinary skill in the art. *See, e.g.*: **The SCAAT method employs a Kalman filter (KF)** in an unusual fashion. T**he Kalman filter is a mathematical procedure that provides an efficient computational (recursive) method for the least-squares estimation of a linear system. It does so in a predictor-corrector fashion, predicting short-term (since the last estimate) changes in the state using a dynamic model, and then correcting them with a measurement and a corresponding measurement model. The extended Kalman filter (EKF) is a variation of the Kalman filter that supports estimation of nonlinear systems, e.g. 3D position and orientation tracking systems.** A basic introduction to the Kalman filter can be found in Chapter 1 of [31], while a more complete introductory discussion can be found in [40], which also contains some interesting historical narrative. More extensive references can be found in [7,18,24,28,31,46]. Welch 1997 at Section 3. **The Kalman filter has been employed previously for virtual environment tracking estimation and prediction.** For example see [2,5,12,14,42], and most recently [32]. In each of these cases however the filter was applied directly and only to the 6D pose estimates delivered by the off-the-shelf tracker. T**he SCAAT approach could be applied to either a hybrid system using off-the shelf and/or custom trackers, or it could be**

Exhibit D-7

CLAIM 51	Welch 1997
	employed by tracker developers to improve the existing systems for the end-user graphics community. Welch 1997 at Section 3. In this section we describe the method in a manner that does not imply a specific tracking system. (In section 3.4 we present experimental results of a specific implementation, a SCAAT wide area optoelectronic tracking system.) In section 3.1 we describe the method for tracking, and in section 3.2 we describe one possible method for concurrent autocalibration. Welch 1997 at Section 3. Throughout we use the following conventions. x = scalar (lower case) $\vec{x}$ = general vector (lower case, arrow) indexed as $\vec{x}[r]$ $\hat{x}$ = filter estimate vector (lower case, hat) A = matrix (capital letters) indexed as $A[r, c]$ A^{-1} = matrix inverse I = the identity matrix β^{-} = matrix/vector *prediction* (super minus) β^{T} = matrix/vector transpose (super T) α_i = matrix/vector/scalar identifier (subscript) $E\{\bullet\}$ = mathematical expectation Welch 1997 at Section 3.

Exhibit D-7

CLAIM 51	Welch 1997
	3.1 Tracking **3.1.1 Main Tracker Filter** The use of a Kalman filter requires a mathematical (state-space) model for the dynamics of the process to be estimated, the target motion in this case. While several possible dynamic models and associated state configurations are possible, we have found a simple *position-velocity* model to suffice for the dynamics of our applications. In fact we use this same form of model, with different parameters, for all six of the position and orientation components $(x, y, z, \phi, \theta, \psi)$. Discussion of some other potential models and the associated trade-offs can be found in [7] pp. 415-420. Because our implementation is discrete with inter sample time δt we model the target's dynamic motion with the following linear difference equation: $\vec{x}(t+\delta t) = A(\delta t)\vec{x}(t) + \vec{w}(\delta t)$. (2) Welch 1997 at Section 3.1.

Exhibit D-7

CLAIM 51	Welch 1997
	In the standard model corresponding to equation (2), the n dimensional Kalman filter *state vector* $\hat{x}(t)$ would completely describe the target position and orientation at any time t. In practice we use a method similar to [2,6] and maintain the complete target orientation externally to the Kalman filter in order to avoid the nonlinearities associated with orientation computations. In the internal state vector $\hat{x}(t)$ we maintain the target position as the Cartesian coordinates (x, y, z), and the *incremental* orientation as small rotations (ϕ, θ, ψ) about the (x, y, z) axis. Externally we maintain the target orientation as the *external quaternion* $\vec{\alpha} = (\alpha_w, (\alpha_x, \alpha_y, \alpha_z))$. (See [9] for discussion of quaternions.) At each filter update step, the incremental orientations (ϕ, θ, ψ) are factored into the external quaternion $\vec{\alpha}$, and then zeroed as shown below. Thus the incremental orientations are linearized for the EKF, centered about zero. We maintain the derivatives of the target position and orientation internally, in the state vector $\hat{x}(t)$. We maintain the angular velocities internally because the angular velocities behave like orthogonal vectors and do not exhibit the nonlinearities of the angles themselves. The target state is then represented by the $n = 12$ element internal state vector $$\hat{x} = \left[x\ y\ z\ \dot{x}\ \dot{y}\ \dot{z}\ \phi\ \theta\ \psi\ \dot{\phi}\ \dot{\theta}\ \dot{\psi}\right]^T \quad (3)$$ and the four-element external orientation quaternion $$\vec{\alpha} = (\alpha_w, (\alpha_x, \alpha_y, \alpha_z)), \quad (4)$$ where the time designations have been omitted for clarity. Welch 1997 at Section 3.1.1.

Exhibit D-7

CLAIM 51	Welch 1997
	The $n \times n$ *state transition matrix* $A(\delta t)$ in (2) projects the state forward from time t to time $t + \delta t$. For our linear model, the matrix implements the relationships $$\begin{aligned} x(t+\delta t) &= x(t) + \dot{x}(t)\delta t \\ \dot{x}(t+\delta t) &= \dot{x}(t) \end{aligned} \quad (5)$$ and likewise for the remaining elements of (3). The $n \times 1$ *process noise vector* $\vec{w}(\delta t)$ in (2) is a normally-distributed zero-mean sequence that represents the uncertainty in the target state over any time interval δt. The corresponding $n \times n$ *process noise covariance matrix* is given by $$E\{\vec{w}(\delta t)\vec{w}^T(\delta t + \varepsilon)\} = \begin{cases} Q(\delta t), & \varepsilon = 0 \\ 0, & \varepsilon \neq 0 \end{cases}. \quad (6)$$ Because our implementation is discrete with inter sample time δt, we can use the transfer function method illustrated by [7] pp. 221-222 to compute a *sampled* process noise covariance matrix. (Because the associated random processes are presumed to be time stationary, we present the process noise covariance matrix as a function of the inter-sample duration δt only.) The non-zero elements of $Q(\delta t)$ are given by $$\begin{aligned} Q(\delta t)[i,i] &= \vec{\eta}[i]\frac{(\delta t)^3}{3} \\ Q(\delta t)[i,j] = Q(\delta t)[j,i] &= \vec{\eta}[i]\frac{(\delta t)^2}{2} \\ Q(\delta t)[j,j] &= \vec{\eta}[i](\delta t) \end{aligned} \quad (7)$$ for each pair $$(i,j) \in \{(x,\dot{x}), (y,\dot{y}), (z,\dot{z}), (\phi,\dot{\phi}), (\theta,\dot{\theta}), (\psi,\dot{\psi})\}.$$ Welch 1997 at Section 3.1.1.

Exhibit D-7

CLAIM 51	Welch 1997
	The $\vec{\eta}[i]$ in (7) are the *correlation kernels* of the (assumed constant) noise sources presumed to be driving the dynamic model. We determined a set of values using Powell's method, and then used these in both simulation and our real implementation. The values can be "tuned" for different dynamics, though we have found that the tracker works well over a broad range of values. The use of a Kalman filter requires not only a dynamic model as described above, but also a *measurement model* for each available type of measurement. The measurement model is used to predict the ideal noise-free response of each sensor and source pair, given the filter's current estimate of the target state as in equations (3) and (4). *It is the nature of the measurement models and indeed the actual sensor measurements that distinguishes a SCAAT Kalman filter from a well-constrained one.* For each sensor *type* σ we define the $m_\sigma \times 1$ *measurement vector* $\vec{z}_\sigma(t)$ and corresponding *measurement function* $\vec{h}_\sigma(\bullet)$ such that $$\vec{z}_{\sigma,t} = \vec{h}_\sigma(\vec{x}(t), \vec{b}_t, \vec{c}_t) + \vec{v}_\sigma(t)\ . \quad (8)$$ Note that in the "purest" SCAAT implementation $m_\sigma = 1$ and the measurements are incorporated as single scalar values. However if it is not possible or necessary to isolate the measurements, e.g. to perform autocalibration, then multi-dimensional measurements can be incorporated also. Guidelines presented in [47] lead to the following heuristic for choosing the SCAAT Kalman filter measurement elements (constraints): *During each SCAAT Kalman filter measurement update one should observe a single sensor and source pair only.* For example, to incorporate magnetic tracker data as an end-user, $m_\sigma = 7$ for the three position and four orientation (quaternion) Welch 1997 at Section 3.1.1.

Exhibit D-7

CLAIM 51	Welch 1997
	elements, while if the manufacturer were to use the SCAAT implementation, $m_\sigma = 3$ for each 3-axis electromagnetic response to a single excitation. For an image-based landmark tracker such as [41] the measurement function would, given estimates of the camera pose and a single landmark location, transform the landmark into camera space and then project it onto the camera image plane. In this case $m_\sigma = 2$ for the 2D image coordinates of the landmark. The $m_\sigma \times 1$ *measurement noise vector* $\vec{v}_\sigma(t)$ in (8) is a normally-distributed zero-mean sequence that represents any random error (e.g. electrical noise) in the measurement. This parameter can be determined from component design specifications, and (or) confirmed by off-line measurement. For our simulations we did both. The corresponding $m_\sigma \times m_\sigma$ *measurement noise covariance matrix* is given by $$E\{\vec{v}_\sigma(t)\vec{v}_\sigma^T(t+\varepsilon)\} = \begin{cases} R_\sigma(t), & \varepsilon = 0 \\ 0, & \varepsilon \neq 0 \end{cases}. \qquad (9)$$ For each measurement function $\vec{h}_\sigma(\bullet)$ we determine the corresponding Jacobian function $$H_\sigma(\vec{x}(t), \vec{b}_t, \vec{c}_t)[i, j] \equiv \frac{\partial}{\partial \vec{x}[j]} \vec{h}_\sigma(\vec{x}(t), \vec{b}_t, \vec{c}_t)[i], \qquad (10)$$ where $1 \leq i \leq m_\sigma$ and $1 \leq j \leq n$. Finally, we note the use of the standard (Kalman filter) $n \times n$ *error covariance matrix* $P(t)$ which maintains the covariance of the error in the estimated state. Welch 1997 at Section 3.1.1.

Exhibit D-7

CLAIM 51	Welch 1997
	3.1.2 Tracking Algorithm Given an initial state estimate $\hat{x}(0)$ and error covariance estimate $P(0)$, the SCAAT algorithm proceeds similarly to a conventional EKF, cycling through the following steps whenever a discrete measurement $\vec{z}_{\sigma, t}$ from some sensor (type σ) and source becomes available at time t: a. Compute the time δt since the previous estimate. b. Predict the state and error covariance. $\hat{x}^- = A(\delta t)\hat{x}(t-\delta t)$ $P^- = A(\delta t)P(t-\delta t)A^T(\delta t) + Q(\delta t)$ (11) c. Predict the measurement and compute the corresponding Jacobian. $\hat{z} = \vec{h}_\sigma(\hat{x}^-, \vec{b}_t, \vec{c}_t)$ $H = H_\sigma(\hat{x}^-, \vec{b}_t, \vec{c}_t)$ (12) d. Compute the *Kalman gain*. $K = P^- H^T(HP^- H^T + R_\sigma(t))^{-1}$ (13) e. Compute the *residual* between the actual sensor measurement $\vec{z}_{\sigma, t}$ and the predicted measurement from (12). $\overrightarrow{\Delta z} = \vec{z}_{\sigma, t} - \hat{z}$ (14) f. Correct the predicted tracker state estimate and error covariance from (11). $\hat{x}(t) = \hat{x}^- + K\overrightarrow{\Delta z}$ $P(t) = (I - KH)P^-$ (15) Welch 1997 at Section 3.1.2.

Exhibit D-7

CLAIM 51	Welch 1997
	g. Update the external orientation of equation (4) per the change indicated by the (ϕ, θ, ψ) elements of the state.* $$\Delta\hat{\alpha} = \text{quaternion}(\hat{x}[\phi], \hat{x}[\theta], \hat{x}[\psi]) \qquad (16)$$ $$\hat{\alpha} = \hat{\alpha} \otimes \Delta\hat{\alpha}$$ h. Zero the orientation elements of the state vector. $$\hat{x}[\phi] = \hat{x}[\theta] = \hat{x}[\psi] = 0 \qquad (17)$$ The equations (11)-(17) may seem computationally complex, however they can be performed quite efficiently. The computations can be optimized to eliminate operations on matrix and vector elements that are known to be zero. For example, the elements of the Jacobian H in (12) that correspond to the velocities in the state $\hat{x}(t)$ will always be zero. In addition, the matrix inverted in the computation of K in (13) is of rank m_σ (2×2 for our example in section 3.4) which is smaller for a SCAAT filter than for a corresponding conventional EKF implementation. Finally, the increased data rate allows the use of the *small angle approximations* $\sin(\theta) = \theta$ and $\cos(\theta) = 1$ in $\vec{h}_\sigma(\bullet)$ and $H_\sigma(\bullet)$. The total *per estimate* computation time can therefore actually be less than that of a corresponding conventional implementation. (We are able to execute the SCAAT filter computations, with the autocalibration computations discussed in the next section, in approximately 100µs on a 200 MHz PC-compatible computer.) Welch 1997 at Section 3.1.2. **3.2.1 Device Filters** For each device (source, sensor, landmark, etc.) we create a distinct device filter as follows. Let $\vec{\pi}$ represent the corresponding device parameter vector and $n_\pi = \text{length}(\vec{\pi})$. a. Allocate an $n_\pi \times 1$ state vector $\hat{x}_\pi$ for the device, initialize with the best *a priori* device parameter estimates, e.g. from design. b. Allocate an $n_\pi \times n_\pi$ noise covariance matrix $Q_\pi(\delta t)$, initialize with the expected parameter variances. c. Allocate an $n_\pi \times n_\pi$ error covariance matrix $P_\pi(t)$, initialize to indicate the level of confidence in the *a priori* device parameter estimates from (a) above. Welch 1997 at Section 3.2.1.

Exhibit D-7

CLAIM 51	Welch 1997
	3.2.2 Revised Tracking Algorithm The algorithm for tracking with concurrent autocalibration is the same as that presented in section 3.1, with the following exceptions. After step (a) in the original algorithm, we form augmented versions of the state vector $$\widehat{x}(t-\delta t) = \left[\hat{x}^T(t-\delta t)\ \ \hat{x}^T_{b,t}(t-\delta t)\ \ \hat{x}^T_{c,t}(t-\delta t)\right]^T, \qquad (18)$$ the error covariance matrix $$\widehat{P}(t-\delta t) = \begin{bmatrix} P(t-\delta t) & 0 & 0 \\ 0 & P_{b,t}(t-\delta t) & 0 \\ 0 & 0 & P_{c,t}(t-\delta t) \end{bmatrix}, \qquad (19)$$ the state transition matrix $$\widehat{A}(\delta t) = \begin{bmatrix} A(\delta t) & 0 & 0 \\ 0 & I & 0 \\ 0 & 0 & I \end{bmatrix}, \qquad (20)$$ and the process noise matrix $$\widehat{Q}(\delta t) = \begin{bmatrix} Q(\delta t) & 0 & 0 \\ 0 & Q_{b,t}(\delta t) & 0 \\ 0 & 0 & Q_{c,t}(\delta t) \end{bmatrix}. \qquad (21)$$ Welch 1997 at Section 3.2.2.

Exhibit D-7

CLAIM 51	Welch 1997
	We then follow steps (b)-(h) from the original algorithm, making the appropriate substitutions of (18)-(21), and noting that the measurement and Jacobian functions used in step (c) have become $\vec{h}_\sigma(\widehat{x}(t))$ and $H_\sigma(\widehat{x}(t))$ because the estimates of parameters $\vec{b}_t$ and $\vec{c}_t$ ($\hat{x}_{b,t}$ and $\hat{x}_{c,t}$) are now contained in the augmented state vector $\widehat{x}$ per (18). After step (h) we finish by extracting and saving the device filter portions of the augmented state vector and error covariance matrix $$\begin{aligned} \hat{x}_{b,t}(t) &= \widehat{x}(t)[i\ldots j] \\ P_{b,t}(t) &= \widehat{P}(t)[i\ldots j, i\ldots j] \\ \hat{x}_{c,t}(t) &= \widehat{x}(t)[k\ldots l] \\ P_{c,t}(t) &= \widehat{P}(t)[k\ldots l, k\ldots l] \end{aligned} \quad (22)$$ where $$\begin{aligned} i &= n+1 \\ j &= n+n_b \\ k &= n+n_b+1 \\ l &= n+n_b+n_c \end{aligned}$$ Welch 1997 at Section 3.2.2.

Exhibit D-7

CLAIM 51	Welch 1997
	and n, n_b, and n_c are the dimensions of the state vectors for the main tracker filter, the source filter, and the sensor filter (respectively). We leave the main tracker filter state vector and error covariance matrix in their augmented counterparts, while we swap the device filter components in and out with each estimate. The result is that individual device filters are updated less frequently than the main tracker filter. The more a device is used, the more it is calibrated. If a device is never used, it is never calibrated. With respect to added time complexity, the computations can again be optimized to eliminate operations on matrix and vector elements that are known to be zero: those places mentioned in section 3.1, and see (19)-(21). Also note that the size of and thus time for the matrix inversion in (13) has not changed. With respect to added space complexity, the autocalibration method requires storing a separate state vector and covariance matrix for each device—a fixed amount of (generally small) space per device. For example, consider autocalibrating the beacon (LED) positions for an optical tracking system with 3,000 beacons. For each beacon one would need 3 words for the beacon state (its 3D position), $3 \times 3 = 9$ words for the noise covariance matrix, and $3 \times 3 = 9$ words for the error covariance matrix. Assuming 8 bytes per word, this is only $3{,}000 \times 8 \times (3 + 9 + 9) = 504{,}000$ bytes. Welch 1997 at Section 3.2.2.

Exhibit D-7

CLAIM 51	Welch 1997
	 Figure 3: The HiBall is shown here with the internal circuitry exposed and the lenses removed. The sensors, which can be seen through the lens openings, are mounted on PC boards that fold-up into the HiBall upon assembly. The mechanical pencil at the bottom conveys an indication of the relative size of the unit. Welch 1997 at Figure 3. 3.3 Stability Because the SCAAT method uses individual measurements with insufficient information, one might be concerned about the potential for instability or divergence. A linear system is said to be stable if its response to any input tends to a finite steady value after the input is removed [24]. For the Kalman filter in general this is certainly not a new concern, and there are standard requirements and corresponding tests that ensure or detect stability (see [18], p. 132): a. The filter must be uniformly completely observable, b. the dynamic and measurement noise matrices in equations (6) and (9) must be bounded from above and below,

CLAIM 51	Welch 1997
	and c. the dynamic behavior represented by in equation (2) must be bounded from above. As it turns out, these conditions and their standard tests are equally applicable to a SCAAT implementation. For the SCAAT method the conditions mean that the user dynamics between estimates must be bounded, the measurement noise must be bounded, one must incorporate a sufficient set of non-degenerate constraints over time. In particular, the constraints must be incorporated in less than 1/2 the time of the user motion time-constant in order to avoid tracking an alias of the true motion. In general these conditions are easily met for systems and circumstances that would otherwise be stable with a multiple-constraint implementation. A complete stability analysis is beyond the scope of this paper, and is presented in [47]. Welch 1997 at Section 3.3. [47] Greg Welch, 1996. "SCAAT: Incremental Tracking with Incomplete Information," University of North Carolina at Chapel Hill, doctoral dissertation, TR 96-051. Welch 1997 at References. *See* Disclosures with respect to Claim 47, *supra*; *see also* Defendants' Invalidity Contentions for further discussion.

N. DEPENDENT CLAIM 52

CLAIM 52	Welch 1997
[52] The method of claim 51 wherein using a stochastic model includes implementing some or all of a Kalman filter in the estimation module.	At least under Plaintiffs' apparent infringement theory, Welch 1997 discloses, either expressly or inherently, the method of claim 51 wherein using a stochastic model includes implementing some or all of a Kalman filter in the estimation module. In the alternative, this element would be obvious over Welch 1997 in light of the other references disclosed in Defendants' Invalidity Contentions and/or the knowledge of one of ordinary skill in the art. *See, e.g.*: **The SCAAT method employs a Kalman filter (KF) in an unusual fashion.** The Kalman filter is a mathematical procedure that provides an efficient computational (recursive) method for the least-squares estimation of a linear system. It does so in a predictor-corrector fashion, predicting short-term (since the last

Exhibit D-7

CLAIM 52	Welch 1997
	estimate) changes in the state using a dynamic model, and then correcting them with a measurement and a corresponding measurement model. The extended Kalman filter (EKF) is a variation of the Kalman filter that supports estimation of nonlinear systems, e.g. 3D position and orientation tracking systems. A basic introduction to the Kalman filter can be found in Chapter 1 of [31], while a more complete introductory discussion can be found in [40], which also contains some interesting historical narrative. More extensive references can be found in [7,18,24,28,31,46]. Welch 1997 at Section 3. The Kalman filter has been employed previously for virtual environment tracking estimation and prediction. For example see [2,5,12,14,42], and most recently [32]. In each of these cases however the filter was applied directly and only to the 6D pose estimates delivered by the off-the-shelf tracker. The SCAAT approach could be applied to either a hybrid system using off-the shelf and/or custom trackers, or it could be employed by tracker developers to improve the existing systems for the end-user graphics community. Welch 1997 at Section 3. In this section we describe the method in a manner that does not imply a specific tracking system. (In section 3.4 we present experimental results of a specific implementation, a SCAAT wide area optoelectronic tracking system.) In section 3.1 we describe the method for tracking, and in section 3.2 we describe one possible method for concurrent autocalibration. Welch 1997 at Section 3.

Exhibit D-7

CLAIM 52	Welch 1997
	Throughout we use the following conventions. x = scalar (lower case) $\vec{x}$ = general vector (lower case, arrow) indexed as $\vec{x}[r]$ $\hat{x}$ = filter estimate vector (lower case, hat) A = matrix (capital letters) indexed as $A[r, c]$ A^{-1} = matrix inverse I = the identity matrix β^{-} = matrix/vector *prediction* (super minus) β^{T} = matrix/vector transpose (super T) α_i = matrix/vector/scalar identifier (subscript) $E\{\bullet\}$ = mathematical expectation Welch 1997 at Section 3. **3.1 Tracking** **3.1.1 Main Tracker Filter** The use of a Kalman filter requires a mathematical (state-space) model for the dynamics of the process to be estimated, the target motion in this case. While several possible dynamic models and associated state configurations are possible, we have found a simple *position-velocity* model to suffice for the dynamics of our applications. In fact we use this same form of model, with different parameters, for all six of the position and orientation components $(x, y, z, \phi, \theta, \psi)$. Discussion of some other potential models and the associated trade-offs can be found in [7] pp. 415-420. Because our implementation is discrete with inter sample time δt we model the target's dynamic motion with the following linear difference equation: $\vec{x}(t+\delta t) = A(\delta t)\vec{x}(t) + \vec{w}(\delta t)$. (2) Welch 1997 at Section 3.1.

Exhibit D-7

CLAIM 52	Welch 1997
	In the standard model corresponding to equation (2), the n dimensional Kalman filter *state vector* $\hat{x}(t)$ would completely describe the target position and orientation at any time t. In practice we use a method similar to [2,6] and maintain the complete target orientation externally to the Kalman filter in order to avoid the nonlinearities associated with orientation computations. In the internal state vector $\hat{x}(t)$ we maintain the target position as the Cartesian coordinates (x, y, z), and the *incremental* orientation as small rotations (ϕ, θ, ψ) about the (x, y, z) axis. Externally we maintain the target orientation as the *external quaternion* $\vec{\alpha} = (\alpha_w, (\alpha_x, \alpha_y, \alpha_z))$. (See [9] for discussion of quaternions.) At each filter update step, the incremental orientations (ϕ, θ, ψ) are factored into the external quaternion $\vec{\alpha}$, and then zeroed as shown below. Thus the incremental orientations are linearized for the EKF, centered about zero. We maintain the derivatives of the target position and orientation internally, in the state vector $\hat{x}(t)$. We maintain the angular velocities internally because the angular velocities behave like orthogonal vectors and do not exhibit the nonlinearities of the angles themselves. The target state is then represented by the $n = 12$ element internal state vector $$\hat{x} = \left[x\ y\ z\ \dot{x}\ \dot{y}\ \dot{z}\ \phi\ \theta\ \psi\ \dot{\phi}\ \dot{\theta}\ \dot{\psi}\right]^T \quad (3)$$ and the four-element external orientation quaternion $$\vec{\alpha} = (\alpha_w, (\alpha_x, \alpha_y, \alpha_z)), \quad (4)$$ where the time designations have been omitted for clarity. Welch 1997 at Section 3.1.1.

Exhibit D-7

CLAIM 52	Welch 1997
	The $n \times n$ *state transition matrix* $A(\delta t)$ in (2) projects the state forward from time t to time $t + \delta t$. For our linear model, the matrix implements the relationships $$\begin{aligned} x(t+\delta t) &= x(t) + \dot{x}(t)\delta t \\ \dot{x}(t+\delta t) &= \dot{x}(t) \end{aligned} \quad (5)$$ and likewise for the remaining elements of (3). The $n \times 1$ *process noise vector* $\vec{w}(\delta t)$ in (2) is a normally-distributed zero-mean sequence that represents the uncertainty in the target state over any time interval δt. The corresponding $n \times n$ *process noise covariance matrix* is given by $$E\{\vec{w}(\delta t)\vec{w}^T(\delta t + \varepsilon)\} = \begin{cases} Q(\delta t), & \varepsilon = 0 \\ 0, & \varepsilon \neq 0 \end{cases}. \quad (6)$$ Because our implementation is discrete with inter sample time δt, we can use the transfer function method illustrated by [7] pp. 221-222 to compute a *sampled* process noise covariance matrix. (Because the associated random processes are presumed to be time stationary, we present the process noise covariance matrix as a function of the inter-sample duration δt only.) The non-zero elements of $Q(\delta t)$ are given by $$\begin{aligned} Q(\delta t)[i,i] &= \vec{\eta}[i]\frac{(\delta t)^3}{3} \\ Q(\delta t)[i,j] = Q(\delta t)[j,i] &= \vec{\eta}[i]\frac{(\delta t)^2}{2} \\ Q(\delta t)[j,j] &= \vec{\eta}[i](\delta t) \end{aligned} \quad (7)$$ for each pair $$(i,j) \in \{(x,\dot{x}), (y,\dot{y}), (z,\dot{z}), (\phi,\dot{\phi}), (\theta,\dot{\theta}), (\psi,\dot{\psi})\}.$$ Welch 1997 at Section 3.1.1.

Exhibit D-7

CLAIM 52	Welch 1997
	The $\vec{\eta}[i]$ in (7) are the *correlation kernels* of the (assumed constant) noise sources presumed to be driving the dynamic model. We determined a set of values using Powell's method, and then used these in both simulation and our real implementation. The values can be "tuned" for different dynamics, though we have found that the tracker works well over a broad range of values. The use of a Kalman filter requires not only a dynamic model as described above, but also a *measurement model* for each available type of measurement. The measurement model is used to predict the ideal noise-free response of each sensor and source pair, given the filter's current estimate of the target state as in equations (3) and (4). *It is the nature of the measurement models and indeed the actual sensor measurements that distinguishes a SCAAT Kalman filter from a well-constrained one.* For each sensor *type* σ we define the $m_\sigma \times 1$ *measurement vector* $\vec{z}_\sigma(t)$ and corresponding *measurement function* $\vec{h}_\sigma(\bullet)$ such that $$\vec{z}_{\sigma,t} = \vec{h}_\sigma(\vec{x}(t), \vec{b}_t, \vec{c}_t) + \vec{v}_\sigma(t) . \quad (8)$$ Note that in the "purest" SCAAT implementation $m_\sigma = 1$ and the measurements are incorporated as single scalar values. However if it is not possible or necessary to isolate the measurements, e.g. to perform autocalibration, then multi-dimensional measurements can be incorporated also. Guidelines presented in [47] lead to the following heuristic for choosing the SCAAT Kalman filter measurement elements (constraints): *During each SCAAT Kalman filter measurement update one should observe a single sensor and source pair only.* For example, to incorporate magnetic tracker data as an end-user, $m_\sigma = 7$ for the three position and four orientation (quaternion) Welch 1997 at Section 3.1.1.

Exhibit D-7

CLAIM 52	Welch 1997
	elements, while if the manufacturer were to use the SCAAT implementation, $m_\sigma = 3$ for each 3-axis electromagnetic response to a single excitation. For an image-based landmark tracker such as [41] the measurement function would, given estimates of the camera pose and a single landmark location, transform the landmark into camera space and then project it onto the camera image plane. In this case $m_\sigma = 2$ for the 2D image coordinates of the landmark. The $m_\sigma \times 1$ *measurement noise vector* $\vec{v}_\sigma(t)$ in (8) is a normally-distributed zero-mean sequence that represents any random error (e.g. electrical noise) in the measurement. This parameter can be determined from component design specifications, and (or) confirmed by off-line measurement. For our simulations we did both. The corresponding $m_\sigma \times m_\sigma$ *measurement noise covariance matrix* is given by $$E\{\vec{v}_\sigma(t)\vec{v}_\sigma^T(t+\varepsilon)\} = \begin{cases} R_\sigma(t), & \varepsilon = 0 \\ 0, & \varepsilon \neq 0 \end{cases}. \quad (9)$$ For each measurement function $\vec{h}_\sigma(\bullet)$ we determine the corresponding Jacobian function $$H_\sigma(\hat{x}(t), \vec{b}_t, \vec{c}_t)[i,j] \equiv \frac{\partial}{\partial \hat{x}[j]} \vec{h}_\sigma(\hat{x}(t), \vec{b}_t, \vec{c}_t)[i], \quad (10)$$ where $1 \leq i \leq m_\sigma$ and $1 \leq j \leq n$. Finally, we note the use of the standard (Kalman filter) $n \times n$ *error covariance matrix* $P(t)$ which maintains the covariance of the error in the estimated state. Welch 1997 at Section 3.1.1.

Exhibit D-7

CLAIM 52	Welch 1997
	3.1.2 Tracking Algorithm Given an initial state estimate $\hat{x}(0)$ and error covariance estimate $P(0)$, the SCAAT algorithm proceeds similarly to a conventional EKF, cycling through the following steps whenever a discrete measurement $\vec{z}_{\sigma,t}$ from some sensor (type σ) and source becomes available at time t: a. Compute the time δt since the previous estimate. b. Predict the state and error covariance. $\hat{x}^- = A(\delta t)\hat{x}(t-\delta t)$ (11) $P^- = A(\delta t)P(t-\delta t)A^T(\delta t)+Q(\delta t)$ c. Predict the measurement and compute the corresponding Jacobian. $\hat{z} = \vec{h}_\sigma(\hat{x}^-, \vec{b}_t, \vec{c}_t)$ (12) $H = H_\sigma(\hat{x}^-, \vec{b}_t, \vec{c}_t)$ d. Compute the *Kalman gain*. $K = P^-H^T(HP^-H^T+R_\sigma(t))^{-1}$ (13) e. Compute the *residual* between the actual sensor measurement $\vec{z}_{\sigma,t}$ and the predicted measurement from (12). $\overrightarrow{\Delta z} = \vec{z}_{\sigma,t} - \hat{z}$ (14) f. Correct the predicted tracker state estimate and error covariance from (11). $\hat{x}(t) = \hat{x}^- + K\overrightarrow{\Delta z}$ (15) $P(t) = (I-KH)P^-$ Welch 1997 at Section 3.1.2.

Exhibit D-7

CLAIM 52	Welch 1997
	g. Update the external orientation of equation (4) per the change indicated by the (ϕ, θ, ψ) elements of the state.* $$\begin{aligned} \Delta\hat{\alpha} &= \text{quaternion}(\hat{x}[\phi], \hat{x}[\theta], \hat{x}[\psi]) \\ \hat{\alpha} &= \hat{\alpha} \otimes \Delta\hat{\alpha} \end{aligned} \quad (16)$$ h. Zero the orientation elements of the state vector. $$\hat{x}[\phi] = \hat{x}[\theta] = \hat{x}[\psi] = 0 \quad (17)$$ The equations (11)-(17) may seem computationally complex, however they can be performed quite efficiently. The computations can be optimized to eliminate operations on matrix and vector elements that are known to be zero. For example, the elements of the Jacobian H in (12) that correspond to the velocities in the state $\hat{x}(t)$ will always be zero. In addition, the matrix inverted in the computation of K in (13) is of rank m_σ (2×2 for our example in section 3.4) which is smaller for a SCAAT filter than for a corresponding conventional EKF implementation. Finally, the increased data rate allows the use of the *small angle approximations* $\sin(\theta) = \theta$ and $\cos(\theta) = 1$ in $\vec{h}_\sigma(\bullet)$ and $H_\sigma(\bullet)$. The total *per estimate* computation time can therefore actually be less than that of a corresponding conventional implementation. (We are able to execute the SCAAT filter computations, with the autocalibration computations discussed in the next section, in approximately $100\mu s$ on a 200 MHz PC-compatible computer.) Welch 1997 at Section 3.1.2. **3.2.1 Device Filters** For each device (source, sensor, landmark, etc.) we create a distinct device filter as follows. Let $\vec{\pi}$ represent the corresponding device parameter vector and $n_\pi = \text{length}(\vec{\pi})$. a. Allocate an $n_\pi \times 1$ state vector $\hat{x}_\pi$ for the device, initialize with the best *a priori* device parameter estimates, e.g. from design. b. Allocate an $n_\pi \times n_\pi$ noise covariance matrix $Q_\pi(\delta t)$, initialize with the expected parameter variances. c. Allocate an $n_\pi \times n_\pi$ error covariance matrix $P_\pi(t)$, initialize to indicate the level of confidence in the *a priori* device parameter estimates from (a) above. Welch 1997 at Section 3.2.1.

Exhibit D-7

CLAIM 52	Welch 1997
	3.2.2 Revised Tracking Algorithm The algorithm for tracking with concurrent autocalibration is the same as that presented in section 3.1, with the following exceptions. After step (a) in the original algorithm, we form augmented versions of the state vector $$\widehat{x}(t-\delta t) = \left[\hat{x}^T(t-\delta t)\ \ \hat{x}^T_{b,t}(t-\delta t)\ \ \hat{x}^T_{c,t}(t-\delta t)\right]^T, \quad (18)$$ the error covariance matrix $$\widehat{P}(t-\delta t) = \begin{bmatrix} P(t-\delta t) & 0 & 0 \\ 0 & P_{b,t}(t-\delta t) & 0 \\ 0 & 0 & P_{c,t}(t-\delta t) \end{bmatrix}, \quad (19)$$ the state transition matrix $$\widehat{A}(\delta t) = \begin{bmatrix} A(\delta t) & 0 & 0 \\ 0 & I & 0 \\ 0 & 0 & I \end{bmatrix}, \quad (20)$$ and the process noise matrix $$\widehat{Q}(\delta t) = \begin{bmatrix} Q(\delta t) & 0 & 0 \\ 0 & Q_{b,t}(\delta t) & 0 \\ 0 & 0 & Q_{c,t}(\delta t) \end{bmatrix}. \quad (21)$$ Welch 1997 at Section 3.2.2.

Exhibit D-7

CLAIM 52	Welch 1997
	We then follow steps (b)-(h) from the original algorithm, making the appropriate substitutions of (18)-(21), and noting that the measurement and Jacobian functions used in step (c) have become $\vec{h}_\sigma(\hat{\vec{x}}(t))$ and $H_\sigma(\hat{\vec{x}}(t))$ because the estimates of parameters $\vec{b}_t$ and $\vec{c}_t$ ($\hat{x}_{b,t}$ and $\hat{x}_{c,t}$) are now contained in the augmented state vector $\hat{\vec{x}}$ per (18). After step (h) we finish by extracting and saving the device filter portions of the augmented state vector and error covariance matrix $$\begin{aligned} \hat{x}_{b,t}(t) &= \hat{\vec{x}}(t)[i \ldots j] \\ P_{b,t}(t) &= \hat{\vec{P}}(t)[i \ldots j, i \ldots j] \\ \hat{x}_{c,t}(t) &= \hat{\vec{x}}(t)[k \ldots l] \\ P_{c,t}(t) &= \hat{\vec{P}}(t)[k \ldots l, k \ldots l] \end{aligned} \qquad (22)$$ where $$\begin{aligned} i &= n+1 \\ j &= n+n_b \\ k &= n+n_b+1 \\ l &= n+n_b+n_c \end{aligned}$$ Welch 1997 at Section 3.2.2.

Exhibit D-7

CLAIM 52	Welch 1997
	and n, n_b, and n_c are the dimensions of the state vectors for the main tracker filter, the source filter, and the sensor filter (respectively). We leave the main tracker filter state vector and error covariance matrix in their augmented counterparts, while we swap the device filter components in and out with each estimate. The result is that individual device filters are updated less frequently than the main tracker filter. The more a device is used, the more it is calibrated. If a device is never used, it is never calibrated. With respect to added time complexity, the computations can again be optimized to eliminate operations on matrix and vector elements that are known to be zero: those places mentioned in section 3.1, and see (19)-(21). Also note that the size of and thus time for the matrix inversion in (13) has not changed. With respect to added space complexity, the autocalibration method requires storing a separate state vector and covariance matrix for each device—a fixed amount of (generally small) space per device. For example, consider autocalibrating the beacon (LED) positions for an optical tracking system with 3,000 beacons. For each beacon one would need 3 words for the beacon state (its 3D position), $3 \times 3 = 9$ words for the noise covariance matrix, and $3 \times 3 = 9$ words for the error covariance matrix. Assuming 8 bytes per word, this is only $3{,}000 \times 8 \times (3 + 9 + 9) = 504{,}000$ bytes. Welch 1997 at Section 3.2.2. 3.3 Stability Because the SCAAT method uses individual measurements with insufficient information, one might be concerned about the potential for instability or divergence. A linear system is said to be stable if its response to any input tends to a finite steady value after the input is removed [24]. For the Kalman filter in general this is certainly not a new concern, and there are standard requirements and corresponding tests that ensure or detect stability (see [18], p. 132): a. The filter must be uniformly completely observable, b. the dynamic and measurement noise matrices in equations (6) and (9) must be bounded from above and below, and c. the dynamic behavior represented by in equation (2) must be bounded from above. As it turns out, these conditions and their standard tests are equally applicable to a SCAAT implementation. **For the SCAAT method the conditions mean that the user dynamics between estimates must be bounded, the**

Exhibit D-7

CLAIM 52	Welch 1997
	measurement noise must be bounded, one must incorporate a sufficient set of non-degenerate constraints over time. In particular, the constraints must be incorporated in less than 1/2 the time of the user motion time-constant in order to avoid tracking an alias of the true motion. In general these conditions are easily met for systems and circumstances that would otherwise be stable with a multiple-constraint implementation. A complete stability analysis is beyond the scope of this paper, and is presented in [47]. Welch 1997 at Section 3.3. [47] Greg Welch, 1996. "SCAAT: Incremental Tracking with Incomplete Information," University of North Carolina at Chapel Hill, doctoral dissertation, TR 96-051. Welch 1997 at References. *See* Disclosures with respect to Claim 51, *supra*; *see also* Defendants' Invalidity Contentions for further discussion.

O. DEPENDENT CLAIM 53

CLAIM 53	Welch 1997
[53] The method of claim 52 wherein implementing some or all of the Kalman filter includes updating error estimates using linearized models of the sensor system.	At least under Plaintiffs' apparent infringement theory, Welch 1997 discloses, either expressly or inherently, the method of claim 52 wherein implementing some or all of the Kalman filter includes updating error estimates using linearized models of the sensor system. In the alternative, this element would be obvious over Welch 1997 in light of the other references disclosed in Defendants' Invalidity Contentions and/or the knowledge of one of ordinary skill in the art. *See, e.g.*: **The SCAAT method employs a Kalman filter (KF) in an unusual fashion. The Kalman filter is a mathematical procedure that provides an efficient computational (recursive) method for the least-squares estimation of a linear system. It does so in a predictor-corrector fashion, predicting short-term (since the last estimate) changes in the state using a dynamic model, and then correcting them with a measurement and a corresponding measurement model. The extended Kalman filter (EKF) is a variation of the Kalman filter that supports estimation of nonlinear systems, e.g. 3D position and orientation tracking systems.** A basic introduction to the Kalman filter can be found in Chapter 1 of [31], while a more complete introductory

Exhibit D-7

CLAIM 53	Welch 1997
	discussion can be found in [40], which also contains some interesting historical narrative. More extensive references can be found in [7,18,24,28,31,46]. Welch 1997 at Section 3. **The Kalman filter has been employed previously for virtual environment tracking estimation and prediction.** For example see [2,5,12,14,42], and most recently [32]. In each of these cases however the filter was applied directly and only to the 6D pose estimates delivered by the off-the-shelf tracker. The SCAAT approach could be applied to either a hybrid system using off-the shelf and/or custom trackers, or it could be employed by tracker developers to improve the existing systems for the end-user graphics community. Welch 1997 at Section 3. In this section we describe the method in a manner that does not imply a specific tracking system. (In section 3.4 we present experimental results of a specific implementation, a SCAAT wide area optoelectronic tracking system.) In section 3.1 we describe the method for tracking, and in section 3.2 we describe one possible method for concurrent autocalibration. Welch 1997 at Section 3. Throughout we use the following conventions. x = scalar (lower case) $\vec{x}$ = general vector (lower case, arrow) indexed as $\vec{x}[r]$ $\hat{x}$ = filter estimate vector (lower case, hat) A = matrix (capital letters) indexed as $A[r, c]$ A^{-1} = matrix inverse I = the identity matrix β^- = matrix/vector *prediction* (super minus) β^T = matrix/vector transpose (super T) α_i = matrix/vector/scalar identifier (subscript) $E\{\bullet\}$ = mathematical expectation Welch 1997 at Section 3.

CLAIM 53	Welch 1997
	3.1 Tracking **3.1.1 Main Tracker Filter** The use of a Kalman filter requires a mathematical (state-space) model for the dynamics of the process to be estimated, the target motion in this case. While several possible dynamic models and associated state configurations are possible, we have found a simple *position-velocity* model to suffice for the dynamics of our applications. In fact we use this same form of model, with different parameters, for all six of the position and orientation components $(x, y, z, \phi, \theta, \psi)$. Discussion of some other potential models and the associated trade-offs can be found in [7] pp. 415-420. Because our implementation is discrete with inter sample time δt we model the target's dynamic motion with the following linear difference equation: $\vec{x}(t + \delta t) = A(\delta t)\vec{x}(t) + \vec{w}(\delta t)$. (2) Welch 1997 at Section 3.1.

Exhibit D-7

CLAIM 53	Welch 1997
	In the standard model corresponding to equation (2), the n dimensional Kalman filter *state vector* $\vec{x}(t)$ would completely describe the target position and orientation at any time t. In practice we use a method similar to [2,6] and maintain the complete target orientation externally to the Kalman filter in order to avoid the nonlinearities associated with orientation computations. In the internal state vector $\vec{x}(t)$ we maintain the target position as the Cartesian coordinates (x, y, z), and the *incremental* orientation as small rotations (ϕ, θ, ψ) about the (x, y, z) axis. Externally we maintain the target orientation as the *external quaternion* $\vec{\alpha} = (\alpha_w, (\alpha_x, \alpha_y, \alpha_z))$. (See [9] for discussion of quaternions.) At each filter update step, the incremental orientations (ϕ, θ, ψ) are factored into the external quaternion $\vec{\alpha}$, and then zeroed as shown below. Thus the incremental orientations are linearized for the EKF, centered about zero. We maintain the derivatives of the target position and orientation internally, in the state vector $\vec{x}(t)$. We maintain the angular velocities internally because the angular velocities behave like orthogonal vectors and do not exhibit the nonlinearities of the angles themselves. The target state is then represented by the $n = 12$ element internal state vector $$\vec{x} = \begin{bmatrix} x & y & z & \dot{x} & \dot{y} & \dot{z} & \phi & \theta & \psi & \dot{\phi} & \dot{\theta} & \dot{\psi} \end{bmatrix}^T \quad (3)$$ and the four-element external orientation quaternion $$\vec{\alpha} = (\alpha_w, (\alpha_x, \alpha_y, \alpha_z)), \quad (4)$$ where the time designations have been omitted for clarity. Welch 1997 at Section 3.1.1.

Exhibit D-7

CLAIM 53	Welch 1997
	The $n \times n$ *state transition matrix* $A(\delta t)$ in (2) projects the state forward from time t to time $t + \delta t$. For our linear model, the matrix implements the relationships $$\begin{aligned} x(t+\delta t) &= x(t) + \dot{x}(t)\delta t \\ \dot{x}(t+\delta t) &= \dot{x}(t) \end{aligned} \quad (5)$$ and likewise for the remaining elements of (3). The $n \times 1$ *process noise vector* $\vec{w}(\delta t)$ in (2) is a normally-distributed zero-mean sequence that represents the uncertainty in the target state over any time interval δt. The corresponding $n \times n$ *process noise covariance matrix* is given by $$E\{\vec{w}(\delta t)\vec{w}^T(\delta t + \varepsilon)\} = \begin{cases} Q(\delta t), & \varepsilon = 0 \\ 0, & \varepsilon \neq 0 \end{cases}. \quad (6)$$ Because our implementation is discrete with inter sample time δt, we can use the transfer function method illustrated by [7] pp. 221-222 to compute a *sampled* process noise covariance matrix. (Because the associated random processes are presumed to be time stationary, we present the process noise covariance matrix as a function of the inter-sample duration δt only.) The non-zero elements of $Q(\delta t)$ are given by $$\begin{aligned} Q(\delta t)[i,i] &= \vec{\eta}[i]\frac{(\delta t)^3}{3} \\ Q(\delta t)[i,j] = Q(\delta t)[j,i] &= \vec{\eta}[i]\frac{(\delta t)^2}{2} \\ Q(\delta t)[j,j] &= \vec{\eta}[i](\delta t) \end{aligned} \quad (7)$$ for each pair $$(i,j) \in \{(x,\dot{x}), (y,\dot{y}), (z,\dot{z}), (\phi,\dot{\phi}), (\theta,\dot{\theta}), (\psi,\dot{\psi})\}.$$ Welch 1997 at Section 3.1.1.

Exhibit D-7

CLAIM 53	Welch 1997
	The $\vec{\eta}[i]$ in (7) are the *correlation kernels* of the (assumed constant) noise sources presumed to be driving the dynamic model. We determined a set of values using Powell's method, and then used these in both simulation and our real implementation. The values can be "tuned" for different dynamics, though we have found that the tracker works well over a broad range of values. The use of a Kalman filter requires not only a dynamic model as described above, but also a *measurement model* for each available type of measurement. The measurement model is used to predict the ideal noise-free response of each sensor and source pair, given the filter's current estimate of the target state as in equations (3) and (4). *It is the nature of the measurement models and indeed the actual sensor measurements that distinguishes a SCAAT Kalman filter from a well-constrained one.* For each sensor *type* σ we define the $m_\sigma \times 1$ *measurement vector* $\vec{z}_\sigma(t)$ and corresponding *measurement function* $\vec{h}_\sigma(\bullet)$ such that $$\vec{z}_{\sigma,t} = \vec{h}_\sigma(\vec{x}(t), \vec{b}_t, \vec{c}_t) + \vec{v}_\sigma(t)\ . \quad (8)$$ Note that in the "purest" SCAAT implementation $m_\sigma = 1$ and the measurements are incorporated as single scalar values. However if it is not possible or necessary to isolate the measurements, e.g. to perform autocalibration, then multi-dimensional measurements can be incorporated also. Guidelines presented in [47] lead to the following heuristic for choosing the SCAAT Kalman filter measurement elements (constraints): *During each SCAAT Kalman filter measurement update one should observe a single sensor and source pair only.* For example, to incorporate magnetic tracker data as an end-user, $m_\sigma = 7$ for the three position and four orientation (quaternion) Welch 1997 at Section 3.1.1.

Exhibit D-7

CLAIM 53	Welch 1997
	elements, while if the manufacturer were to use the SCAAT implementation, $m_\sigma = 3$ for each 3-axis electromagnetic response to a single excitation. For an image-based landmark tracker such as [41] the measurement function would, given estimates of the camera pose and a single landmark location, transform the landmark into camera space and then project it onto the camera image plane. In this case $m_\sigma = 2$ for the 2D image coordinates of the landmark. The $m_\sigma \times 1$ *measurement noise vector* $\vec{v}_\sigma(t)$ in (8) is a normally-distributed zero-mean sequence that represents any random error (e.g. electrical noise) in the measurement. This parameter can be determined from component design specifications, and (or) confirmed by off-line measurement. For our simulations we did both. The corresponding $m_\sigma \times m_\sigma$ *measurement noise covariance matrix* is given by $$E\{\vec{v}_\sigma(t)\vec{v}_\sigma^T(t+\varepsilon)\} = \begin{cases} R_\sigma(t), & \varepsilon = 0 \\ 0, & \varepsilon \neq 0 \end{cases}. \quad (9)$$ For each measurement function $\vec{h}_\sigma(\bullet)$ we determine the corresponding Jacobian function $$H_\sigma(\hat{x}(t), \vec{b}_t, \vec{c}_t)[i, j] \equiv \frac{\partial}{\partial \hat{x}[j]} \vec{h}_\sigma(\hat{x}(t), \vec{b}_t, \vec{c}_t)[i], \quad (10)$$ where $1 \leq i \leq m_\sigma$ and $1 \leq j \leq n$. Finally, we note the use of the standard (Kalman filter) $n \times n$ *error covariance matrix* $P(t)$ which maintains the covariance of the error in the estimated state. Welch 1997 at Section 3.1.1.

Exhibit D-7

CLAIM 53	Welch 1997
	3.1.2 Tracking Algorithm Given an initial state estimate $\hat{x}(0)$ and error covariance estimate $P(0)$, the SCAAT algorithm proceeds similarly to a conventional EKF, cycling through the following steps whenever a discrete measurement $\vec{z}_{\sigma,t}$ from some sensor (type σ) and source becomes available at time t: a. Compute the time δt since the previous estimate. b. Predict the state and error covariance. $$\begin{aligned} \hat{x}^- &= A(\delta t)\hat{x}(t-\delta t) \\ P^- &= A(\delta t)P(t-\delta t)A^T(\delta t) + Q(\delta t) \end{aligned} \quad (11)$$ c. Predict the measurement and compute the corresponding Jacobian. $$\begin{aligned} \hat{z} &= \vec{h}_\sigma(\hat{x}^-, \vec{b}_t, \vec{c}_t) \\ H &= H_\sigma(\hat{x}^-, \vec{b}_t, \vec{c}_t) \end{aligned} \quad (12)$$ d. Compute the *Kalman gain*. $$K = P^- H^T (HP^- H^T + R_\sigma(t))^{-1} \quad (13)$$ e. Compute the *residual* between the actual sensor measurement $\vec{z}_{\sigma,t}$ and the predicted measurement from (12). $$\overrightarrow{\Delta z} = \vec{z}_{\sigma,t} - \hat{z} \quad (14)$$ f. Correct the predicted tracker state estimate and error covariance from (11). $$\begin{aligned} \hat{x}(t) &= \hat{x}^- + K\overrightarrow{\Delta z} \\ P(t) &= (I - KH)P^- \end{aligned} \quad (15)$$ Welch 1997 at Section 3.1.2.

Exhibit D-7

CLAIM 53	Welch 1997
	g. Update the external orientation of equation (4) per the change indicated by the (ϕ, θ, ψ) elements of the state. $$\begin{aligned}\Delta\hat{\alpha} &= \text{quaternion}(\hat{x}[\phi], \hat{x}[\theta], \hat{x}[\psi]) \\ \hat{\alpha} &= \hat{\alpha} \otimes \Delta\hat{\alpha}\end{aligned} \quad (16)$$ h. Zero the orientation elements of the state vector. $$\hat{x}[\phi] = \hat{x}[\theta] = \hat{x}[\psi] = 0 \quad (17)$$ The equations (11)-(17) may seem computationally complex, however they can be performed quite efficiently. The computations can be optimized to eliminate operations on matrix and vector elements that are known to be zero. For example, the elements of the Jacobian H in (12) that correspond to the velocities in the state $\hat{x}(t)$ will always be zero. In addition, the matrix inverted in the computation of K in (13) is of rank m_σ (2×2 for our example in section 3.4) which is smaller for a SCAAT filter than for a corresponding conventional EKF implementation. Finally, the increased data rate allows the use of the *small angle approximations* $\sin(\theta) = \theta$ and $\cos(\theta) = 1$ in $\vec{h}_\sigma(\bullet)$ and $H_\sigma(\bullet)$. The total *per estimate* computation time can therefore actually be less than that of a corresponding conventional implementation. (We are able to execute the SCAAT filter computations, with the autocalibration computations discussed in the next section, in approximately $100\mu s$ on a 200 MHz PC-compatible computer.) Welch 1997 at Section 3.1.2. **3.2.1 Device Filters** For each device (source, sensor, landmark, etc.) we create a distinct device filter as follows. Let $\vec{\pi}$ represent the corresponding device parameter vector and $n_\pi = \text{length}(\vec{\pi})$. a. Allocate an $n_\pi \times 1$ state vector $\hat{x}_\pi$ for the device, initialize with the best *a priori* device parameter estimates, e.g. from design. b. Allocate an $n_\pi \times n_\pi$ noise covariance matrix $Q_\pi(\delta t)$, initialize with the expected parameter variances. c. Allocate an $n_\pi \times n_\pi$ error covariance matrix $P_\pi(t)$, initialize to indicate the level of confidence in the *a priori* device parameter estimates from (a) above. Welch 1997 at Section 3.2.1.

Exhibit D-7

CLAIM 53	Welch 1997
	3.2.2 Revised Tracking Algorithm The algorithm for tracking with concurrent autocalibration is the same as that presented in section 3.1, with the following exceptions. After step (a) in the original algorithm, we form augmented versions of the state vector $$\widehat{x}(t-\delta t) = \left[\hat{x}^T(t-\delta t)\ \ \hat{x}^T_{b,t}(t-\delta t)\ \ \hat{x}^T_{c,t}(t-\delta t)\right]^T, \quad (18)$$ the error covariance matrix $$\widehat{P}(t-\delta t) = \begin{bmatrix} P(t-\delta t) & 0 & 0 \\ 0 & P_{b,t}(t-\delta t) & 0 \\ 0 & 0 & P_{c,t}(t-\delta t) \end{bmatrix}, \quad (19)$$ the state transition matrix $$\widehat{A}(\delta t) = \begin{bmatrix} A(\delta t) & 0 & 0 \\ 0 & I & 0 \\ 0 & 0 & I \end{bmatrix}, \quad (20)$$ and the process noise matrix $$\widehat{Q}(\delta t) = \begin{bmatrix} Q(\delta t) & 0 & 0 \\ 0 & Q_{b,t}(\delta t) & 0 \\ 0 & 0 & Q_{c,t}(\delta t) \end{bmatrix}. \quad (21)$$ Welch 1997 at Section 3.2.2.

Exhibit D-7

CLAIM 53	Welch 1997
	We then follow steps (b)-(h) from the original algorithm, making the appropriate substitutions of (18)-(21), and noting that the measurement and Jacobian functions used in step (c) have become $\tilde{h}_\sigma(\widehat{x}(t))$ and $H_\sigma(\widehat{x}(t))$ because the estimates of parameters $\tilde{b}_t$ and $\tilde{c}_t$ ($\hat{x}_{b,t}$ and $\hat{x}_{c,t}$) are now contained in the augmented state vector $\widehat{x}$ per (18). After step (h) we finish by extracting and saving the device filter portions of the augmented state vector and error covariance matrix $$\begin{aligned} \hat{x}_{b,t}(t) &= \widehat{x}(t)[i \ldots j] \\ P_{b,t}(t) &= \widehat{P}(t)[i \ldots j, i \ldots j] \\ \hat{x}_{c,t}(t) &= \widehat{x}(t)[k \ldots l] \\ P_{c,t}(t) &= \widehat{P}(t)[k \ldots l, k \ldots l] \end{aligned} \quad (22)$$ where $$\begin{aligned} i &= n+1 \\ j &= n+n_b \\ k &= n+n_b+1 \\ l &= n+n_b+n_c \end{aligned}$$ Welch 1997 at Section 3.2.2.

Exhibit D-7

CLAIM 53	Welch 1997
	and n, n_b, and n_c are the dimensions of the state vectors for the main tracker filter, the source filter, and the sensor filter (respectively). We leave the main tracker filter state vector and error covariance matrix in their augmented counterparts, while we swap the device filter components in and out with each estimate. The result is that individual device filters are updated less frequently than the main tracker filter. The more a device is used, the more it is calibrated. If a device is never used, it is never calibrated. With respect to added time complexity, the computations can again be optimized to eliminate operations on matrix and vector elements that are known to be zero: those places mentioned in section 3.1, and see (19)-(21). Also note that the size of and thus time for the matrix inversion in (13) has not changed. With respect to added space complexity, the autocalibration method requires storing a separate state vector and covariance matrix for each device—a fixed amount of (generally small) space per device. For example, consider autocalibrating the beacon (LED) positions for an optical tracking system with 3,000 beacons. For each beacon one would need 3 words for the beacon state (its 3D position), $3 \times 3 = 9$ words for the noise covariance matrix, and $3 \times 3 = 9$ words for the error covariance matrix. Assuming 8 bytes per word, this is only $3{,}000 \times 8 \times (3 + 9 + 9) = 504{,}000$ bytes. Welch 1997 at Section 3.2.2. 3.3 Stability Because the SCAAT method uses individual measurements with insufficient information, one might be concerned about the potential for instability or divergence. A linear system is said to be stable if its response to any input tends to a finite steady value after the input is removed [24]. For the Kalman filter in general this is certainly not a new concern, and there are standard requirements and corresponding tests that ensure or detect stability (see [18], p. 132): a. The filter must be uniformly completely observable, b. the dynamic and measurement noise matrices in equations (6) and (9) must be bounded from above and below, and c. the dynamic behavior represented by in equation (2) must be bounded from above. As it turns out, these conditions and their standard tests are equally applicable to a SCAAT implementation. **For the SCAAT method the conditions mean that the user dynamics between estimates must be bounded, the**

Exhibit D-7

CLAIM 53	Welch 1997
	measurement noise must be bounded, one must incorporate a sufficient set of non-degenerate constraints over time. In particular, the constraints must be incorporated in less than 1/2 the time of the user motion time-constant in order to avoid tracking an alias of the true motion. In general these conditions are easily met for systems and circumstances that would otherwise be stable with a multiple-constraint implementation. A complete stability analysis is beyond the scope of this paper, and is presented in [47]. Welch 1997 at Section 3.3. [47] Greg Welch, 1996. "SCAAT: Incremental Tracking with Incomplete Information," University of North Carolina at Chapel Hill, doctoral dissertation, TR 96-051. Welch 1997 at References. *See* Disclosures with respect to Claim 52, *supra*; *see also* Defendants' Invalidity Contentions for further discussion.

P. DEPENDENT CLAIM 59

CLAIM 59	Welch 1997
[59] The method of claim 47 wherein providing configuration information from the sensor modules includes providing information characterizing a type of a sensor associated with a sensor module.	At least under Plaintiffs' apparent infringement theory, Welch 1997 discloses, either expressly or inherently, the method of claim 47 wherein providing configuration information from the sensor modules includes providing information characterizing a type of a sensor associated with a sensor module. In the alternative, this element would be obvious over Welch 1997 in light of the other references disclosed in Defendants' Invalidity Contentions and/or the knowledge of one of ordinary skill in the art. *See, e.g.*:

Exhibit D-7

CLAIM 59	Welch 1997
	3.1 Tracking **3.1.1 Main Tracker Filter** The use of a Kalman filter requires a mathematical (state-space) model for the dynamics of the process to be estimated, the target motion in this case. While several possible dynamic models and associated state configurations are possible, we have found a simple *position-velocity* model to suffice for the dynamics of our applications. In fact we use this same form of model, with different parameters, for all six of the position and orientation components $(x, y, z, \phi, \theta, \psi)$. Discussion of some other potential models and the associated trade-offs can be found in [7] pp. 415-420. Because our implementation is discrete with inter sample time δt we model the target's dynamic motion with the following linear difference equation: $\vec{x}(t+\delta t) = A(\delta t)\vec{x}(t) + \vec{w}(\delta t)$. (2) Welch 1997 at Section 3.1.

Exhibit D-7

CLAIM 59	Welch 1997
	In the standard model corresponding to equation (2), the n dimensional Kalman filter *state vector* $\vec{x}(t)$ would completely describe the target position and orientation at any time t. In practice we use a method similar to [2,6] and maintain the complete target orientation externally to the Kalman filter in order to avoid the nonlinearities associated with orientation computations. In the internal state vector $\vec{x}(t)$ we maintain the target position as the Cartesian coordinates (x, y, z), and the *incremental* orientation as small rotations (ϕ, θ, ψ) about the (x, y, z) axis. Externally we maintain the target orientation as the *external quaternion* $\vec{\alpha} = (\alpha_w, (\alpha_x, \alpha_y, \alpha_z))$. (See [9] for discussion of quaternions.) At each filter update step, the incremental orientations (ϕ, θ, ψ) are factored into the external quaternion $\vec{\alpha}$, and then zeroed as shown below. Thus the incremental orientations are linearized for the EKF, centered about zero. We maintain the derivatives of the target position and orientation internally, in the state vector $\vec{x}(t)$. We maintain the angular velocities internally because the angular velocities behave like orthogonal vectors and do not exhibit the nonlinearities of the angles themselves. The target state is then represented by the $n = 12$ element internal state vector $$\vec{x} = \begin{bmatrix} x & y & z & \dot{x} & \dot{y} & \dot{z} & \phi & \theta & \psi & \dot{\phi} & \dot{\theta} & \dot{\psi} \end{bmatrix}^T \quad (3)$$ and the four-element external orientation quaternion $$\vec{\alpha} = (\alpha_w, (\alpha_x, \alpha_y, \alpha_z)), \quad (4)$$ where the time designations have been omitted for clarity. Welch 1997 at Section 3.1.1.

Exhibit D-7

CLAIM 59	Welch 1997
	The $n \times n$ *state transition matrix* $A(\delta t)$ in (2) projects the state forward from time t to time $t + \delta t$. For our linear model, the matrix implements the relationships $$\begin{aligned} x(t+\delta t) &= x(t) + \dot{x}(t)\delta t \\ \dot{x}(t+\delta t) &= \dot{x}(t) \end{aligned} \quad (5)$$ and likewise for the remaining elements of (3). The $n \times 1$ *process noise vector* $\vec{w}(\delta t)$ in (2) is a normally-distributed zero-mean sequence that represents the uncertainty in the target state over any time interval δt. The corresponding $n \times n$ *process noise covariance matrix* is given by $$E\{\vec{w}(\delta t)\vec{w}^T(\delta t + \varepsilon)\} = \begin{cases} Q(\delta t), & \varepsilon = 0 \\ 0, & \varepsilon \neq 0 \end{cases}. \quad (6)$$ Because our implementation is discrete with inter sample time δt, we can use the transfer function method illustrated by [7] pp. 221-222 to compute a *sampled* process noise covariance matrix. (Because the associated random processes are presumed to be time stationary, we present the process noise covariance matrix as a function of the inter-sample duration δt only.) The non-zero elements of $Q(\delta t)$ are given by $$\begin{aligned} Q(\delta t)[i,i] &= \vec{\eta}[i]\frac{(\delta t)^3}{3} \\ Q(\delta t)[i,j] = Q(\delta t)[j,i] &= \vec{\eta}[i]\frac{(\delta t)^2}{2} \\ Q(\delta t)[j,j] &= \vec{\eta}[i](\delta t) \end{aligned} \quad (7)$$ for each pair $$(i,j) \in \{(x,\dot{x}), (y,\dot{y}), (z,\dot{z}), (\phi,\dot{\phi}), (\theta,\dot{\theta}), (\psi,\dot{\psi})\}.$$ Welch 1997 at Section 3.1.1.

Exhibit D-7

CLAIM 59	Welch 1997
	The $\vec{\eta}[i]$ in (7) are the *correlation kernels* of the (assumed constant) noise sources presumed to be driving the dynamic model. We determined a set of values using Powell's method, and then used these in both simulation and our real implementation. The values can be "tuned" for different dynamics, though we have found that the tracker works well over a broad range of values. The use of a Kalman filter requires not only a dynamic model as described above, but also a *measurement model* for each available type of measurement. The measurement model is used to predict the ideal noise-free response of each sensor and source pair, given the filter's current estimate of the target state as in equations (3) and (4). *It is the nature of the measurement models and indeed the actual sensor measurements that distinguishes a SCAAT Kalman filter from a well-constrained one.* For each sensor *type* σ we define the $m_\sigma \times 1$ *measurement vector* $\vec{z}_\sigma(t)$ and corresponding *measurement function* $\vec{h}_\sigma(\bullet)$ such that $\vec{z}_{\sigma,t} = \vec{h}_\sigma(\vec{x}(t), \vec{b}_t, \vec{c}_t) + \vec{v}_\sigma(t)$. (8) Note that in the "purest" SCAAT implementation $m_\sigma = 1$ and the measurements are incorporated as single scalar values. However if it is not possible or necessary to isolate the measurements, e.g. to perform autocalibration, then multi-dimensional measurements can be incorporated also. Guidelines presented in [47] lead to the following heuristic for choosing the SCAAT Kalman filter measurement elements (constraints): *During each SCAAT Kalman filter measurement update one should observe a single sensor and source pair only.* For example, to incorporate magnetic tracker data as an end-user, $m_\sigma = 7$ for the three position and four orientation (quaternion) Welch 1997 at Section 3.1.1.

Exhibit D-7

CLAIM 59	Welch 1997
	elements, while if the manufacturer were to use the SCAAT implementation, $m_\sigma = 3$ for each 3-axis electromagnetic response to a single excitation. For an image-based landmark tracker such as [41] the measurement function would, given estimates of the camera pose and a single landmark location, transform the landmark into camera space and then project it onto the camera image plane. In this case $m_\sigma = 2$ for the 2D image coordinates of the landmark. The $m_\sigma \times 1$ *measurement noise vector* $\vec{v}_\sigma(t)$ in (8) is a normally-distributed zero-mean sequence that represents any random error (e.g. electrical noise) in the measurement. This parameter can be determined from component design specifications, and (or) confirmed by off-line measurement. For our simulations we did both. The corresponding $m_\sigma \times m_\sigma$ *measurement noise covariance matrix* is given by $$E\{\vec{v}_\sigma(t)\vec{v}_\sigma^T(t+\varepsilon)\} = \begin{cases} R_\sigma(t), & \varepsilon = 0 \\ 0, & \varepsilon \neq 0 \end{cases}. \quad (9)$$ For each measurement function $\vec{h}_\sigma(\bullet)$ we determine the corresponding Jacobian function $$H_\sigma(\hat{x}(t), \vec{b}_t, \vec{c}_t)[i, j] \equiv \frac{\partial}{\partial \hat{x}[j]} \vec{h}_\sigma(\hat{x}(t), \vec{b}_t, \vec{c}_t)[i], \quad (10)$$ where $1 \leq i \leq m_\sigma$ and $1 \leq j \leq n$. Finally, we note the use of the standard (Kalman filter) $n \times n$ *error covariance matrix* $P(t)$ which maintains the covariance of the error in the estimated state. Welch 1997 at Section 3.1.1. *See* Disclosures with respect to Claim 47, *supra*; *see also* Defendants' Invalidity Contentions for further discussion.

Q. DEPENDENT CLAIM 60

CLAIM 60	Welch 1997
[60] The method of claim 47 wherein	At least under Plaintiffs' apparent infringement theory, Welch 1997 discloses, either expressly or inherently, the method of claim 47 wherein providing configuration information from the sensor modules includes providing

Exhibit D-7

CLAIM 60	Welch 1997
providing configuration information from the sensor modules includes providing information characterizing a position or an orientation of a sensor associated with a sensor module.	information characterizing a position or an orientation of a sensor associated with a sensor module. In the alternative, this element would be obvious over Welch 1997 in light of the other references disclosed in Defendants' Invalidity Contentions and/or the knowledge of one of ordinary skill in the art. *See, e.g.*: We present a promising new mathematical method for **tracking a user's pose (position and orientation) for interactive computer graphics.** The method, which is applicable to a wide variety of both commercial and experimental systems, improves accuracy by properly assimilating sequential observations, filtering sensor measurements, and by concurrently autocalibrating source and sensor devices. It facilitates user motion prediction, multisensor data fusion, and higher report rates with lower latency than previous methods. Welch 1997 at Abstract. Tracking systems determine the user's pose by measuring signals from low-level hardware sensors. For reasons of physics and economics, most systems make multiple sequential measurements which are then combined to produce a single tracker report. For example, commercial magnetic trackers using the SPASYN (*Space Synchro*) system sequentially measure three magnetic vectors and then combine them mathematically to produce a report of the sensor pose. Welch 1997 at Abstract. **Our new approach produces tracker reports as each new low-level sensor measurement is made rather than waiting to form a complete collection of observations**. Because single observations under-constrain the mathematical solution, we refer to our approach as single-constraint-at-a-time or SCAAT tracking. The key is that the single observations provide some information about the user's state, and thus can be used to incrementally improve a previous estimate. We recursively apply this principle, incorporating new sensor data as soon as it is measured. With this approach we are able to generate estimates more frequently, with less latency, and with improved accuracy. We present results from both an actual implementation, and from extensive simulations. Welch 1997 at Abstract.

Exhibit D-7

CLAIM 60	Welch 1997
	1.1 Incomplete Information The idea that one might build a tracking system that generates a new estimate with each individual sensor measurement or *observation* is a very interesting one. After all, individual observations usually provide only partial information about a user's complete state (pose), i.e. they are "incomplete" observations. For example, for a camera observing landmarks in a scene, only limited information is obtained from observations of any single landmark. In terms of control theory, a system designed to operate with only such incomplete measurements is characterized as *unobservable* because the user state cannot be observed (determined) from the measurements. The notion of observability can also be described in terms of constraints on the unknown parameters of the system being estimated, e.g. constraints on the unknown elements of the system state. Given a particular system, and the corresponding set of unknowns that are to be estimated, let C be defined as the minimal number of independent simultaneous constraints necessary to uniquely determine a solution, let N be the number actually used to generate a new estimate, and let N_{ind} be the number of *independent* constraints that can be formed from the N constraints. For any $N \geq N_{ind}$ constraints, if $N_{ind} = C$ the problem is *well constrained*, if $N_{ind} > C$ it is *over constrained*, and if $N_{ind} < C$ it is *under-constrained*. (See Figure 1.) Welch 1997 at Section 1.1.

Exhibit D-7

CLAIM 60	Welch 1997
	1.2 Landmark Tracking Consider for example a system in which a single camera is used to observe known scene points to determine the camera position and orientation. In this case, the constraints provided by the observations are multi-dimensional: 2D image coordinates of 3D scene points. Given the internal camera parameters, a set of four known coplanar scene points, and the corresponding image coordinates, the camera position and orientation can be uniquely determined in closed-form [16]. In other words if $N = C = 4$ constraints (2D image points) are used to estimate the camera position and orientation, the system is completely observable. On the other hand, if $N < C$ then there are multiple solutions. For example with only $N = 3$ non-collinear points, there are up to 4 solutions. Even worse, with $N = 2$ or $N = 1$ points, there are infinite combinations of position and orientation that could result in the same camera images. Welch 1997 at Section 1.2. In general, for closed-form tracking approaches, a well or over-constrained system with $N \geq C$ is observable, an under-constrained system with $N < C$ is not. Therefore, if the individual observations provide only partial information, i.e. the measurements provide insufficient constraints, then multiple devices or landmarks must be excited and (or) sensed prior to estimating a solution. Sometimes the necessary observations can be obtained simultaneously, and sometimes they can not. Magnetic trackers such as those made by Polhemus and Ascension perform three *sequential* source excitations, each in conjunction with a complete sensor unit observation. And while a camera can indeed observe multiple landmarks simultaneously in a single image, the image processing to identify and locate the individual landmarks must be done sequentially for a single CPU system. If the landmarks can move independently over time, for example if they are artificial marks placed on the skin of an ultrasound patient for the purpose of landmark-based tracking [41], batch processing of the landmarks can reduce the effectiveness of the system. A SCAAT implementation might grab an image, extract a *single* landmark, update the estimates of both the camera *and* landmark positions, and then throw-away the image. In this way estimates are generated faster and with the most recent landmark configurations. Welch 1997 at Section 1.2.

Exhibit D-7

CLAIM 60	Welch 1997
	1.3 Putting the Pieces Together Given a tracker that uses multiple constraints that are each individually incomplete, a *measurement model* for any one of incomplete constraints would be characterized as *locally unobservable*. Such a system must incorporate a sufficient set of these incomplete constraints so that the resulting overall system is observable. The corresponding aggregate measurement model can then be characterized as *globally observable*. Global observability can be obtained over *space* or over *time*. The SCAAT method adopts the latter scheme, even in some cases where the former is possible. Welch 1997 at Section 1.3. *See* Disclosures with respect to Claim 47, *supra*; *see also* Defendants' Invalidity Contentions for further discussion.

R. DEPENDENT CLAIM 61

CLAIM 61	Welch 1997
[61] The method of claim 47 wherein providing configuration information from the sensor modules includes providing information characterizing one or more calibration parameters of a sensor associated with a sensor module.	At least under Plaintiffs' apparent infringement theory, Welch 1997 discloses, either expressly or inherently, the method of claim 47 wherein providing configuration information from the sensor modules includes providing information characterizing one or more calibration parameters of a sensor associated with a sensor module. In the alternative, this element would be obvious over Welch 1997 in light of the other references disclosed in Defendants' Invalidity Contentions and/or the knowledge of one of ordinary skill in the art. *See, e.g.*:

Exhibit D-7

CLAIM 61	Welch 1997
	2 MOTIVATION **2.1 The Simultaneity Assumption** Several well-known virtual environment tracking systems collect position and orientation constraints (sensor measurements) sequentially. For example, tracking systems developed by Polhemus and Ascension depend on sensing a sequence of variously polarized electromagnetic waves or fields. A system that facilitated simultaneous polarized excitations would be very difficult if not impossible to implement. Similarly both the original UNC optoelectronic tracking system and the newer HiBall version are designed to observe only one ceiling-mounted LED at a time. Based on the available literature [25,27,37] these systems currently assume (mathematically) that their sequential observations were collected simultaneously. We refer to this as the *simultaneity assumption*. If the target remains motionless this assumption introduces no error. However if the target is moving, the violation of the assumption introduces error. To put things into perspective, consider that typical arm and wrist motion can occur in as little as 1/2 second, with typical "fast" wrist tangential motion occurring at 3 meters/second [1]. For the current versions of the above systems such motion corresponds to approximately 2 to 6 centimeters of translation *throughout* the sequence of measurements required for a single estimate. For systems that attempt sub-millimeter accuracies, even slow motion occurring during a sequence of sequential measurements impacts the accuracy of the estimates. Welch 1997 at Section 2.1.

Exhibit D-7

CLAIM 61	Welch 1997
	The error introduced by violation of the simultaneity assumption is of greatest concern perhaps when attempting any form of system *autocalibration*. Gottschalk and Hughes note that motion during their autocalibration procedure must be severely restricted in order to avoid such errors [19]. Consider that for a multiple-measurement system with 30 milliseconds total measurement time, motion would have to be restricted to approximately 1.5 centimeters/second to confine the translation (throughout a measurement sequence) to 0.5 millimeters. For complete autocalibration of a large (wide-area) tracking system, this restriction results in lengthy specialized sessions. Welch 1997 at Section 2.1. **2.2 Device Isolation & Autocalibration** Knowledge about source and sensor imperfections can be used to improve the accuracy of tracking systems. While intrinsic sensor parameters can often be determined off-line, e.g. by the manufacturer, this is generally not the case for extrinsic parameters. For example it can be difficult to determine the exact geometric relationship between the various sensors of a hybrid system. Consider that the coordinate system of a magnetic sensor is located at some unknown location inside the sensor unit. Similarly the precise geometric relationship between visible landmarks used in a vision-based system is often difficult to determine. Even worse, landmark positions can change over time as, for example, a patient's skin deforms with pressure from an ultrasound probe. In general, goals such as flexibility, ease of use, and lower cost, make the notion of self-calibration or *autocalibration* attractive. Welch 1997 at Section 2.2.

Exhibit D-7

CLAIM 61	Welch 1997
	The general idea for autocalibration is not new. See for example [19,45]. However, because the SCAAT method *isolates* the measurements provided by each sensor or modality, the method provides a new and elegant means to autocalibrate concurrently while tracking. Because the SCAAT method isolates the individual measurements, or measurement dimensions, individual source and sensor imperfections are more easily identified and dealt with. Furthermore, because the simultaneity assumption is avoided, the motion restrictions discussed in section 2.1 would be removed, and autocalibration could be performed *while concurrently tracking a target*. The isolation enforced by the SCAAT approach can improve results even if the constraints are obtained simultaneously through multidimensional measurements. An intuitive explanation is that if the elements (dimensions) are corrupted by independent noise, then incorporating the elements independently can offer improved filtering over a batch or ensemble estimation scheme. Welch 1997 at Section 2.2.

CLAIM 61	Welch 1997
	2.3 Temporal Improvements Per Shannon's sampling theorem [24] the measurement or *sampling* frequency should be at least twice the true target motion bandwidth, or an estimator may track an alias of the true motion. Given that common arm and head motion bandwidth specifications range from 2 to 20 Hz [13,14,36], the *sampling* rate should ideally be greater than 40 Hz. Furthermore, the *estimate* rate should be as high as possible so that normally-distributed white estimate error can be discriminated from any non-white error that might be observed during times of significant target dynamics, and so estimates will always reflect the most recent user motion. In addition to increasing the estimate rate, we want to reduce the latency associated with generating an improved estimate, thus reducing the overall latency between target motion and visual feedback in virtual environment systems [34]. If too high, such latency can impair adaptation and the illusion of presence [22], and can cause motion discomfort or sickness. Increased latency also contributes to problems with head-mounted display registration [23] and with motion prediction [4,15,29]. Finally, post-rendering Welch 1997 at Section 2.3.

Exhibit D-7

CLAIM 61	Welch 1997
	image deflection techniques are sometimes employed in an attempt to address latency variability in the rendering pipeline [32,39]. Such methods are most effective when they have access to (or generate) accurate motion predictions and low-latency tracker updates. With accurate prediction the best possible position and orientation information can be used to render a preliminary image. With fast tracker updates there is higher probability that when the preliminary image is ready for final deflection, recent user motion has been detected and incorporated into the deflection. With these requirements in mind, let us examine the effect of the measurements on the estimate latency and rate. Let t_m be the time needed to determine one constraint, e.g. to measure a sensor or extract a scene landmark, let N be the number of (sequential) constraints used to compute a complete estimate, and let t_c be the time needed to actually compute that estimate. Then the estimate latency t_e and rate r_e are $$t_e = Nt_m + t_c \ , \quad r_e = \frac{1}{t_e} = \frac{1}{Nt_m + t_c} \ . \qquad (1)$$ Welch 1997 at Section 2.3.

CLAIM 61	Welch 1997
	As the number of constraints N increases, equation (1) shows how the estimate latency and rate increase and decrease respectively. For example the Polhemus Fastrak, which uses the SPASYN (*Space Synchro*) method for determining relative position and orientation, employs $N = 3$ sequential electromagnetic excitations and measurements per estimate [25,27,37], the original University of North Carolina (UNC) optoelectronic tracking system sequentially observed $10 \le N \le 20$ beacons per estimate [3,44], and the current UNC hybrid landmark-magnetic tracking system extracts (from a camera image) and then incorporates $N = 4$ landmarks per update. The SCAAT method seeks to improve the latencies and data rates of such systems by updating the current estimate with each new (individual) constraint, i.e. by fixing N at 1. In other words, it increases the estimate rate to approximately the rate that individual constraints can be obtained and likewise decreases the estimate latency to approximately the time required to obtain a single constraint, e.g. to perform a single measurement of a single sensor, or to extract a single landmark. Welch 1997 at Section 2.3.

Exhibit D-7

CLAIM 61	Welch 1997
	Figure 2 illustrates the increased data rate with a timing diagram that compares the SPASYN (Polhemus Navigation Systems) magnetic position and orientation tracking system with a hypothetical SCAAT implementation. In contrast to the SPASYN system, a SCAAT implementation would generate a new estimate after sensing each *individual* excitation vector rather than waiting for a complete pattern. 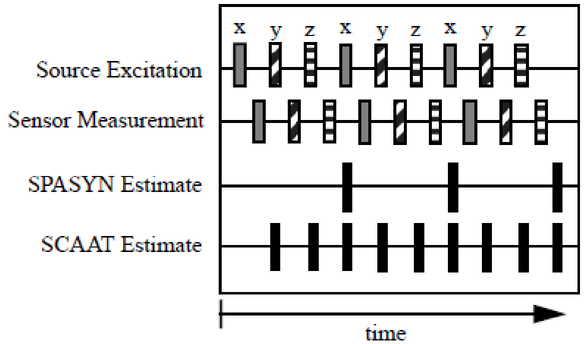 Figure 2: A timing diagram comparing the SPASYN (Polhemus Navigation Systems) magnetic position and orientation tracking system with a hypothetical SCAAT implementation. Welch 1997 at Section 2.3.

Exhibit D-7

CLAIM 61	Welch 1997
	3.2 Autocalibration The method we use for autocalibration involves *augmenting* the *main tracker filter* presented in section 3.1 to effectively implement a distinct *device filter*, a Kalman filter, for each source or sensor to be calibrated. (We use the word "device" here to include for example scene landmarks which can be thought of as passive sources, and cameras which are indeed sensors.) In general, any constant device-related parameters used by a measurement function $\vec{h}_{\sigma}(\bullet)$ from (8) are candidates for this autocalibration method. We assume that the parameters to be estimated are contained in the device parameter vectors $\vec{b}_t$ and $\vec{c}_t$, and we also present the case where both the source and sensor are to be calibrated since omission of one or the other is trivial. We note the following new convention. $\widehat{\alpha}$ = augmented matrix/vector (wide hat) Welch 1997 at Section 3.2. **3.2.1 Device Filters** For each device (source, sensor, landmark, etc.) we create a distinct device filter as follows. Let $\vec{\pi}$ represent the corresponding device parameter vector and $n_{\pi} = \text{length}(\vec{\pi})$. a. Allocate an $n_{\pi} \times 1$ state vector $\hat{x}_{\pi}$ for the device, initialize with the best *a priori* device parameter estimates, e.g. from design. b. Allocate an $n_{\pi} \times n_{\pi}$ noise covariance matrix $Q_{\pi}(\delta t)$, initialize with the expected parameter variances. c. Allocate an $n_{\pi} \times n_{\pi}$ error covariance matrix $P_{\pi}(t)$, initialize to indicate the level of confidence in the *a priori* device parameter estimates from (a) above. Welch 1997 at Section 3.2.1.

Exhibit D-7

CLAIM 61	Welch 1997
	3.2.2 Revised Tracking Algorithm The algorithm for tracking with concurrent autocalibration is the same as that presented in section 3.1, with the following exceptions. After step (a) in the original algorithm, we form augmented versions of the state vector $$\widehat{x}(t-\delta t) = \left[\hat{x}^T(t-\delta t)\;\; \hat{x}^T_{b,t}(t-\delta t)\;\; \hat{x}^T_{c,t}(t-\delta t)\right]^T, \quad (18)$$ the error covariance matrix $$\widehat{P}(t-\delta t) = \begin{bmatrix} P(t-\delta t) & 0 & 0 \\ 0 & P_{b,t}(t-\delta t) & 0 \\ 0 & 0 & P_{c,t}(t-\delta t) \end{bmatrix}, \quad (19)$$ the state transition matrix $$\widehat{A}(\delta t) = \begin{bmatrix} A(\delta t) & 0 & 0 \\ 0 & I & 0 \\ 0 & 0 & I \end{bmatrix}, \quad (20)$$ and the process noise matrix $$\widehat{Q}(\delta t) = \begin{bmatrix} Q(\delta t) & 0 & 0 \\ 0 & Q_{b,t}(\delta t) & 0 \\ 0 & 0 & Q_{c,t}(\delta t) \end{bmatrix}. \quad (21)$$ Welch 1997 at Section 3.2.2.

Exhibit D-7

CLAIM 61	Welch 1997
	We then follow steps (b)-(h) from the original algorithm, making the appropriate substitutions of (18)-(21), and noting that the measurement and Jacobian functions used in step (c) have become $\vec{h}_\sigma(\widehat{\vec{x}}(t))$ and $H_\sigma(\widehat{\vec{x}}(t))$ because the estimates of parameters $\vec{b}_t$ and $\vec{c}_t$ ($\hat{x}_{b,t}$ and $\hat{x}_{c,t}$) are now contained in the augmented state vector $\widehat{\vec{x}}$ per (18). After step (h) we finish by extracting and saving the device filter portions of the augmented state vector and error covariance matrix $$\begin{aligned} \hat{x}_{b,t}(t) &= \widehat{\vec{x}}(t)[i \ldots j] \\ P_{b,t}(t) &= \widehat{P}(t)[i \ldots j, i \ldots j] \\ \hat{x}_{c,t}(t) &= \widehat{\vec{x}}(t)[k \ldots l] \\ P_{c,t}(t) &= \widehat{P}(t)[k \ldots l, k \ldots l] \end{aligned} \quad (22)$$ where $$\begin{aligned} i &= n+1 \\ j &= n+n_b \\ k &= n+n_b+1 \\ l &= n+n_b+n_c \end{aligned}$$ and n, n_b, and n_c are the dimensions of the state vectors for the main tracker filter, the source filter, and the sensor filter (respectively). We leave the main tracker filter state vector and error covariance matrix in their augmented counterparts, while we swap the device filter components in and out with each estimate. The result is that individual device filters are updated less frequently than the main tracker filter. The more a device is used, the more it is calibrated. If a device is never used, it is never calibrated. Welch 1997 at Section 3.2.2.

CLAIM 61	Welch 1997
	With respect to added time complexity, the computations can again be optimized to eliminate operations on matrix and vector elements that are known to be zero: those places mentioned in section 3.1, and see (19)-(21). Also note that the size of and thus time for the matrix inversion in (13) has not changed. With respect to added space complexity, the autocalibration method requires storing a separate state vector and covariance matrix for each device—a fixed amount of (generally small) space per device. For example, consider autocalibrating the beacon (LED) positions for an optical tracking system with 3,000 beacons. For each beacon one would need 3 words for the beacon state (its 3D position), $3 \times 3 = 9$ words for the noise covariance matrix, and $3 \times 3 = 9$ words for the error covariance matrix. Assuming 8 bytes per word, this is only $3{,}000 \times 8 \times (3 + 9 + 9) = 504{,}000$ bytes. Welch 1997 at Section 3.2.2. **3.2.3 Discussion** The ability to simultaneously estimate two dependent sets of unknowns (the target and device states) is made possible by several factors. First, the dynamics of the two sets are very different as would be reflected in the process noise matrices. We assume the target is undergoing some random (constant) acceleration, reflected in the noise parameter η of $Q(\delta t)$ in (6). Conversely, we assume the device parameters are constant, and so the elements of $Q_\pi(\delta t)$ for a source or sensor simply reflect any allowed variances in the corresponding parameters: usually zero or extremely small. In addition, while the target is expected to be moving, the filter expects the motion between any two estimations to closely correspond to the velocity estimates in the state (3). If the tracker estimate rate is high enough, poorly estimated device parameters will result in what appears to be almost instantaneous target motion. The increased rate of the SCAAT method allows such motion to be recognized as unlikely, and attributed to poorly estimated device parameters. Welch 1997 at Section 3.2.3 *See* Disclosures with respect to Claim 47, *supra*; *see also* Defendants' Invalidity Contentions for further discussion.